



No. 110 – December 2002

Installation and Commissioning of FLAMES, the VLT Multifibre Facility

L. PASQUINI¹, G. AVILA¹, A. BLECHA², C. CACCIARI³, V. CAYATTE⁴, M. COLLESS⁵, F. DAMIANI⁶, R. DE PROPRIIS⁵, H. DEKKER¹, P. DI MARCANTONIO⁷, T. FARRELL⁸, P. GILLINGHAM⁸, I. GUINOARD⁴, F. HAMMER⁴, A. KAUFER⁹, V. HILL⁴, M. MARTEAUD⁴, A. MODIGLIANI¹, G. MULAS¹⁰, P. NORTH², D. POPOVIC⁸, E. ROSSETTI³, F. ROYER², P. SANTIN⁷, R. SCHMUTZER⁹, G. SIMOND², P. VOLA⁴, L. WALLER⁸, M. ZOCCALI¹

¹European Southern Observatory, Garching, Germany; ²Observatoire de Genève, Sauverny, Suisse;

³INAF-OABo, Bologna, Italy; ⁴Observatoire de Paris-Meudon, Meudon, France;

⁵Research School of Astronomy and Astrophysics, Australian National University, Canberra, Australia;

⁶INAF-OAPa, Palermo, Italy; ⁷INAF-OATs, Trieste, Italy; ⁸Anglo Australian Observatory, Sydney, Australia;

⁹European Southern Observatory, Chile; ¹⁰INAF-OACa, Capoterra, Cagliari, Italy

Introduction

FLAMES (Fibre Large Array Multi Element Spectrograph) is the VLT Fibre Facility, installed and commissioned at the Nasmyth A focus of UT2 (Kueyen Telescope). FLAMES was built and assembled in about four years through an international collaboration between ten institutes in six countries and three continents. It had first light with the fibre link to the red arm of UVES on April 1, and with the GIRAFFE spectrograph on

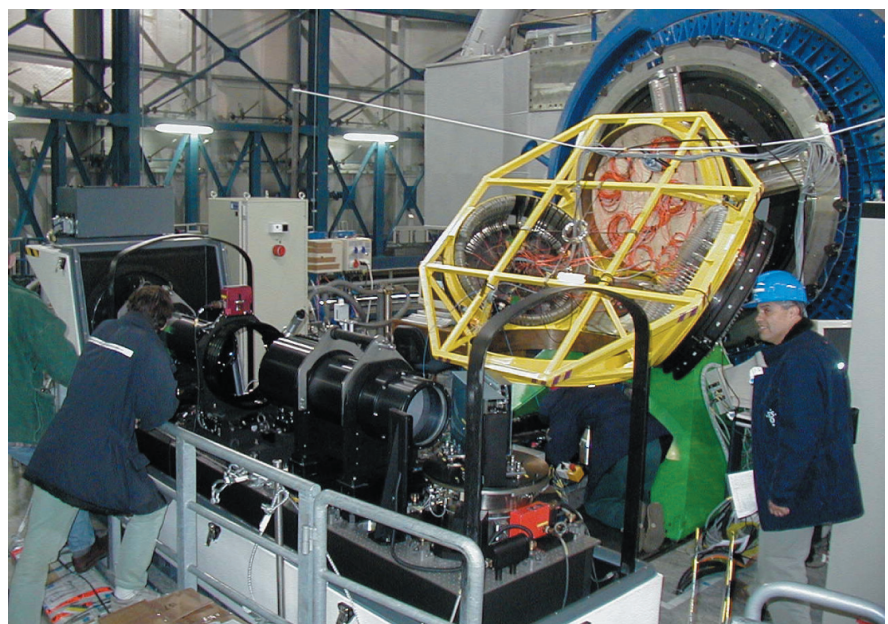


Figure 1: The fibre positioner and GIRAFFE as seen during the GIRAFFE integration on the Nasmyth platform. The positioner is looking towards the Nasmyth Focus, where the corrector is placed (only the corrector support is visible). GIRAFFE is open, and all the optomechanics components are visible. The picture was taken when the OzPoz enclosure had not yet been installed.

Table 1. Observational capabilities of FLAMES.

Spectrograph	Mode	Nr. Objects	Aperture	R	Coverage (nm)
UVES8 Red Arm (with sky)		8	1	47000	200, 400
UVES7 Red Arm (with sky)	Simult. Calibration	7	1	47000	200
GIRAFFE	MEDUSA	132 (with sky)	1.2	20500*	$\lambda/22^*$
GIRAFFE	MEDUSA	132 (with sky)	1.2	7000*	$\lambda/7^*$
GIRAFFE	IFU	15 (+15 sky)	2×3	33000*	$\lambda/22^*$
GIRAFFE	IFU	15 (+15 sky)	2×3	11000*	$\lambda/7^*$
GIRAFFE	ARGUS	1	11.5 \times 7.3 Or 6.6 \times 4.2	33000*	$\lambda/22^*$
GIRAFFE	ARGUS	1	11.5 \times 7.3 Or 6.6 \times 4.2	11000*	$\lambda/7^*$

*The GIRAFFE resolving power (R) and wavelength coverage given here are only average values. They will vary for the different set-ups by $\pm \sim 20\%$. Aperture is in arcseconds.

July 3. We report here on the complex process of integration and commissioning, and we compare the expected and observed astronomical requirements.

Overview

FLAMES is the multi-object, intermediate and high-resolution fibre facility of the VLT. Mounted at the Nasmyth A platform of UT2 it offers a large corrected field of view (25 arcmin diameter) and it consists of several components, developed by several consortia (Australis (AAO/ANU/UNSW), Paris-Meudon (OPM), Geneva and Lausanne (OGL), Bologna, Cagliari, Palermo and Trieste (ITAL Consortium)) and ESO:

- An optical *Corrector*, providing excellent image quality and telecentricity over the full field of view of 25 arcmin diameter (developed at ESO).

- A *Fibre Positioner* hosting two plates. While one plate is observing, the other one is positioning the fibres for the subsequent observations, therefore limiting the dead time between observations (developed at AAO).

- A link to the *UVES* spectrograph (Red Arm) via eight single object fibres/plate (developed at OPM in collaboration with ESO).

- A high and intermediate resolution optical spectrograph, *GIRAFFE* (developed at OPM and ESO).

- Three types of fibre systems: MEDUSA, IFU, ARGUS (developed at OPM).

- A coordinating observing software, that allows *simultaneous UVES* and *GIRAFFE* observations (developed at ITAL Consortium in collaboration with ESO).

- As for all VLT instruments, a full Data Reduction Software (*DRS*) package is provided, integrated in the ESO Data Flow Software (developed at OGL with contributions from OPM (*GIRAFFE*) and ITAL Consortium (*UVES-Fibre*)).

The FLAMES components are described in detail elsewhere (cf. e.g. Avila et al. 2002, Blecha et al. 2000, Gillingham et al. 2000, 2002, Jocou et al. 2000, Mulas et al. 2002, Pasquini et al. 2000, Royer et al. 2002), on the ESO web site and in the FLAMES User Manual

(www.eso.org/instruments/FLAMES/manuals).

The characteristics of the different observing modes are given in Table 1, which summarizes the observational capabilities of FLAMES.

UVES-Fibre

UVES is the high-resolution spectrograph of the VLT UT2 (D’Odorico et al. 2000). Each positioner plate has eight fibres connected to the UVES Red Arm. With an aperture on the sky of 1 arcsec, the fibres project to five UVES pixels giving a resolving power of $\sim 47,000$. Only the three standard UVES Red set-ups are offered, with central wavelengths of 520, 580 and 860 nm, respectively.

GIRAFFE

GIRAFFE is a medium-high resolution spectrograph ($R = 6000\text{--}33,000$) for the entire visible range (370–950 nm). It is equipped with two echelles for low and high resolution and uses interference order sorting filters to select the required spectral range within an order. The typical spectral coverage in one exposure is 60–100 nm in low resolution and 20–40 nm in high resolution.

The fibre system feeding GIRAFFE consists of the following components (cf. Avila et al. 2002 for details):

- *MEDUSA* fibre slits, one per positioner plate. Up to 132 separate objects (including sky fibres) are accessible in MEDUSA single fibre mode, each with an aperture of 1.2 arcsec on the sky.

- *IFU* slits. 15 deployable Integral Field Units (IFU) per plate, each consisting of an array of 20 square micro-lenses, for a total (almost rectangular) aperture of $\sim 3 \times 2$ arcsec. For each plate there are also 15 IFU dedicated to sky measurements.

- *1 ARGUS* slit. A large integral unit consisting of a rectangular array of 22 by 14 micro-lenses, fixed at the centre of one positioner plate. Two scales are available: one with a sampling of 0.52 arcsec/micro-lens and a total aperture of 12 by 7 arcsec, and one with a sam-

pling of 0.3 arcsec/micro-lens and a total coverage of 6.6 by 4.2 arcsec. 15 deployable ARGUS single sky fibres are also available.

GIRAFFE is operated with 30 fixed set-ups (22 high-resolution + 8 low-resolution modes). For performance estimates (based on expected transmission curves and performances) the user is referred to the Exposure Time Calculator (ETC), available at the ESO ETC web page: www.eso.org/observing/etc

The FLAMES observing software (OS) is coordinating the operations of the Telescope, the Positioner and the UVES and GIRAFFE spectrographs. In addition, it allows COMBINED observations: that is the simultaneous acquisition of UVES and GIRAFFE spectra with the specific observing modes listed in Table 1.

LAYOUT

Figure 1 shows a view of the main components of the FLAMES facility, the fibre Positioner and GIRAFFE, as seen on the telescope platform. The Corrector support is also visible, attached at the Nasmyth rotator.

1. Corrector

The optical corrector is a big doublet of 880 mm free aperture. The function of the corrector is to give an excellent image quality over the whole 25 arcmin FLAMES field of view and to provide a pupil located at the centre of curvature of the focal plate, to avoid vignetting for off-axis fibres. When the whole optical train is taken into account (including telescope optics and vignetting), the effective transmission of the corrector depends on the observing wavelength and on the distance of the object to the field centre, varying from about 78% at 370 nm to 90% in the visible, and 82% at 1 micron.

A system of lamps has been installed to illuminate the Nasmyth screen, which is located in the telescope centrepiece, about 2 m in front of the focal plane.

2. Fibre Positioner (OzPoz)

The Fibre Positioner (OzPoz) is at the core of the FLAMES facility. OzPoz is a rather large and complex system equipped with four plates, two of which are currently in use (cf. Gillingham et al. 2002). The Positioner can be subdivided into the following subsystems:

- Plates: Two metallic disks, on which the magnetic buttons holding the fibres are attached. Each of the plates has a hole in the centre. In one plate this hole hosts ARGUS. Each plate has a curvature of 3950 mm to match the curvature of the corrector focal surface.

- Retractors: Mechanical systems maintaining the fibres in constant tension. Each fibre is equipped with one retractor. The retractors are externally the same for all fibres.

- Exchanger: Main structure holding the plates. The exchanger can perform two main movements: it can retract (or approach) the Nasmyth adapter to engage the plate (or disengage it). Furthermore, it can rotate the upper part in order to perform the plate exchange.

- r- θ system and Gripper: This unit grips and releases the magnetic buttons at the positions reached via the r- θ (polar) robot. The gripper requires a back-illumination system, sending a brief light flash along each fibre from the spectrograph towards the plate. A camera records this back-illumination light and performs an image analysis. The back-illumination light is used for several purposes: to reach the required positioning accuracy and to detect if the magnetic button was properly lifted from the plate.

- OzPoz is equipped with a calibration box which can direct the light either from a tungsten, or from a Th-Ar, or from a Ne lamp. In this way FF, Th-Ar and Ne calibrations can be obtained for GIRAFFE and for UVES.

- Field Acquisition Bundles (FACBs): Four magnetic buttons on each plate are equipped with a system of 19 coherent fibres each. This bundle is used to obtain images of fiducial stars, one per button. The four images are viewed by an ESO technical CCD; the image centroids are computed and the proper offsets are calculated to centre the fiducial stars into the bundles. Each FACB bundle has an effective diameter of 2.4 arcseconds.

- Positioning Software: It is written around the so-called delta-task program, developed initially for the 2dF system at AAO. This program allows crossing between the fibres and it determines the button movements sequence.

3. Buttons and Fibre Systems

FLAMES is equipped with different types of fibres for UVES and for the dif-

ferent modes for GIRAFFE. It is worth mentioning that, in addition to the object or sky fibres coming from the Positioner, each GIRAFFE fibre slit has five fibres devoted to *simultaneous wavelength calibration*, which provide simultaneous calibration spectra for each observation acquired with GIRAFFE (Hammer et al. 1999).

The histogram distribution of the transmission is given in Figure 2 for the different fibre types. The FLAMES fibres have been proven very robust, so that out of more than 1000 fibres, only a few were broken (and replaced) at the end of the whole process.

3.1 UVES fibres

Each of the positioner plates hosts eight 55-metre fibres to guide the light to the UVES spectrograph located on the opposite Nasmyth Platform. From the UVES simultaneous calibration box, one additional 5-metre fibre reaches the UVES-Fibre slit. The fibre centres are separated by 1.7 fibre core, implying that there is some degree of contamination between adjacent fibres; the UVES-Fibre Data Reduction Software (Mulas et al. 2002) has been developed to obtain a complete de-blending of the spectra.

3.2 MEDUSA fibres

Each plate also hosts 132 MEDUSA fibres. The separation between each of the MEDUSA fibres in a sub-slit is $2.26 \times$ the fibre core; this ensures a fibre-to-fibre contamination below 0.5 per cent.

During our tests we have experienced some (about 2%) increased stray light due to reflections from the filter and the (polished) exit slit. We will attempt to reduce this with a stray light mask that reduces the width of the reflecting exit slit viewed from the side of the filter.

3.3 IFU fibres

Each Integral Field Unit (IFU) button is composed of twenty micro-lenses arranged in a rectangular shape. The micro-lenses are $0.52''$ squares. The movable IFUs are a unique characteristic of GIRAFFE and can be placed all over the FLAMES field of view, with the exception of a small fraction of the centre annulus. Each plate hosts fifteen IFUs plus fifteen Sky IFUs. The separation between the fibres' centre is only

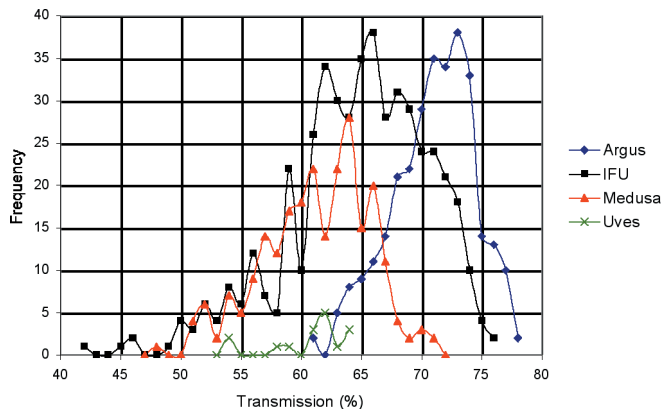


Figure 2: Transmission distribution of all GIRAFFE fibres, as measured in the laboratory.

1.47 times the fibre diameter core, which implies that the contamination between adjacent fibres is about 10 per cent. With the chosen arrangement of the fibres this is acceptable since in normal seeing conditions a higher level of contamination will be present at the fibre entrance level.

3.4 ARGUS fibres

The ARGUS system is a fixed array of 14×22 micro-lenses, similar to the IFUs, located in the middle of Plate 2. ARGUS is also equipped with a lens to switch between a scale of $0.52''/\text{micro-lens}$ to a finer scale of $0.3''/\text{pixel}$. An ADC ensures that the object images at different wavelengths are maintained in the same locations up to a Zenithal distance of 60 degrees. In addition to the object fibres, fifteen ARGUS sky fibres are present on the plate.

4. GIRAFFE

GIRAFFE is a fully dioptic spectrograph. The fibres are arranged in 5 long slits (IFU 1/2, MEDUSA 1/2, ARGUS) at the curved focal plane of the collimator. One of these fibre slits is placed in the working position by a translation stage. The other slits are masked. After leaving the fibres at F/5, the light first passes through one order sorting filter be-

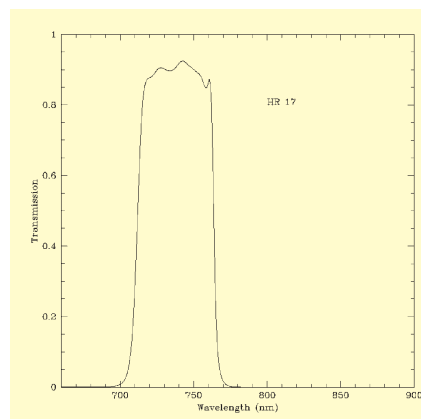


Figure 3: Transmission of order sorting filter HR 17.

Table 2. Summary of GIRAFFE construction characteristics.

Fibre slit height	76.8 mm
Type	Echelle + Order selection Filters
Collimator aperture	F/5
Collimator beam	18 cm
H-R Echelle	204 × 408 mm, 316 lines/mm, 63.4° Blaze
L-R Echelle	156 × 204 mm, 600 lines/mm, 33.7° Blaze
Reimager demagnification ratio	2.5
Effective Camera Focal Length	360 mm
Detector	2048 × 4096, 15 μm EEV CCD
Scale	0.20 arcsec/pixel

fore it is directed to the collimator by a 45-degree mirror. The collimated beam is dispersed by one of the two echelle gratings that are mounted back to back on the grating turret. After passing through the collimator again an intermediate spectrum is produced. Finally, a re-imaging system (“camera”) produces a 2.5 times demagnified image on the 2K × 4K CCD at F/2. A view of GIRAFFE is given in Figure 1. GIRAFFE has been conceived to minimize maintenance and night calibrations; special requirements have been introduced to reduce set-up shifts and to obtain accurate re-positioning, to be able to use wavelength calibrations and flats obtained in the afternoon. To be able to monitor instrument drifts, five fibres are always used to obtain simultaneous calibration spectra.

A summary of the most relevant GIRAFFE characteristics is given in Table 2

GIRAFFE is operated with 30 fixed set-ups; 22 are used to cover the whole spectral range with the high resolution grating, 8 with the low resolution grating. The different GIRAFFE sub-units are described in more detail in the following sections.

4.1 Slit Unit

The slit unit is the most complex GIRAFFE mechanical subsystem, because it needs a very high stability and reproducibility. It has two linear movements: one to exchange the fibre slit, the other one is used for focusing and to press the non-used slits against a baffle that is also used for back-illumi-

nation. The slit unit is equipped with a number of back-illumination LEDs, which are switched on before pick-up and after placing a fibre, to allow the gripper camera to view the fibre output.

4.2 Filters

After the fibre slit, an order-sorting interference filter is placed in the beam. These filters must have excellent transmission and steep bandpass edges and out-of-band blocking, in order to avoid pollution from adjacent spectral orders. One example of filter transmission is given in Figure 3. The transmissions of all filters, averaged over each set-up, are given in Figure 4. This figure shows also the efficiencies of other GIRAFFE components, as well as the overall GIRAFFE efficiency.

4.3 Optics and gratings

The gratings are placed back to back on a turntable. The high-dispersion grating is a MgF₂/Ag coated, 204 × 408 mm 63.6 degree echelle with a large groove density (316 lines/mm). The 370–950 nm spectral range is covered by twenty-two set-ups in grating orders 15 to 6. Silver was selected because of its good VIS/NIR efficiency and the low polarization it produces on this grating. While the efficiency on one edge of the grating is good through the used spectrum, the efficiency degrades below 500 nm as one approaches the other edge. This is due to inhomogeneity in the MgF₂ layer. We are working to find a replacement up to specifications.

The low-resolution grating has 600

lines/mm coated with MgF₂/Al. Its first-order blaze lies at 1.96 μm, so in the range 370–950 nm it works in orders 5–2; eight set-ups are needed to cover the full range. After being dispersed, the light passes again through the collimator, forms a real image at an intermediate focal plane and is finally imaged by an F/2 reimaging camera with 7 elements.

4.4 Spectral Format and Efficiency

In GIRAFFE the spectra are parallel in dispersion along the long side of the detector (readout direction), while the short side is along the slit direction. Spectra are slightly curved due to optical distortion and lateral chromatism, with the central part closer to each other than the edges. As is the case in any long-slit spectrograph, the lines of constant wavelength are arranged on low-curvature arcs. An example of a Th-A spectrum taken with MEDUSA is given in Figure 5.

The resolving power and coverage are both a function of the grating angle and grating order: two or three different grating angles are required to fully cover a grating order, which causes the differences in resolution and spectral coverage between the different set-ups. The higher resolving power of the IFU and ARGUS modes (compared to the MEDUSA mode) is due to the smaller size of the fibres, which projects to ~2.2 pixels instead of ~4.3 pixels of MEDUSA, but the spectral coverage for a given set-up is the same in the MEDUSA, IFU and ARGUS modes.

5. Integration and Commissioning Results

FLAMES components were installed between October 2001 and April 2002 on UT2. The integration sequence has roughly followed the light path: Corrector, UVES fibres, Positioner, GIRAFFE. GIRAFFE had first light in Europe in December 2001 and was re-assembled in Paranal in April 2002 without major inconveniences, after the re-integration of the positioner and in perfect timing with the rest of the project.

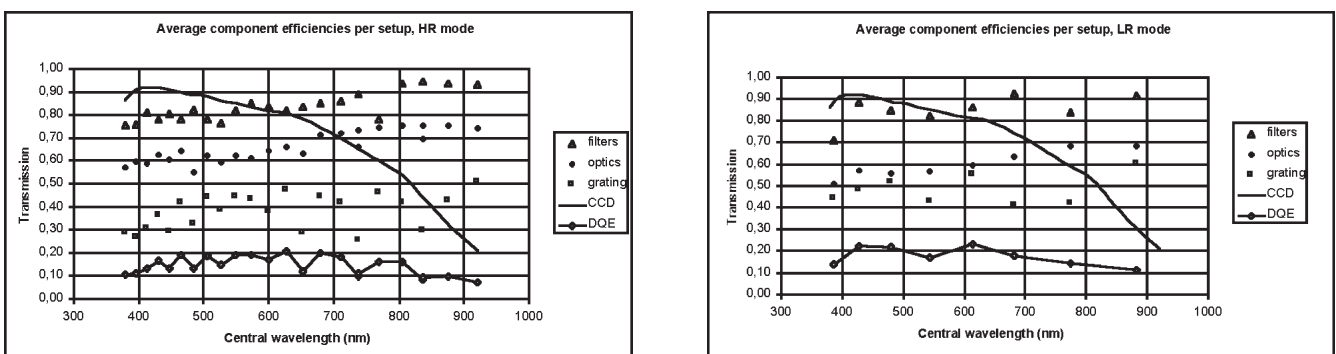


Figure 4: Component efficiencies per set-up and the resulting overall DQE (slit to detected photoelectrons) of GIRAFFE. All reported values are averages; note that grating efficiencies can vary by up to a factor of two within a set-up. The optics efficiency includes vignetting at the grating, this is why the reported LR values are slightly lower than HR values at the same wavelengths.

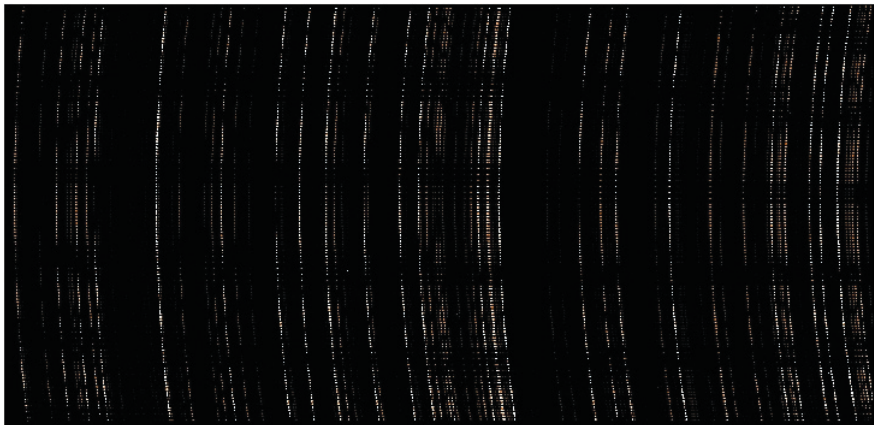


Figure 5: Th-A spectrum taken with a MEDUSA slit. The fibres in the centre of the slit have lines moved towards smaller pixels; e.g. fibres corresponding to the central fibres have slightly redder wavelength coverage than the ones at the CCD edges.

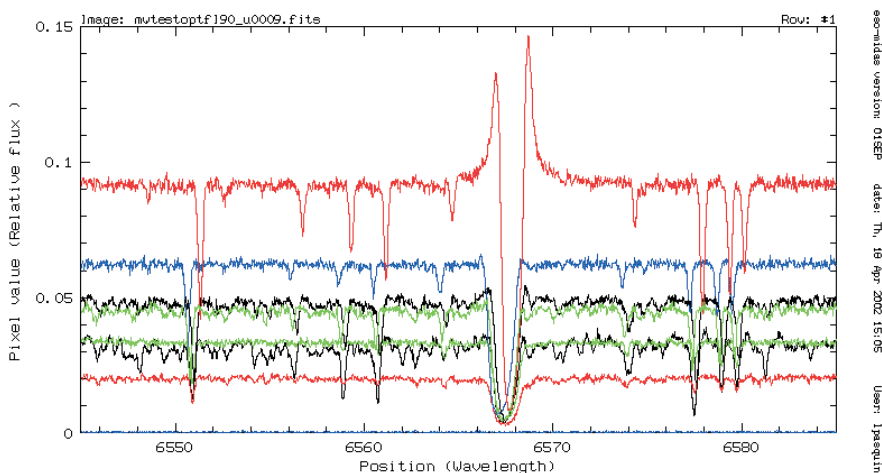


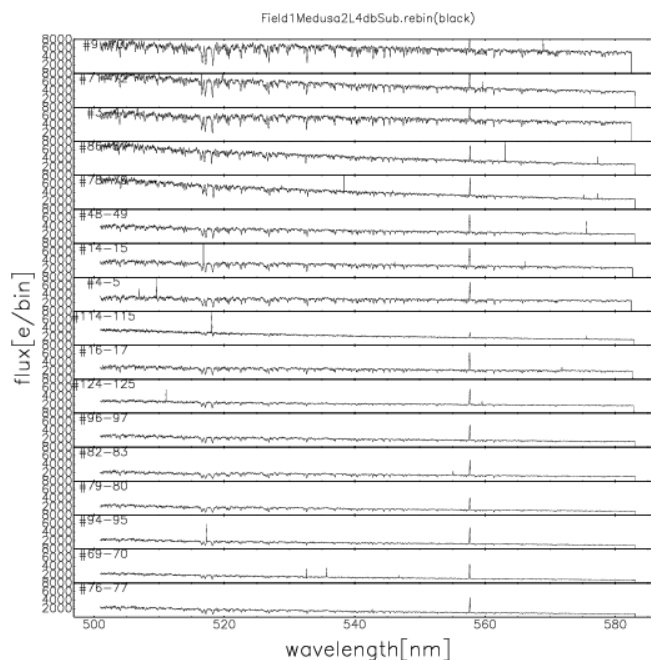
Figure 6: Reduced spectra of 7 giants in the globular cluster Omega Cen taken with UVES-fibre around the H α line.

During the first run at the end of March 2002 the Positioner was integrated and tested and we could gather the first light with UVES-Fibres. Three 10-minute spectra were obtained for 7 stars (one fibre was dedicated to sky) belonging to the Globular cluster Omega Cen. Three of them were previously observed with UVES in long slit mode (Pancino et al. 2002). A small portion of the spectra around the line H α line is shown in Figure 6. The stars had magnitude varying between V = 11.5 and 12.9. After data reduction the equivalent widths of a few hundred lines were compared for the UVES – Fibre and UVES-long slit spectra of the same star, finding an excellent agreement: $EQW(\text{Fibre}) = EQW(\text{Slit}) + A$ with A in the range of 4–6 mÅ, with an rms of 4–7 mÅ, which is largely due to equivalent widths measurement uncertainties.

During this March run, malfunctions were experienced in the positioner robot, due to the lower temperature at the telescope compared to those prevailing during the tests in Australia and in the Assembly Hall in Paranal. We temporarily fixed this using three heaters,

clearly not a suitable permanent solution. This was corrected prior to a second commissioning period in June but new mechanical problems, related to the interface with the telescope rotator-

Figure 7: Reduced spectra of GIRAFFE from the first commissioning run: the stars belong to an astrometric field. The Mg triplet and the 557 nm sky emission line are clearly visible in all spectra.



adapter were encountered. These problems were cured in advance of the August commissioning run. On July 3, first GIRAFFE spectra could be obtained. Two sets of spectra of stars in an astrometric field were acquired, each of 10 minutes. The set-up used was LR4, Low Resolution centred at a wavelength close to the V filter. 66 MEDUSA fibres were positioned (some in sky positions), and the reduced spectra of some of them are shown in Figure 7. The stars have R magnitudes between 13 and 14. In all spectra the Magnesium triplet at 518 nm is clearly visible, as well as the 557 sky emission line.

The stability and repeatability of GIRAFFE on the telescope, measured by taking a ThAr spectrum every 4 hours over a period of 2 weeks is shown in Figures 8 and 9.

The tests have been very satisfactory, showing that the instrument exceeds specifications.

A further commissioning took place in August 2002, enabling us to advance the commissioning tests. Many MEDUSA ‘rasters’ have been performed, to determine the telescope-plate geometry.

In these rasters an astrometric field is observed with MEDUSA and the telescope is offset along a grid around the pointing position. For every star, the distance between its nominal position (the centre of the grid) and the positions of its maximum flux is then computed and used to correct the astrometric model. The results have been so far very encouraging, and the found residuals are shown in Figure 10, with an RMS of 0.15 arcseconds, which is very good when considering that this number includes all sources of errors, e.g., the accuracy of the stellar astrometry. In Figure 11 we show the image of 4

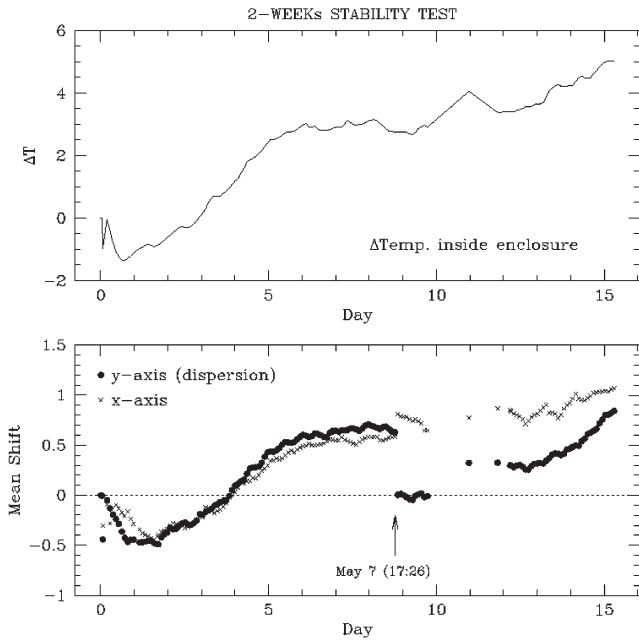
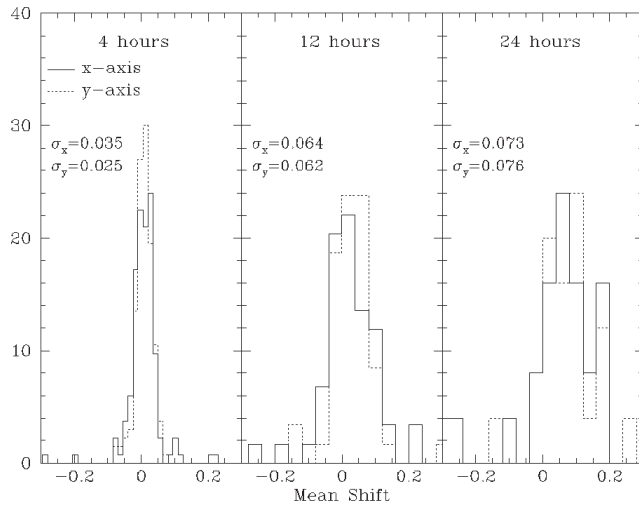


Figure 8: the average position of ThAr lines in a time series that was taken at 4-h intervals over a period of 2 weeks. Shifts are given in pixels relative to the first exposure. These exposures were taken in Medusa HR mode, with configuration changes between exposures. The jump on May 7 cannot be correlated to any known event like an earthquake.



▲ Figure 9: Histogram of relative shifts after 4, 12 and 24 hours, using the time series of Figure 12. In HR mode, 0.1 pixel corresponds to about 300 m/sec. These plots show the intrinsic stability of Giraffe and will be helpful to plan the frequency of calibrations. Note that we expect to obtain higher radial velocity precision by using the simultaneous calibration fibres.

stars from the Tycho catalogue well centred in the FACBs after the telescope field acquisition has been completed.

Two recurrent questions when using fibres are the capability of obtaining good flat field corrections, and to subtract the sky. Sky subtraction tests are under way, while flat field correction capabilities have been evaluated. In Figure 12 is shown the comparison between the measured S/N ratio in a por-

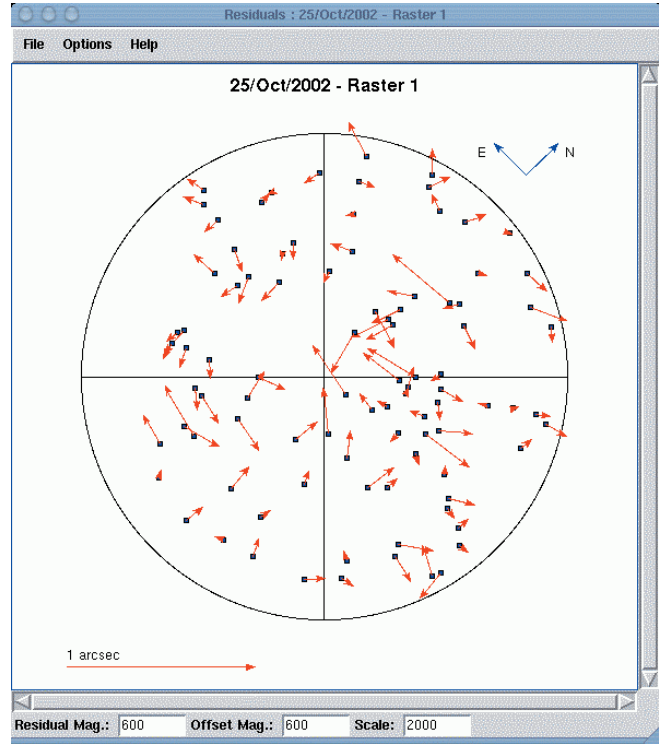


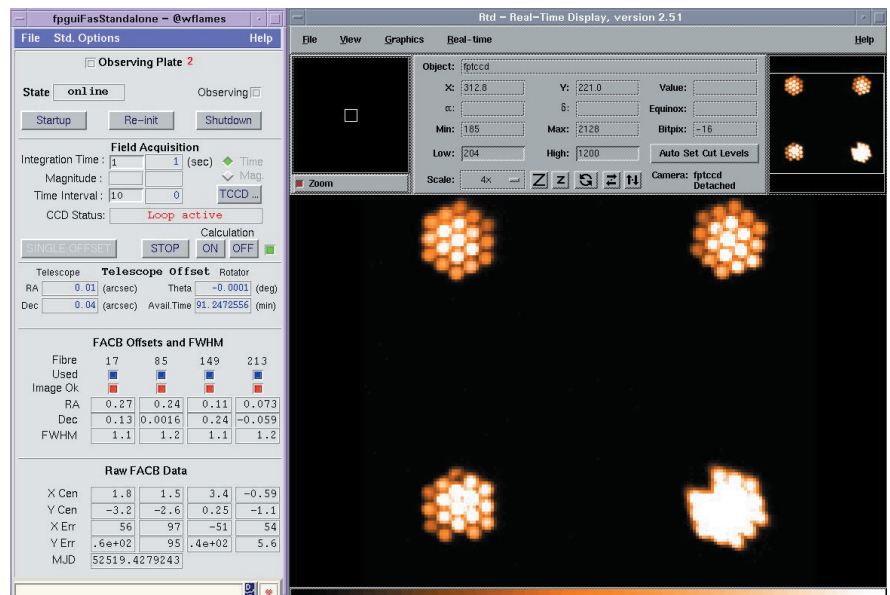
Figure 10: Residuals vectors after the subtraction of the position centroid from the object fibre, after a successful modelling of the plate geometry.

tion of the spectra of several stars in the SMC, acquired with the L8 set-up, a spectral range plagued by strong fringing. We searched for a 'line free' region in the spectra and the S/N ratio has been computed in this small (typically less than 2 nm) spectral region. In ordinate the Poisson noise

based on the number of detected electrons is given. The agreement between the measured and Poisson S/N ratio is quite good.

In the past, several groups have reported problems in obtaining accurate

Figure 11: After a successful acquisition is completed, the four fiducial stars should be well centred in the FACBs, as in the case of these 4 stars from the Tycho Catalogue. The observations were made at airmass 1.8 which shows the good handling of atmospheric effects by the positioner SW. The figure shows the Graphic User Interface at the UT2 Console.



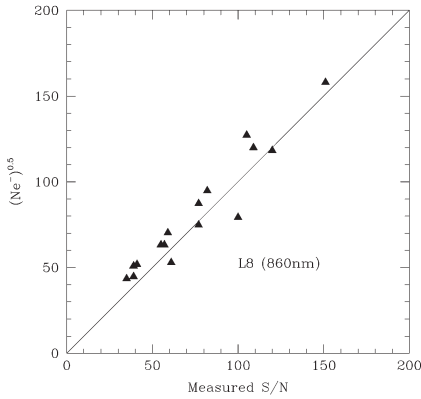


Figure 12: S/N ratio as measured in clean regions of spectra taken in the L8 set-up, compared with the Poisson S/N ratio expected on the number of counts recorded.

flat fielding while using fibres, because, if spatial filters are present in the optical path, variable fringing pattern can be produced in the spectra.

By dividing 3 FF taken with the fibre positioner by the mean of 36 FF taken with the Nasmyth screen, a S/N ratio of 400 was obtained. This S/N ratio obtained was less than what expected by Poisson noise statistics, but it shows that this problem is limited in the FLAMES system to very high S/N observations. Note that the 3 positioner FF represent the standard calibrations that the observer will receive. Similarly we have tested the stability of photometric response of the fibres to torsion and movements: by taking Nasmyth FF and after rotating by a full circle, the photometric stability has been shown to be better than 0.5 %. Finally, in order to perform an accurate sky subtraction, the relative fibre transmission needs to be known accurately. By comparing fibre to fibre transmission by using 3 positioner flats (standard calibrations) with that obtained by the average of the 36 Nasmyth flats, we find that the two measurements agree to better than 3% rms. This is a good result, although not yet within the specifications (2%).

We have performed several comparisons with the ESO Exposure Time Calculator (ETC, www.eso.org/observing/etc). In Figure 13 we show the results of the comparison between the flux observed vs. the flux predicted as obtained by observing an astrometric field (the astrometric solution in use in this test had a residual rms of 0.24 arcseconds). The Figure shows the number of counts recorded vs. R magnitude, while the curve shows the prediction by the ETC in the L8 set-up for a G0 star and the parameters (seeing, exposure time) appropriate for the observation. As shown in the bottom panel, at any given magnitude, the number of collected e^- per object is represented by a relatively broad distribution. This is due to several factors, such as the variation in the fibre transmission,

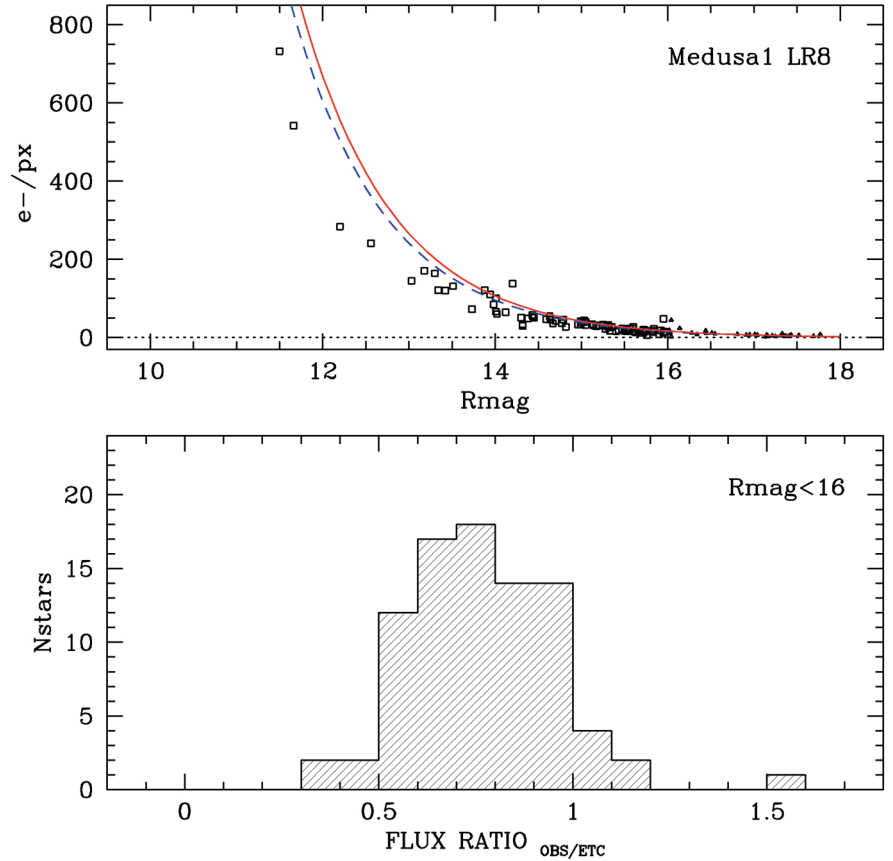


Figure 13: Comparison between observed flux and predicted ETC flux for an astrometric field with the L8 set-up. The histogram shows the ratio measured/expected. The ETC calculations are based on a G0 spectral type.

the poor astrometry of some targets, and the difference in spectral type among the stars in the catalogue. On

the other hand, it is important that the potential users become familiar with the concept that for FLAMES the S/N

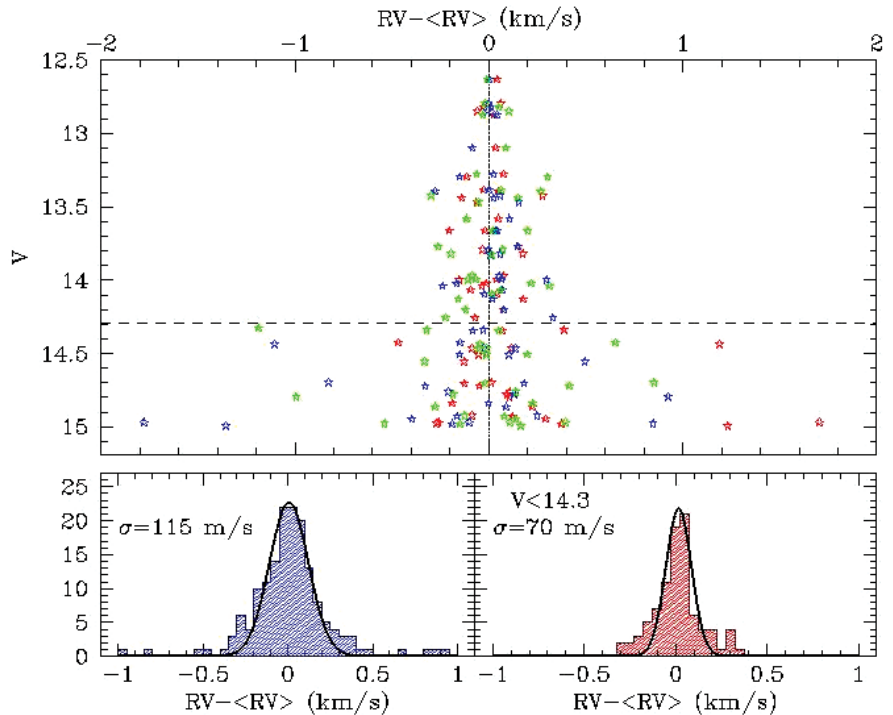


Figure 14: Distribution of the difference between RV single measurements and RV mean for 3 exposures taken in 1 night of 60 stars of the globular cluster NGC 6809, shown vs. the stellar magnitude. Points from the different observations are shown with different colours. In the lower panel, the left distribution refers to all the measurements, irrespective of stellar magnitude. The right distribution includes only the bright ($V < 14.3$) subsample.

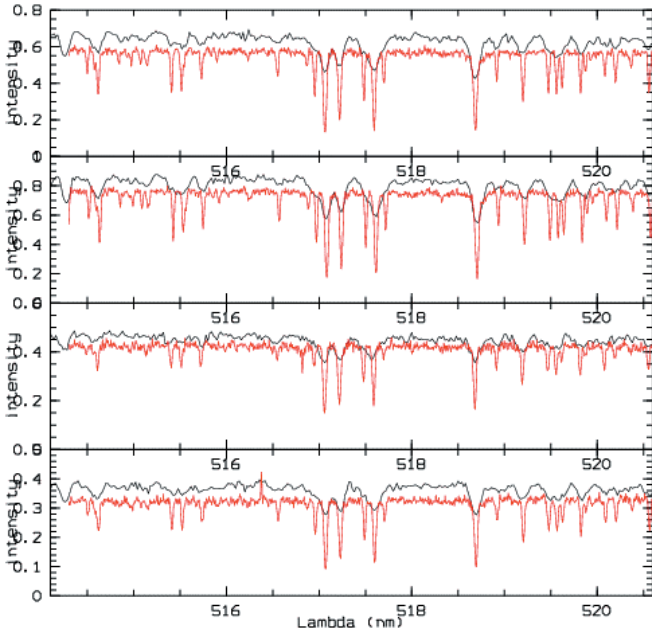


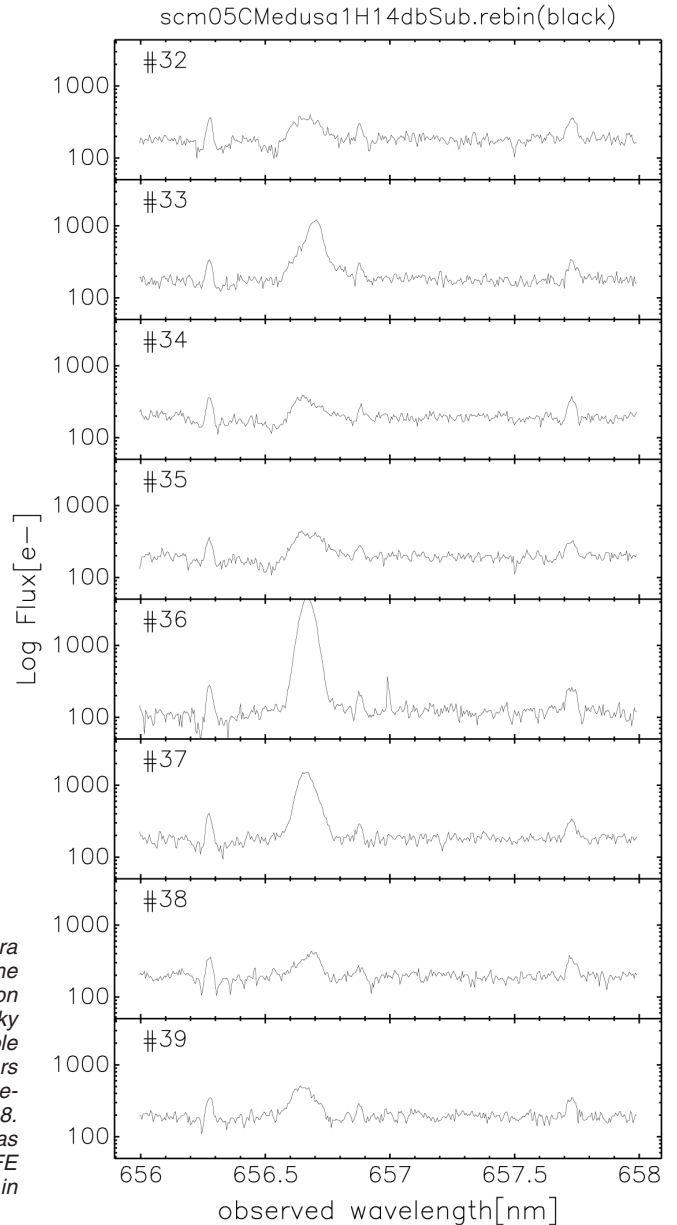
Figure 15: GIRAFFE Low (L4, black lines) and High (H9, red lines) resolution spectra of 4 giants belonging to the Globular Cluster NGC 6809

ratio predicted by the ETC will always have to be intended in a statistical sense.

A number of tests have been performed to characterize the GIRAFFE radial velocity (RV) capabilities, observing the same objects several time in a night, as well as in different nights. Three not consecutive observations of 15 minutes in the GIRAFFE H9 set-up were obtained in the same night for 96 giants at the centre of the Globular Cluster NGC6809. The stars were selected between magnitude 13 and 15 and the observations made with a non optimal astrometric model. Out of the full sample (96 stars) we analysed only 60 objects giving a well determined cross correlation peak.

Out of these 11 were further excluded because their RV were either discordant from the bulk of the cluster, or because they showed a very large RV difference in the 3 measurements (4 stars). Based on the 3 measurements of the 49 stars left, the cluster velocity is found at 178.81 km/sec (note that this RV is computed with respect to our digital mask, no attempt has been made to transform it to an absolute RV), with a dispersion of 4.057 km/sec. In Figure 14 the distribution of the differences of all the measurements with respect to their mean values are shown. This figure clearly shows how the Radial Velocity accuracy degrades with increasing stellar magnitude (and therefore decreasing fluxes); the three observation points are indicated with different colours. When taking all the points, irrespective of the stellar magnitudes, the σ of the distribution is of 113 m/sec, while if only the bright end is considered, $V < 14.3$, the σ decreases

Figure 16: $H\alpha$ Spectra of 8 red giants in the SMC, no sky subtraction was performed, and sky $H\alpha$ in emission is visible at 6562.8 nm. The stars have V magnitude between 18.5 and 18.8. The exposure time was 1 hour, in the GIRAFFE H14 setup. Fluxes are in Log scale.



to 70 m/sec. These numbers are indicative of the accuracy reached in the time scale of a few hours and normal operations. Royer et al. (2002) have reached a short-term accuracy of 13 m/sec with GIRAFFE, in a more stable environment, using much higher S/N observations of the solar light in the Garching Integration Hall.

We had the opportunity to observe the same NGC 6809 field also with GIRAFFE in low resolution mode (L4) and in Figure 15 a fraction of the spectra of the same stars (4 giants belonging to the cluster) observed in L4 and H9 at a resolving power of $R = 6000$ and $R = 26,000$ respectively are shown. The integration time in the HR9 was 2 times longer than in the LR4 .

We are acquiring spectra to verify the behaviour of the instruments at the faint end of the magnitude range; Figure 16 shows a collection of $H\alpha$ spectra taken with the high resolution grating of GIRAFFE (set-up H14) of giants on the

Red Giant Branch of the Small Magellanic Cloud; the magnitudes vary between $V = 18.5$ and 18.8, the exposure time was of 1 hour with an 0.9 arc-second seeing.

Spectra were acquired for a field of galaxies with the Giraffe IFUs, and their reduction is not yet completed. We aim at making a release of FLAMES commissioning data in the first quarter of 2003.

6. Acknowledgements

The development of FLAMES, which was recommended by the ESO STC in 1998, presented some remarkable aspects, showing the feasibility of a complex, multi-institute facility in a short time. This could not have been possible without appropriate structures but mostly without the dedicated work of a very large number of people, whose names do not appear in the author list. We thank all the persons at ESO

(Garching and Paranal) and at the different institutions who have contributed to the realization of this ambitious project: J. Alonso, P. Ballester, J.-L. Beckers, P. Biereichel, B. Buzzoni, C. Cavadore, N. Cretton, C. Cumani, B. Delabre, A.V. Kesteren, H. Kotzlowski, J.-L. Lizon, R.S. Moreau, W. Nees, R. Palsa, E. Pozna, (ESO), P. Barriga, R. Castillo, J. Spyromilio AND MANY OTHERS at Paranal, C. Evans, R. Haynes, U. Klauser, B. Hingley, D. Mayfield, S. Miziarski, R. Muller, W. Saunders, G. Schafer, K. Shortridge, (AAO), L. Jocou and the fibre team, T. Melse and the mechanics workshop team, S. Baratchart, L. Chemin, H. Flores, D. Horville, J.M., Huet, F. Rigaud, F. Sayède (GEPI, OPM), F.R. Ferraro,

P. Molaro, R. Pallavicini, I. Porceddu (ITAL Consortium).

References

Avila, G. Guinouard, I., Jocou, L., Guillon, F., Balsamo, F. 2002, in *Instrument Design and Performance for Optical/Infrared Ground-Based Telescopes* Proc. SPIE **4841** (in press).
 Blecha, A., North, P., Cayatte, V., Royer, F., Simond, G. 2000, Proc. SPIE Vol. **4008**, p. 467.
 D'Odorico, S. et al. 2000, Proc. SPIE Vol. **4005**, p. 121.
 Gillingham, P., Miziarski, S., Klauser, U. 2000, Proc. SPIE Vol. **4008**, p. 914.
 Gillingham P.R., Popovic D., Waller L.G., Farrell T.J. 2002, in *Instrument Design and Performance for Optical/Infrared Ground-Based Telescopes*, Proc. SPIE **4841** (in press).

Hammer, F., Hill, V., Cayatte, V. 1999, *Journal des Astronomes Français*, **60**, 19.
 Jocou, I. et al. 2000, Proc. SPIE Vol. **4008**, p. 475.
 Mulas, G., Modigliani, A., Porceddu, I., Damiani, F. 2002, in *Instrument Design and Performances for Optical/Infrared Ground-Based Telescopes*, Proc. SPIE **4841** (in press).
 Pancino, E. et al. 2002: *ApJ* **568**, L101.
 Pasquini, L. et al. 2000, Proc. SPIE Vol. **4008**, p. 129.
 Pasquini, L. et al. 2002, in *Instrument Design and Performances for Optical/Infrared Ground-Based Telescopes*, Proc. SPIE **4841** (in press).
 Royer, F., Blecha, A., North, P., Simond, G., Baratchart, S., Cayatte, V., Chemin, L., Palsa, R. 2002, in *Astronomical Data Analysis II*, Proc SPIE **4847** (in press).

HARPS: ESO's Coming Planet Searcher

Chasing Exoplanets with the La Silla 3.6-m Telescope

F. PEPE¹, M. MAYOR¹, G. RUPPRECHT³

email: Francesco.Pepe@obs.unige.ch; Michel.Mayor@obs.unige.ch; grupprec@eso.org

with the collaboration of the HARPS Team: G. AVILA³, P. BALLESTER³, J.-L. BECKERS³, W. BENZ⁵, J.-L. BERTAUX⁶, F. BOUCHY¹, B. BUZZONI³, C. CAVADORE³, S. DEIRIES³, H. DEKKER³, B. DELABRE³, S. D'ODORICO³, W. ECKERT², J. FISCHER⁵, M. FLEURY¹, M. GEORGE¹, A. GILLIOTTE², D. GOJAK^{2,3}, J.-C. GUZMAN², F. KOCH³, D. KOHLER⁴, H. KOTZLOWSKI, D. LACROIX³, J. LE MERRER¹⁰, J.-L. LIZON³, G. LO CURTO², A. LONGINOTTI³, D. MEGEVAND¹, L. PASQUINI³, P. PETITPAS⁴, M. PICHARD¹, D. QUELOZ¹, J. REYES³, P. RICHAUD⁴, J.-P. SIVAN⁴, D. SOSNOWSKA¹, R. SOTO², S. UDRY¹, E. URETA², A. VAN KESTEREN³, L. WEBER¹, U. WEILENMANN², A. WICENEC³, G. WIELAND³ and advice by the Instrument Science Team: J. CHRISTENSEN-DALSGAARD⁷, D. DRAVINS⁸, A. HATZES⁹, M. KÜRSTER⁹, F. PARESCE³, A. PENNY¹¹

¹Observatoire de Genève; ²ESO, La Silla; ³ESO, Garching; ⁴Observatoire de Haute Provence; ⁵Physikalisches Institut, Bern; ⁶Service d'Aéronomie du CNRS; ⁷Aarhus University, ⁸Lund Observatory, ⁹Tautenburger Landessternwarte; ¹⁰Laboratoire d'Astrophysique de Marseille; ¹¹Rutherford Appleton Laboratory

Introduction

An extensive review of past, present and future research on extrasolar planets is given in the article "Extrasolar Planets" by N. Santos et al. in the present issue of *The Messenger*. Here we want to mention only that the search for extrasolar planets and the interpretation of the scientific results have evolved in recent years into one of the most exciting and dynamic research topics in modern astronomy.

As a consequence, ESO decided to have a dedicated spectrograph built to be installed at the La Silla 3.6-m telescope. An Announcement of Opportunity was issued in 1998 and a consortium chosen for the realization of the project which consists of Observatoire de Haute Provence (F), Physikalisches

Institut der Universität Bern (CH) and Service d'Aéronomie du CNRS (F) under the leadership of the Observatoire de Genève (CH) where the Principal Investigator and the Project Office are located. Further contributions come from ESO-La Silla and ESO Headquarters (Garching). The agreement was finally signed in August 2000.

According to this agreement, the HARPS Consortium bears the cost for the spectrograph and all its components whereas ESO provides the Cassegrain Fibre Adapter, the fibre link, the dedicated HARPS room in the telescope building and the complete detector system. In return, the HARPS Consortium will be granted 100 HARPS observing nights per year for a period of 5 years after successful Provisional Acceptance in Chile. HARPS will of

course also be offered to the astronomical community like any other ESO instrument.

The Radial Velocity Method: Error Sources

A description of the radial velocity method for the detection of extrasolar planets in general and of the CORALIE spectrograph installed at the Swiss Leonhard Euler Telescope at La Silla in particular was given by Queloz & Mayor (2001); it describes the technique applied also with HARPS and the spectrograph which is its direct ancestor. An instrument like CORALIE achieves an accuracy in radial velocity determination of about 3 m/s, and with this accuracy planets down to a minimum mass of about one third the mass of Saturn

have been discovered. For HARPS an accuracy of 1 m/s RMS is specified. To achieve this goal, we have to analyse the limitations that are encountered by a spectrograph in order to overcome them.

Photon noise

The contribution of photon noise to the radial-velocity (RV) measurement error can be expressed, according to Hatzes & Cochran (1992), by the generic formula

$$\sigma_{RV} \propto S^{-0.5} \cdot \lambda \lambda^{-0.5} \cdot R^{-1.5}. \quad (1)$$

The measurement precision is proportional to the square root of the flux S and the wavelength range $\lambda\lambda$ of the spectrograph. It should be mentioned that in practice it is not the wavelength range that determines the precision, but rather the number of spectral lines and their depth, since the information on RV is contained in the stellar absorption lines. Nevertheless, the formula tells us that we must maximize the amount of light entering the spectrograph. This goal can be reached by increasing the spectral range, maximizing the optical efficiency of the instrument, and, of course, by using the largest telescope available.

The UVES-like optical design as well as the choice of the optical components make HARPS an efficient spectrograph. However, this is not sufficient to get a precise RV spectrograph, since,

again according to formula (1), higher precision is obtained when the spectral resolution R is increased. Unfortunately, telescope diameter D , spectral resolution R , and fibre diameter ϕ (projected on the sky) are not independent, but linked by the formula

$$R_{\max} = \frac{2 \cdot \tan \beta \cdot h}{\phi \cdot D}, \quad (2)$$

where h is the diameter of the collimated beam on the echelle grating and $\tan \beta$ is the tangent of the echelle grating angle. In other words, if we want to increase the spectral resolution we have to increase the collimated beam diameter, or restrict the field of view ϕ and consequently decrease the slit efficiency.

A trade-off therefore had to be made between spectrograph size, spectral resolution, and slit efficiency. Our solution consists in building an instrument using the largest monolithic echelle grating available to date (a 837×208 mm grating developed for UVES) and to balance spectral resolution against slit efficiency. The compromise led to a spectral resolution of $R = 93,000$ which in most cases is sufficient to resolve the stellar absorption lines. Going beyond would not reduce the photon noise but only increase slit losses. At the selected resolution the fibre covers 1 arcsec on the sky. The resulting slit losses are about 50% on average. It should be recalled however that the goal was to optimize the instrument for RV precision, which is proportional to $R^{1.5}$ but only

proportional to the square root of S . Thus, a fibre twice as large would collect twice the amount of light, but would also reduce the spectral resolution by a factor of 2. The resulting RV precision would be reduced by a factor 2.

Instrumental errors

If we want to detect RV variations of 1 ms^{-1} we must be able to detect changes in the stellar absorption line position which are

smaller than 1/1000 of a CCD pixel. A temperature variation by 1°C or the change of atmospheric pressure by 1 mbar would already produce effects of the order of 100 ms^{-1} ! We have therefore decided to act on different fronts:

- Stabilize the spectrograph environment. HARPS is installed in vacuum to remove effects caused by varying ambient pressure. In addition, the temperature of the whole instrument is actively controlled.

- Simplify the opto-mechanical design, avoid any moving or movable components, design a robust spectrograph.

- Use a spectral reference to track residual instrumental drifts.

Since it is impossible to avoid drifts of 10 nm on the instrument, the spectral reference is mandatory. On HARPS we will have the possibility of using either a ThAr spectral lamp in simultaneous reference mode, or an iodine absorption cell in self-calibrating mode. Both techniques attain to date similar performance at the level of about 3 ms^{-1} . The main mode of HARPS will be the ThAr simultaneous reference, since it allows to cover a spectral range 3 times larger than with the iodine cell, which in addition absorbs about 50% of the light. The efficiency is thus 6 times higher using the ThAr simultaneous reference mode.

Often, stability of the instrumental profile (IP) is associated with the RV precision of an instrument. In practice, both spectral reference methods allow to avoid errors produced by internal IP variations. It is however true that the ThAr simultaneous reference technique does not account for variations of the slit illumination. This technique works therefore only if combined with a fibre feed and with an image scrambler, whose sole function is to "scramble" the light entering the fibre at the telescope. The goal is to avoid a change in spectrograph illumination when the position of the star on the fibre entrance changes. We estimate that the residual effects are of the order of 0.25 ms^{-1} and can thus be neglected. It is worth mentioning that good telescope guiding and high spectral resolution reduce these kinds of error sources even further.

External errors

We should not forget that RV measurements may be influenced by error sources related neither to the instrument nor to the telescope. Any of those can produce RV errors of the order of several ms^{-1} if not correctly accounted for. Without going into detail, we mention the following:

- Atmospheric absorption lines which vary in relative position and intensity compared to the stellar spectrum
- Atmospheric dispersion



Figure 1: The finished HARPS Cassegrain Fibre Adapter ready to be shipped from La Silla to Geneva for system tests.

- Sunlight reflected by the moon and superimposed on the stellar spectrum
- Stellar companions close to the target star may contaminate its spectrum, depending on seeing conditions
- Stellar jitter, intrinsic variability of the star

HARPS: The Implementation

The La Silla 3.6-m telescope

As already mentioned, ESO decided early on to install HARPS at the La Silla 3.6-m telescope. This telescope recently underwent a major overhaul and was retrofitted with a new control system based on the VLT software and data flow. These improvements, together with the obvious fact that a 4-m-class telescope is ideal in providing the large number of photons required for high signal-to-noise ratio spectra, make this telescope a superb complement to our new instrument.

The HARPS Cassegrain Fibre Adapter (HCFA)

To connect the fibre link (see below) to the telescope, the La Silla Engineering Department designed and manufactured a new fibre adapter for the Cassegrain focus. The HCFA fulfils a number of functions: It allows the remotely controlled exchange of the fibres for HARPS and the CES and provides both fibre feeds with an atmospheric dispersion compensator (ADC) and the possibility to use the telescope's guide camera for guiding on the respective fibre entrance. For HARPS, there is also a neutral density filter and a feed for the calibration fibre which carries the light from a separate calibration unit (see below). This is a crucial part of the calibration concept of HARPS (described in Queloz & Mayor 2001). As a unique feature, HARPS will offer the observer two options for precise wavelength calibration: the default Thorium-Argon method and the use of the Iodine absorption cell. This Iodine cell is also mounted in the HCFA and can be moved in and out of the telescope beam under remote control. Figure 1 shows the finished HCFA.

Calibration unit

The HARPS calibration unit provides the instrument with light for wavelength and flatfield calibration. For this purpose it contains a set of hollow-cathode Thorium-Argon and halogen lamps which can be remotely switched on and off. A motorized exchange mechanism allows to position the calibration fibre in front of any desired lamp. The calibration fibre pair connects the calibration unit, which is located next to the air-conditioned HARPS enclosure in the coudé west room, with the fibre adapter at the Cassegrain focus.



Figure 2: The closed HARPS vacuum vessel in the Geneva integration laboratory.

Fibre links, image scramblers

Strictly speaking HARPS is a distributed system, and one of the most important components connecting its various parts is the observation fibre link. Its purpose is to feed the spectrograph down in the telescope building with (a) the star light collected at the Cassegrain focus and with (b) either the ThAr spectrum for the simultaneous calibration or with light from the night sky for better sky subtraction. For HARPS we chose two 70 μ m fibres (type FVP made by Polymicro), corresponding to 1 arc-second on the sky, and put it in a "shower tube" made of sturdy steel mesh for mechanical protection. The total length of the fibres from the Cassegrain focus to the spectrograph entrance (by way of the declination bearing, telescope fork, northern telescope mount bearing and into the coudé west room) is 38 metres.

To minimize focal ratio degradation, the light is coupled into the object and reference fibres by means of two micro lens doublets per fibre. By projecting the image on the fibre input end, the telescope pupil is at infinity. This design combines an excellent image quality with easy, uncritical alignment.

A double image scrambler is located at the entrance of the object/reference fibres into the vacuum vessel of the spectrograph. In combination with the fibre feed, it serves to stabilize the spectrograph illumination: the object may move at the fibre entrance due to guiding errors or seeing, but the intensity distribution at the fibre exit, i.e. the spectrograph entrance, will not change. In addition the scrambler serves as the feed-through for the fibres into the vacuum and it also

houses, on the atmosphere side, the exposure shutter.

The light is finally led to the spectrograph entrance inside the vacuum vessel by means of two short (2-metre) pieces of fibre. The coupling to the spectrograph is again achieved by a pair of doublet microlenses per fibre.

The second fibre link leads, as mentioned before, from the calibration unit in the coudé west room up to the Cassegrain focus. It is therefore also about 38 metres long, consisting of a pair of 300 μ m core diameter fibres (type FVP made by Polymicro).

Vacuum vessel with spectrograph

The vacuum vessel has the purpose of protecting the spectrograph proper from temperature variations and from the effects of refractive index variations of air. This vessel has a volume of approximately 2 m³. It is evacuated by means of a turbo molecular pump before the start of operations; we expect to repeat the regeneration of the vacuum about once or twice per month.

Since the long-term stability of the spectrograph is of paramount importance for the success of the exoplanet search, the vacuum should be broken as seldom as possible. For this reason there are no moving functions inside the vacuum except the focussing mechanism of the camera. This will however be adjusted and locked before the vessel is finally closed. Figure 2 shows the closed vessel in the Geneva integration hall.

The spectrograph itself is a cross dispersed echelle spectrograph, very similar to UVES at the VLT. It is a white pupil design with the grism cross disperser placed in the white pupil. The



Figure 3: The open HARPS vacuum vessel. The back side of the echelle grating is visible on top of the optical bench as well as the rail system used for moving the large parts of the vessel.

echelle grating, a copy of the UVES mosaic, is operated in quasi-Littrow condition. An $f/2.1$ parabolic mirror serves as collimator and is used in triple pass. A dioptric camera images the cross-dispersed spectra (one each from the object and reference fibres) side by side onto a mosaic of two $2k \times 4k$ EEV CCDs. 68 orders cover a spectral range from 380–690 nm. At a spectral resolution RS of 90,000, determined by the fibre diameter, a spectral resolution element is sampled by 4 pixels. All optical components are mounted on a stainless steel optical bench. The optical parameters are listed in Table 1.

Procurement of the optics turned out to be the most demanding of all. The first company charged with the production of the cross disperser grism failed to deliver and a new contract had to be negotiated with another supplier. The collimator mirror also failed to materialize, both within schedule and with acceptable quality. The mirror which was finally delivered had to be re-polished by another company to meet our requirements.

In order to improve the observing efficiency by always applying the correct exposure time (according to the selected signal-to-noise ratio SNR) we fitted an exposure meter, again following the example of UVES. Two photon counters are used to separately measure the light coming from the object and ref-

erence fibres which is reflected off the gap on the echelle between the two gratings comprising the mosaic.

Detector system

HARPS employs a mosaic of two EEV type 44-82 CCDs (nicknamed *Jasmin* and *Linda*). The spectral format

is thus 4096^2 pixels ($15 \mu\text{m}$ square) of which a field of $62.7 \times 61.4 \text{ mm}$ is actually used at a sampling of 4 pixels per spectral element. The performance of the chips is summarized in Table 2.

As HARPS is a stationary instrument, its detectors are cooled by a continuous-flow cryostat (CFC) of the current ESO standard design. A special feature of the HARPS cryostat is however the fact that the detector head (visible on the left in Fig. 4) is mounted to the spectrograph bench inside the vacuum vessel, with the actual CFC outside. Both are connected by a stainless steel bellows which protects the detector high vacuum (10^{-6} mbar) from the mere “emptiness” (10^{-2} mbar) of the spectrograph vessel. The detector head window also serves as field lens of the camera optics.

As a consequence of this configuration, all cables connecting the detector head to the FIERA controller have to pass through vacuum feed troughs.

Thermal enclosure

In order to keep the spectrograph temperature as constant as possible it was decided to put the vacuum vessel in an additional thermal enclosure. This is a well insulated room on the coude floor of the 3.6-m telescope building which is itself already temperature stabilized. Based on preliminary measurements we expect to keep the temperature variations of the spectrograph

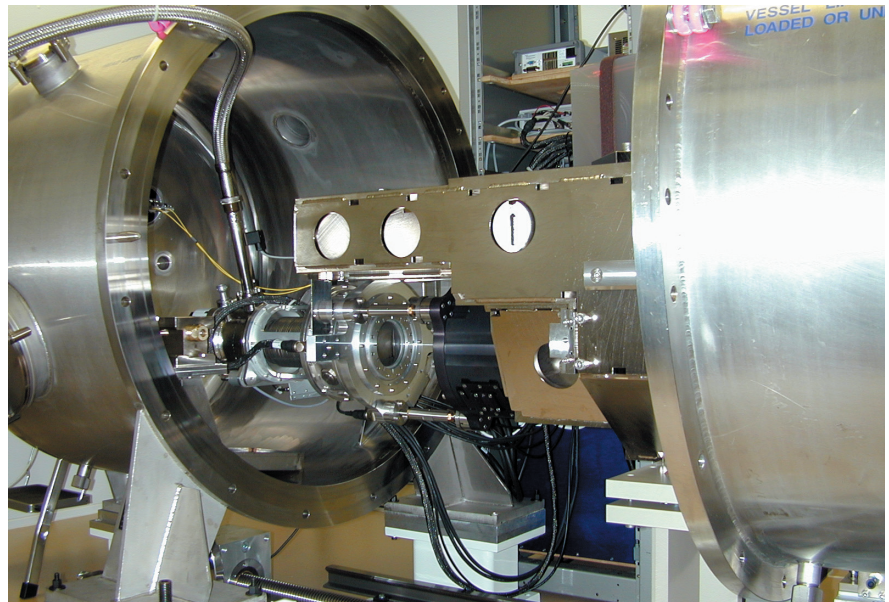


Figure 4: The figure shows the CCD detector system mounted below the spectrograph bench. Visible are also the field lens and a holder which still connects the head and the CFC. In the final configuration the CFC will be mounted outside the vacuum vessel.

Table 1 Summary of the HARPS spectrograph optics.

System	2 fibres (1" dia.), spectral range 380–690 nm, collimated beam diameter 208 mm
Echelle	R4, 31.6 gr/mm, blaze angle 75° , mosaic 2×1 on Zerodur monolith $840 \times 214 \times 125 \text{ mm}$, efficiency $> 65\%$ in the visible
Cross disperser	FK5 grism, 257.17 gr/mm blazed at 480 nm, $240 \times 230 \times 50 \text{ mm}$, $T = 73\%$ (av)
Collimator	Zerodur, $f = 1560 \text{ mm}$, used diameter 730 mm, triple pass
Camera	All dioptric, 6 elements in 6 groups, $f = 728 \text{ mm}$, $f/3.3$, $T > 85\%$

Table 2: Properties of the HARPS detector system.

DQE	82–85% peak, 70% minimum
Read-out noise	~ 3e ⁻ at 50 kpx/sec (2 ports/chip)
CTE	0.999999 (horizontal+vertical) at 166 kpx/sec
Cosmetics	Science grade (grade 1)
Read-out modes	50 kpx/sec and 625 kpx/sec, one or two ports per chip

bench inside the vacuum vessel (the only place that really matters) below 0.1K, ideally at 0.01K!

Performance

The instrument

Recently we have completed the integration of HARPS at the Geneva Observatory. Tests of the complete spectrograph have been carried out, and the spectroscopic characteristics verified. The spectral format recorded corresponds well to the calculated values. All the orders – except order 115 which falls between the two CCDs – could be localized and extracted using a tungsten flat-field lamp (Fig. 5), while the wavelength calibration was done using the ThAr spectral lamp. In Figure 6 we show a small segment of the extracted and wavelength-calibrated ThAr spectrum. About 3500 spectral lines covering a large intensity range could be detected and identified. From the spectrum shown, which was recorded during an exposure of 7 s, we estimate that the internal photon noise on the radial velocity is only 10 cm s⁻¹. This represents a large gain compared to CORALIE, in part due to the higher optical efficiency of the spectrograph, but mainly due to the higher spectral resolution. Indeed, the Gaussian fit of a single ThAr line indicates a spectral resolution of $R = 98,000$, which is about 5% higher than expected.

As mentioned above, HARPS is equipped with an iodine cell for the self-calibration mode. We have recorded a spectrum of our iodine cell by sending the white light of the tungsten lamp through it. The extracted and wavelength-calibrated spectrum is shown in Figure 7. The intensity of the continuum varies strongly across the echelle order because of the blaze re-

sponse of the grating. The angle of the echelle grating was not centred correctly at that time thus delivering an asymmetric blaze response. This was corrected later by tilting the echelle grating physically by 0.25°.

The total efficiency of the instrument has not yet been determined. This measurement will be done during Commissioning using a reference star. Nevertheless, the optical components were measured individually. Table 3 summarizes the expected optical efficiency of HARPS derived from these measurements. From this, and based on data recorded with the CORALIE instrument at La Silla (see Queloz &

Mayor (2001)), we have estimated the RV precision of HARPS as a function of stellar magnitude (see their Fig. 14). The total RV efficiency of HARPS is thus about 75 times higher than that of CORALIE. This extraordinary RV efficiency will offer exciting new possibilities in other research fields, for example in asteroseismology.

Operations

Often neglected, observational efficiency also plays an important role. In fact, searching for exoplanets requires that many measurements per object are carried out. Telescope time must therefore be used efficiently.

From the beginning, strong emphasis was put on efficient operations scenarios to optimize the yield from an observing run. Most important is certainly the adoption of the VLT Data Flow System, from the preparation of Observation Blocks with P2PP through the use of BOB at the telescope to the imple-

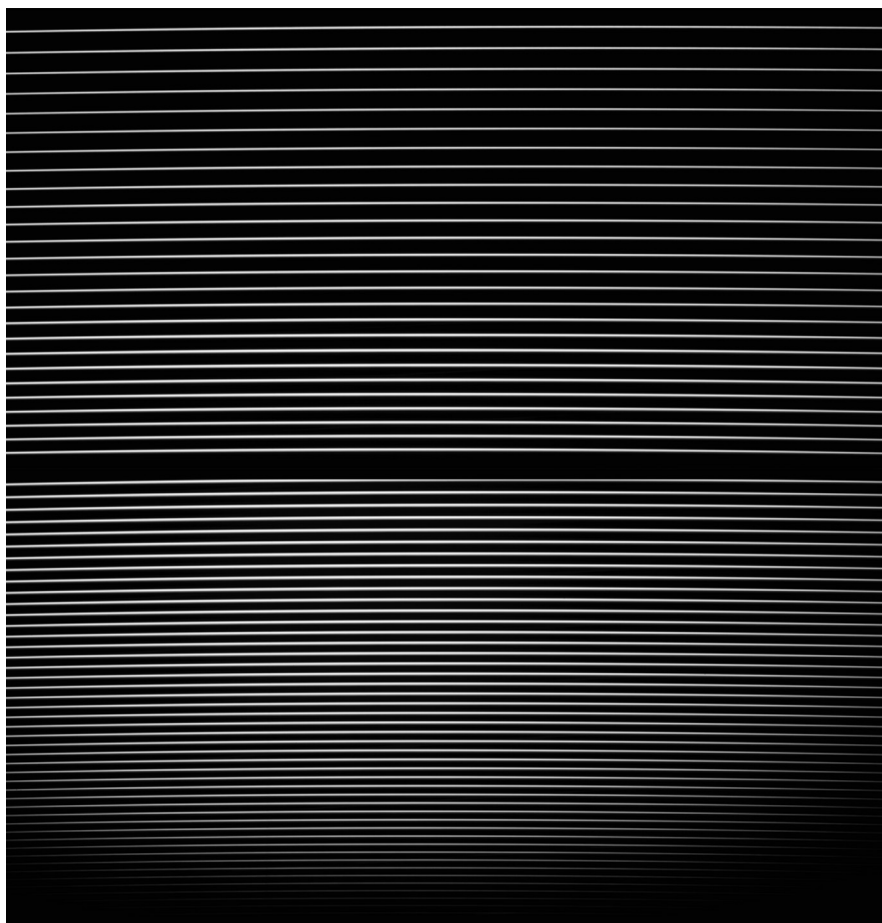


Figure 5: Spectral flat-field of HARPS using the tungsten lamp. Only one fibre (object) is illuminated for the localization of the orders.

Table 3: Optical efficiency of HARPS.

Wavelength	380 nm	400 nm	450 nm	500 nm	550 nm	600 nm	650 nm	690 nm
Tel. + atm.	44%	47%	54%	57%	59%	59%	61%	63%
“Slit”	46%	47%	48%	49%	50%	50%	51%	52%
Instrument	8%	11%	15%	15%	17%	17%	15%	12%
CCD	65%	78%	85%	85%	81%	79%	76%	72%
Total	1.0%	1.9%	3.2%	3.5%	4.0%	3.9%	3.4%	2.9%

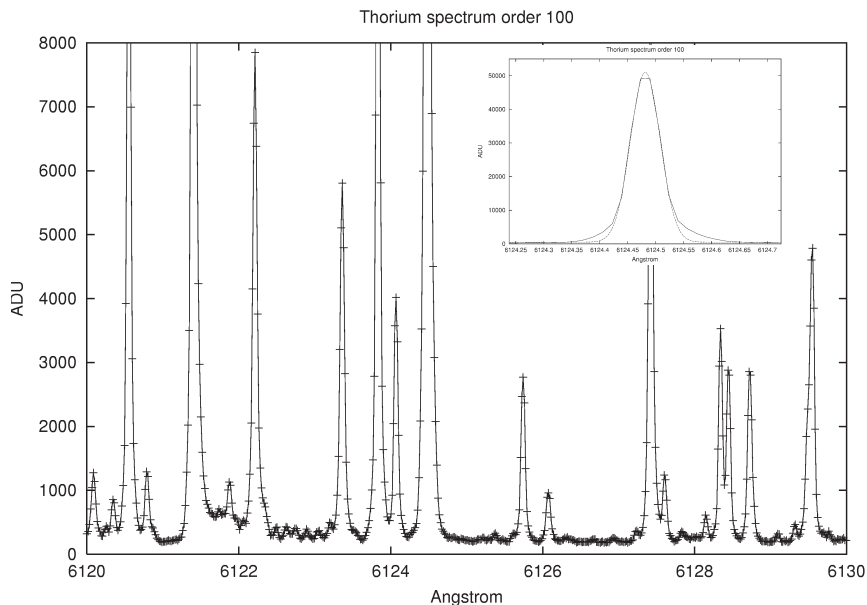


Figure 6: Segment of the extracted ThAr spectrum. In the small window one single line is shown. The FWHM of the superimposed Gaussian (dashed line) corresponds to a spectral resolution of $R = 98,000$.

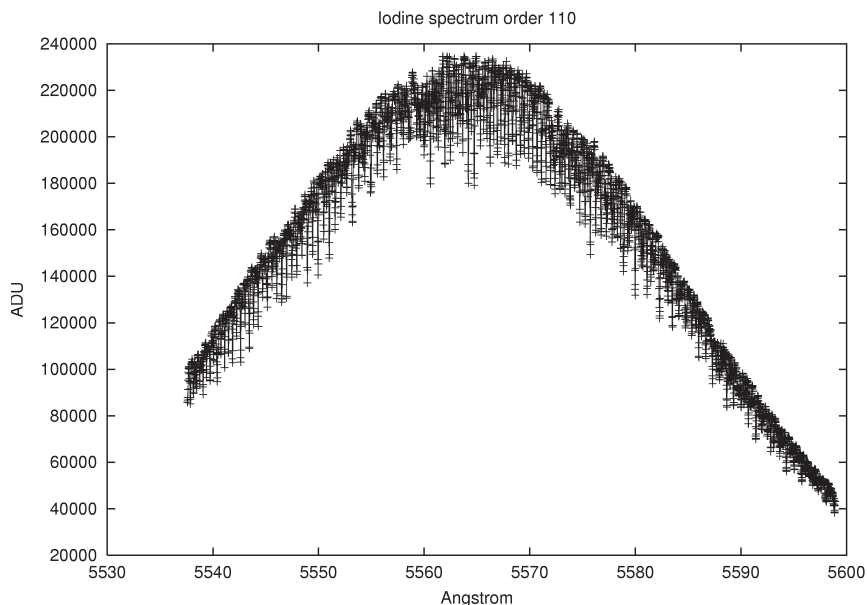


Figure 7: Portion of the extracted and wavelength-calibrated iodine spectrum. The intensity variation across the echelle order is caused by the blaze response of the grating.

mentation of a full online data reduction pipeline. A sophisticated software tool will support the observer during the run: it will allow online calculation of the exposure time (based on the brightness of the star, the actual brightness of the night sky, the seeing and the desired

SNR) and enable him to optimize during the night the short-term scheduling of observations of targets in a pre-prepared object catalogue.

All raw data are then stored in the local archive. In addition, observations in the high-precision ThAr mode are auto-

matically reduced in near real time by a pipeline running on a dedicated workstation: at the end of the night the observer will have available all final radial velocities, ready for publication! All data can be immediately written to DVD-ROM and are also archived in the central Garching science archive.

Outlook

The HARPS project is now close to completion. Following the initial Announcement of Opportunity in 1998 were the project kick-off in February 2000, optics Final Design Review (FDR) in April 2000, Preliminary Design Review in July 2000, FDR in March 2001, and software FDR in July 2001. HARPS is currently undergoing extended system tests at Geneva Observatory (see Pepe et al. 2002). As soon as these are finished, we will perform Preliminary Acceptance (Europe), scheduled for December 2002. After the transport to La Silla and the subsequent re-integration and functional tests we plan to have First Light in February 2003, followed by two commissioning runs of 2 weeks duration each. HARPS should then be available to the ESO astronomical community from Period 72 on. At the specified performance, it will be a marvellous radial velocity machine which will among others serve to strengthen the leading role European astronomers play in the new and exciting field of extrasolar planet research.

Acknowledgements

Like many major instrument projects these days, HARPS would not have become a reality without the enthusiastic effort of a large number of people in several institutes on different continents. The main players in the HARPS Team are listed at the beginning of this article.

Industry played a further crucial role in the project by providing key components. The major contractors are listed in Table 4.

The HARPS Consortium acknowledges financial support from various foundations and institutions in Switzerland and France.

References

- Hatzes, A., Cochran, W. in *Proceedings ESO Workshop on High-Resolution Spectroscopy with the VLT*, M. Ulrich, ed., ESO, (ESO Garching), 1992
- Santos, N. et al.: this *Messenger*.
- Pepe, F. et al., "Performance Verification of HARPS – First Laboratory Results", in *Astronomical Telescopes and Instrumentation 2002: Ground-based Telescopes and Instrumentation*, Proc. SPIE Vol. **4841**, (2002, in print).
- Queloz, D., Mayor, M. 2001, From CORALIE to HARPS, *The Messenger*, **105**, 1–7.

Table 4. The main HARPS industrial contractors.

Vacuum vessel	APCO Technology (CH)
Optical bench	Deshors Ets. (F), Acrodur (F)
Crossdisperser grism	Cybernetix (F), Thermo RGL (USA)
Echelle grating	Thermo RGL (USA)
Camera, collimator	SESO (F), SAGEM (F)
Coatings	SAGEM (F), Gretag TFP (CH)
Optical fibres	SEDI (F)
Iodine cell	Hellma (D), Physikalisch-Technische Bundesanstalt (D)

OmegaCAM: the 16k×16k CCD Camera for the VLT Survey Telescope

K. KUIJKEN^{1,2}, R. BENDER³, E. CAPPELLARO⁴, B. MUSCHIELOK³, A. BARUFFOLO⁵, E. CASCONI⁴, O. IWERT⁶, W. MITSCH³, H. NICKLAS⁷, E.A. VALENTIJN², D. BAADE⁶, K.G. BEGEMAN², A. BORTOLUSSI⁵, D. BOXHOORN², F. CHRISTEN^{2,6}, E.R. DEUL¹, C. GEIMER⁶, L. GREGGIO⁵, R. HARKE⁷, R. HÄFNER³, G. HESS⁶, H.-J. HESS³, U. HOPP³, I. ILIJEVSKI³, G. KLINK⁸, H. KRAVCAR³, J. L. LIZON⁶, C. E. MAGAGNA⁵, PH. MÜLLER⁹, R. NIEMECZEK⁶, L. DE PIZZOL⁵, H. POSCHMANN⁸, K. REIF⁸, R. RENGELINK¹, J. REYES⁶, A. SILBER⁶, W. WELLEM⁷

¹Leiden Observatory; ²NOVA/Kapteyn Astronomical Institute, Groningen;

³Universitäts-Sternwarte München; ⁴INAF - Osservatorio Astronomico di Capodimonte, Napoli;

⁵INAF – Osservatorio Astronomico di Padova; ⁶ESO, Garching; ⁷Universitäts-Sternwarte Göttingen;

⁸Sternwarte Bonn; ⁹Radioastronomisches Institut Bonn

1. Introduction

In 2004, OmegaCAM will start operations on Paranal as the sole instrument on the 2.6-m VLT Survey Telescope. OmegaCAM is a huge optical CCD imaging camera: its 16k × 16k CCD pixels cover the square degree field of view of the VST almost entirely. The primary function of the VST and its instrument is to provide surveys in support of VLT science, be it in the form of large homogeneous multi-colour imaging surveys which form the basis for large-scale spectroscopic follow-up work, or in its ability to find rare or extreme astronomical objects for further study.

The designs of both VST and OmegaCAM try to take full advantage of natural good seeing, so it should also be a superb instrument for weak gravitational lensing surveys, or for monitoring projects designed to detect micro-

lensing or supernovae. In fact, applications are manifold: one has only to look at the exciting science that is now coming out of the Sloan Digitized Sky Survey to realize the potential of VST/OmegaCAM, which has a comparable field of view to the SDSS camera, but will operate continuously, with better image quality and higher throughput.

The scale of the instrument means that once operations start the challenge is not at all over: OmegaCAM will generate of order 50 GByte of raw data per night, year after year, and such a volume of data can only be digested by means of a strict observing protocol (encoded in the Observation Blocks) combined with highly automated processing of the data. Exciting and challenging times are ahead!

In this article, the OmegaCAM consortium presents the basic features and design of the instrument.

2. The VLT Survey Telescope

The VST (Arnaboldi et al. 1998), now under construction in Naples, is a 2.6-m modified Ritchey-Crétien telescope which will stand next to the four UT's on Paranal. It is specifically designed for wide-field imaging, and has been optimized for excellent image quality in natural seeing. Thus, it will have active primary and secondary mirrors, a retractable atmospheric dispersion corrector, a constant focal plane scale of 0.21 arcsec per 15 μm pixel over a 1.4 degree diameter field, and a theoretical PSF with 80% of its energy in a 2 × 2 pixel area over the whole field. OmegaCAM will be the sole instrument on the telescope, and will be mounted at the Cassegrain focus.

3. Overview of the Instrument

3.1 Detector system

The heart of OmegaCAM is the CCD mosaic (Fig. 1), being built at ESO headquarters in Garching. It consists of a 'science array' of 32 thinned, low-noise (5e⁻) 3-edge buttable 2 × 4k Marconi (now E2V) 44-82 devices, for a total area of 16384 × 16384 15 μm pixels (26 × 26 cm!). The science array fits snugly into the fully corrected field of view in the focal plane of the VST, and covers an area of 1 × 1 degree at 0.21 arcsec/pixel. Around this science array lie four 'auxiliary CCDs', of the same format. Two of these are used for autoguiding (on opposite sides of the field: the field is so large that also field rotation will be auto-guided), and the other two for on-line image analysis. For this purpose the latter CCDs are deliberately mounted out of focus (one 2 mm in front, one 2 mm behind the focal plane), and the resulting defocused images can be analysed on-line and used to infer aberration coefficients such as defocus, coma, or astigmatism every

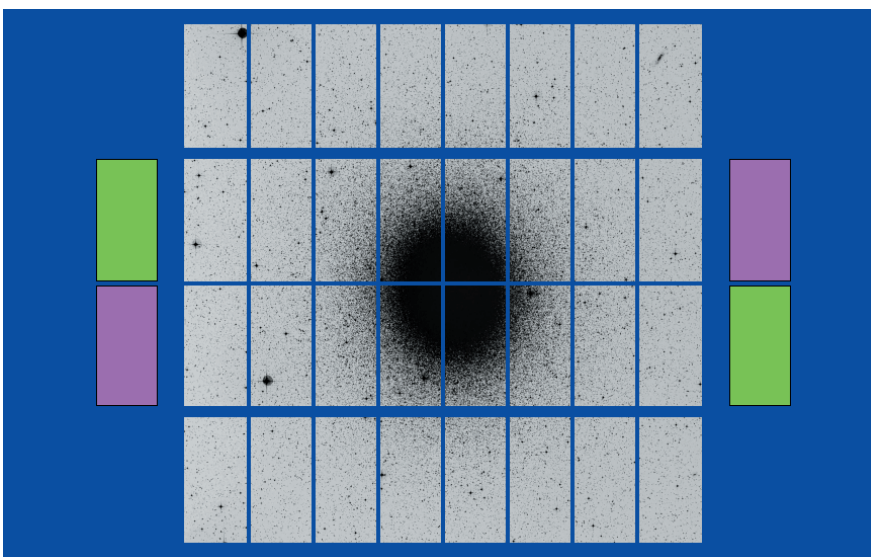


Figure 1: Layout of CCDs in the focal plane. This arrangement minimizes the amount of dead space between devices, given the constraints imposed by connecting the read-out ports. The globular cluster ω Cen is superimposed on the field, which covers a 1×1 degree area. The auxiliary CCDs, shown in green and purple, are used for autoguiding and for online wavefront analysis.

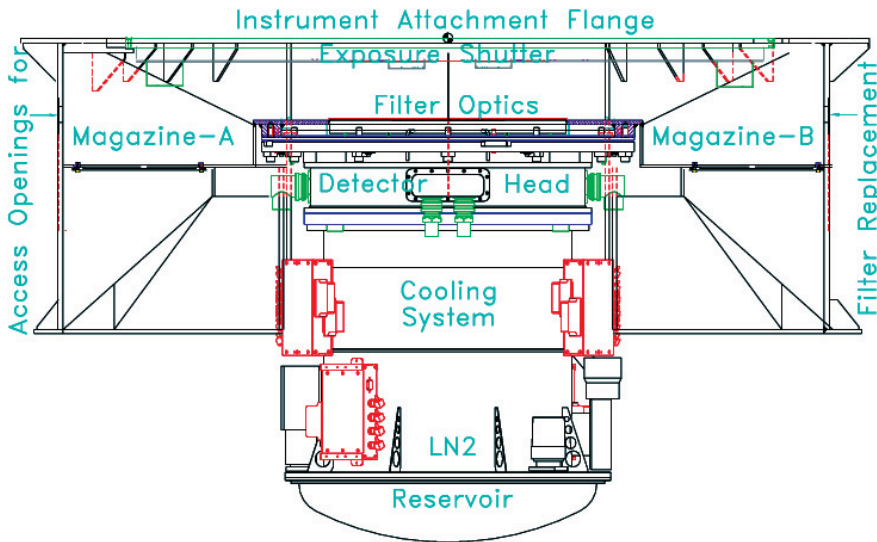


Figure 2: General drawing of the OmegaCAM instrument. The view is dominated by the cryogenic cooling system (with pre-amplifiers, vacuum equipment, etc. attached on the outside) and the detector head on top of it containing the CCD mosaic. Above the CCDs, obscuring the curved dewar window, is the filter exchange system (shown in blue), which moves filters between the two magazines and the beam. The exposure shutter is mounted at the top of the instrument, just below the telescope flange.

minute. The whole detector system is mounted behind a large, curved dewar window (the final optical element in the VST design) and is cooled using a 40-l Nitrogen cryostat. Readout of the full mosaic takes 45 s, and is accomplished by two FIERA controllers (a third FIERA takes care of the four guiding and image analysis CCDs).

The OmegaCAM detector team at ESO is led by O. Iwert.

3.2 Hardware

In front of the dewar window is the mechanical part of OmegaCAM: closest to the CCD window sits the filter exchange mechanism, and above that the shutter. Both components have to fit into a design space of a mere 16 cm between the dewar window and the VST's Shack-Hartmann unit. The housing provides the mechanical link between the telescope flange and the detector/cryostat system.

Figure 2 gives a section view of the final design that foresees a cylindrical housing with a spoke-like rib structure to support the axisymmetrical loads at the Cassegrain focus. The housing can be seen in Figure 3.

The filters are stored in two magazines which can move up and down, either side of the focal plane, through large shafts in the housing. A linear stage slides filters into the beam, where they are locked into place by means of movable notches. High-precision filter positioning ensures that intensity variations in the flat fields due to optical imperfections in the filters (dust grains, etc.) are less than 0.1%. The filter exchange unit is built in such a way that it allows one filter to be pulled into the beam while the previous one is pushed

out, allowing efficient observing in spite of the rather large distance the filters have to travel.

The filters are large (in the language of our latest ESO member state: a square foot) and heavy: when fully loaded with 12 filters, the instrument will contain 40 kg (90 lbs.) of filter glass alone!

The exposure shutter (Reif et al. 2002) is one of the key units of OmegaCAM (Fig. 4). It consists of two carbon fibre blades which open and close the light path. They are driven by micro-stepper motors and move smoothly on linear motion guides. These movements are controlled such that each individual CCD pixel 'sees'

the opening edge of the one blade and the closing edge of the other blade with an identical time difference, even if the blades are still accelerating – this provides an impact-free, high-accuracy photometric shutter. Tests of the shutter confirm that it meets the key technical specification: for an exposure time as short as 1 second, deviations from a homogeneous exposure are well below $\pm 0.2\%$ over the whole field of view.

The OmegaCAM control electronics are based on VME-based local Control Units (LCUs), with a higher level of Unix-based workstations to manage the user interface, coordination, testing and maintenance. The LCU is a stand-alone VME crate equipped with a Motorola CPU board, an Ethernet board, the real time operating system VxWorks, as well as specialized control and interface boards. All the controlled functions are standardized as much as possible, and the modular design facilitates the maintenance and should ensure efficient and reliable operations.

The mechanics are designed and built by the German consortium partners in Göttingen (H. Nicklas – housing, filter exchanger) and Bonn (K. Reif – shutter). More details can be found in Nicklas et al. (2002) and Reif et al. (2002). The control electronics were designed at INAF-Naples by E. Cascone, and are being assembled at Munich University Observatory under W. Mitsch.

3.3 Optics

The VST telescope will work in two configurations, which can be selected remotely. In the standard configuration, foreseen for work at small zenith distances, a two-lens field corrector is

Figure 3: The 1.5-m diameter housing structure during a test assembly of the main units: the two storage magazines (to be inserted into the big shaft at left and hidden right), the filter exchange unit with the exchange carriage and a 420 × 320 mm² opaque, aluminium 'filter' (at the bottom left).



used. The second configuration replaces this corrector with one including an Atmospheric Dispersion Corrector (ADC), consisting of one lens and two counter-rotating prism pairs. The operating wavelength ranges are 320–1014 nm and 365–1014 nm for the two-lens corrector and corrector + ADC respectively.

The only optical parts located in the instrument are the filters, and the entrance window to the cryostat, which doubles as a field lens.

The primary filter set of OmegaCAM will be a set of Sloan u' , g' , r' , i' and z' filters. In addition, there will be Johnson B and V filters for stellar work and for cross-calibrating the photometric systems, a Strömgren ν filter, an $H\alpha$ filter consisting of 4 segments with redshifts of up to 10,000 km/sec, and a segmented ugri filter for efficient photometric monitoring of the sky.

The procurement of large format filters of the required size turned into a challenging task. Only one manufacturer (the French company SAGEM, formerly REOSC, who figured the VLT primary mirrors) could make an offer for producing the primary set of filters without resorting to a segmented design, which would have created vignetting shadows on the detector array. Rather than using coloured glass – barely available in the required size – the filter passband is generated by means of multiple layer coating of up to 5 surfaces in a sandwich of three plates. The expected throughputs of the Sloan filters are very high (Fig. 5).

Filter procurement is coordinated by U. Hopp and B. Muschielok.

3.4 Control Software

All instrument functions (filter exchange, shutter, detector readout, as well as monitoring the instrument state) are controlled in software. The programming environment is defined and provided by ESO through the releases of the VLT Common Software which has to be used as the basis for design and development. The partitioning of the OmegaCAM Instrument Software (OmegaCAM INS) into software subsystems also follows the VLT standards. Nevertheless there were several challenges peculiar to OmegaCAM.

The Autoguiding Software and Image Analysis modules normally belong to the Telescope Control Software. In the case of OmegaCAM it was necessary to move these functionalities to the INS because during normal operations the VST guiding arm will not be used, as it slightly vignets the science array. A new software algorithm was developed to extract optical aberration coefficients from the out-of-focus images recorded on the Image Analysis CCDs. On the detector software side, particular attention had to be paid to the coordination



Figure 4: The OmegaCAM exposure shutter. The aperture size is 370×292 mm, the shortest possible exposure time is smaller than 1 msec, the deviations of the effective exposure time from pixel to pixel (homogeneity) are smaller than $\pm 0.2\%$ for a 100-msec exposure, the exposure time accuracy is about 0.3 msec. (The laptop computer gives an idea of the scale.)

of the readouts by the different FIERA's, and to the efficient storage of the data on disk.

The Instrument Software is being produced by the Italian part of the consortium, headed by A. Baruffolo (INAF-Padua), and is described in more detail in Baruffolo et al. (2002).

4. Calibration and Data Reduction Software

The amount of data produced by OmegaCAM will be truly huge. We estimate that there will be over 15 Terabyte of raw data per year. This raw data volume contains roughly 5 Terabyte of calibration data and 10 Terabyte of raw science data. Data processing will then produce another 10 Terabyte of reduced science data and may create, with about 100,000 astronomical objects per OmegaCAM field, enormous catalogues. To efficiently handle this data volume the data acquisition, calibrations and the pipeline reductions are strictly procedurized, a key aim being to

maintain the *instrument*, not individual data sets, calibrated at all times. ESO will operate the instrument in service mode, optimizing the observing programme to ambient conditions, and routinely taking calibration data. Thus each night the instrument's overall responsiveness and also the transmission of the atmosphere will be monitored in the u' , g' , r' and i' bands irrespective of the schedule of science observations. Data reduction recipes, run in ESO's DFS, will provide a continuous characterization of the behaviour of the instrument in these key bands. When other filters are used, the calibration plan foresees a cross calibration of these filters versus these key bands.

The basic technique to overcome any gaps or artefacts in the CCD pixels is to take more exposures of the same field with slightly shifted field centre and to co-add the images off-line. We distinguish the following observing modes:

- *Dither* has offsets matching the maximum gap between CCDs, ~ 400 pixels (5.6 mm). It will be operated with

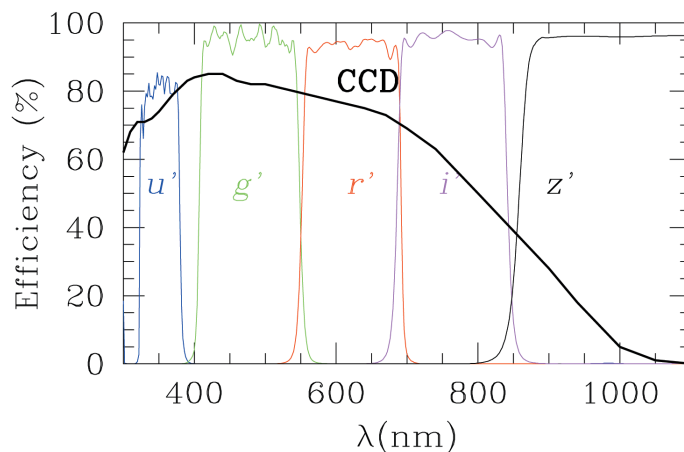


Figure 5: Theoretical throughput curves from SAGEM for the SDSS filter set, and measured quantum efficiency of one of the OmegaCAM CCDs.

N (with 5 as the default value) pointings on the sky. Although this will nearly cover all the gaps in the focal plane and maximizes the sky coverage, the context map of such data is complex. An advantage is that it will be relatively easy to couple the photometry among the individual CCDs.

- *Jitter* has offsets matching the smallest gaps in CCDs ~ 5 pixels. This mode optimizes the homogeneity of the context map and will be used during observations for which the wide gaps are not critical, but which, for instance, require a well-mapped smoothly varying PSF.

- *Stare* allows re-observing one fixed pointing position multiple times. It is the main workhorse for monitoring the instrument and allows detection of optical transients.

- *SSO* is the mode for observing Solar System Objects, which requires non-sidereal tracking.

For all these modes dedicated observing templates are being developed.

An observing strategy employs one or a combination of the basic observing modes. It also defines a number of additional instructions for scheduling of the observations. We distinguish the following strategies:

- *Standard* which consists of a single observation (observation block)

- *Deep* which does deep integrations, possibly taken at selected atmospheric conditions over several nights

- *Freq* which frequently visits (monitors) the same field on time scales ranging from minutes to months and has overriding priority on the telescope schedule

- *Mosaic* maps areas of the sky larger than 1 degree, which is essentially an item for the scheduling, as the pipeline has to produce uniform quality data anyway. The combination of various field centres into one image is not considered a standard pipeline task.

The observing modes and strategies are fully integrated with the data reduction software being developed by the OmegaCAM consortium. We distinguish between a calibration pipeline producing and qualifying calibration files, and an image pipeline that applies the calibration files to raw data and transforms them into astrometrically and photometrically calibrated images. ESO users will be provided with the output of the image pipeline, run in Garching, on the data contained in a single OB. The nominal photometric accuracy of this pipeline will be ± 0.05 mag, exceptionally ± 0.01 mag. The nominal accuracy for the astrometry is ± 0.1 arcsec rms over the entire field of view.

As part of the contract, the OmegaCAM consortium will deliver software modules that ESO will integrate into the image pipeline. In addition, a project has been set up among European wide-field imaging groups to provide a 'wide-field imaging survey system' that will combine pipeline processing of image data with archiving and data mining tools. Further details can be found on <http://www.astrowise.org>, and in Valentijn & Kuijken (2002).

The development of the analysis software is being done by a team based in Groningen and Leiden, led by E. Valentijn.

5. Current Status

The OmegaCAM project is now well into the manufacturing phase. Most of the CCDs have been delivered and tested; most of the mechanics exist and are ready to be integrated; instrument control and data analysis software is being coded. Extensive tests in Europe are foreseen for the second half of 2003, and the camera should see first light early in 2004. Exciting times!

Acknowledgements

The consortium was formed in 1998 in response to an announcement of opportunity from ESO, and comprises institutes in the Netherlands (NOVA, in particular the Kapteyn Institute Groningen and Leiden Observatory), Germany (in particular University Observatories of Munich, Göttingen and Bonn) and Italy (INAF, in particular Padua and Naples observatories). The ESO Optical Detector Team provides the detector system at cost to the consortium. OmegaCAM is headed by PI K. Kuijken (Groningen and Leiden University) and co-PI's R. Bender (Munich USM/MPE) and Cappellaro (INAF Naples/Padua), and project management is done by B. Muschielok and R. Häfner (USM).

OmegaCAM is funded by grants from the Dutch Organization for Research in Astronomy (NOVA), the German Federal Ministry of Education, Science, Research and Technology (grants 05 AV9MG1/7, AV9WM2/5, 05 AV2MGA/6 and 05 AV2WM1/2), and the Italian Consorzio Nazionale per l'Astronomia e l'Astrofisica (CNAA) and Istituto Nazionale di Astrofisica (INAF), in addition to manpower and materials provided by the partner institutes.

References

- Arnaboldi, M., Capaccioli, M., Mancini, D., Rafanelli, P., Scaranella, R., Sedmak, G. and Vettolani, G. P., 1998. *The Messenger* **93**, 30.
- Baruffolo, A., Bortolussi, A., De Pizzol, L. 2002, Proc. *SPIE* 4848, in press.
- Nicklas, H., Harke, R., Wellem, W., Reif, K. 2002, Proc. *SPIE* 4836-34, in press.
- Reif, K., Klink, G., Müller, Ph. and Poschmann, H. 2002 in *Scientific Detectors for Astronomy*, Beletic, Amico eds., Astrophysics and Space Sciences Library (Kluwer: Dordrecht), in press.
- Valentijn, E.A. & Kuijken, K. 2002 in *Toward an International Virtual Observatory*, Quinn, P., ed., ESO Astrophysics Symposia Series (Springer-Verlag), in press.

The VLTI – 20 Months after First Fringes

A. GLINDEMANN, ESO

1. Introduction

In 2002, the second year of fringes at Paranal, the VLTI has made substantial progress. The highlight was the completion of the combination in pairs of all four Unit Telescopes on September 15/16 and 16/17 using a total of five different baselines. Only the combination MELIPAL – YEPUN could not be provided due to the current configuration of delay lines in the interferometric tunnel.

Of equal importance was the start of a total of 150 hours shared risk science operations with the VLTI in October.

Forty proposals from the community were received representing about 10% of all proposals submitted to ESO for the VLT observatory. A summary of the first semester with VLTI science operations will be given at the end of this semester. For Period 71, the shared risk science operations became a part of the ESO Call for Proposals with 25 proposals submitted for the VLTI. A number of observation preparation tools have been developed in collaboration with the Jean-Marie Mariotti Centre for Interferometry (JMMC) in Grenoble. Two of them are now available on the web

(<http://www.eso.org/observing/etc/preview.html>). In the course of the year, all science data between First Fringes in March 2001 and September 2002 have been released through the archive resulting in first scientific results which are described in [1]–[4]. A summary of the first results is given in [5]. In the context of science operations, the results of the on-going observations of calibrator stars are reported in [6], in collaboration with the NOVA ESO VLTI Expertise Centre (NEVEC) in Leiden.

Amongst the runners-up for achievements are the integrated optics beam

combiner IONIC for VINCI, the acceptance of the science instrument MIDI in Heidelberg in September (currently being integrated at Paranal), and three new contracts to extend the VLTI infrastructure: Delay Lines 4, 5 and 6 were ordered at Fokker Space in Leiden, and the installation of the required rail systems in the Delay Line Tunnel started in August. The contract for the fourth Auxiliary Telescope was signed with AMOS in Liège at the beginning of September (see [7]). The first PRIMA contract for the delivery of the fringe sensor unit was signed with ALENIA Spazio, Torino, in July, and the second contract for the star separator unit will follow soon. The PRIMA laser metrology system will be an in-house development. These three subsystems will form the first phase of PRIMA.

IONIC was provided by the Observatoire de Grenoble. IONIC is a beam combiner for VINCI that can be used instead of VINCI's fibre beam combiner MONA. In IONIC, the beams are guided through two silicon fibres into an integrated optics (IO) component where the beam combination takes place. At the exit of the IO component, fibers are attached guiding the light to the infrared detector. Since the fibre connectors are identical to those used in MONA, the optical integration was just a matter of disconnecting and connecting a few fibres. Unlike the K-band beam combiner MONA, IONIC, having silicon fibres and substrates, works in the H-band. The VLTI had first fringes with IONIC on July 18, producing an interferometric transfer function above 80% with an accuracy of 1% which is as good as MONA (see [8]).

Last but not least there is also progress with the adaptive optics systems for the VLTI. The Paranalization of the tip-tilt sensors STRAP on two Unit Telescopes is finished, and MACAO, the high-order adaptive optics system (see [9]), saw first light in the laboratory in Garching in August, closing the loop on an artificial star.

2. Four Eyes Are Better

Why should one attempt to use more than two telescopes if the interferometric instrument can only combine two beams? First of all, this exercise demonstrated the ability to provide multiple beams in the VLTI laboratory without losing time for mirror realignment or for other reconfigurations. In 2003, AMBER, the near infrared science instrument, will see first fringes. Then we will have an instrument combining up to three telescopes simultaneously.

In addition, multiple baselines are the key to efficient interferometric imaging. The result of the observations of the star Achernar in September, shown in Figure 1, gives an impression of the angular resolution capability of the VLTI

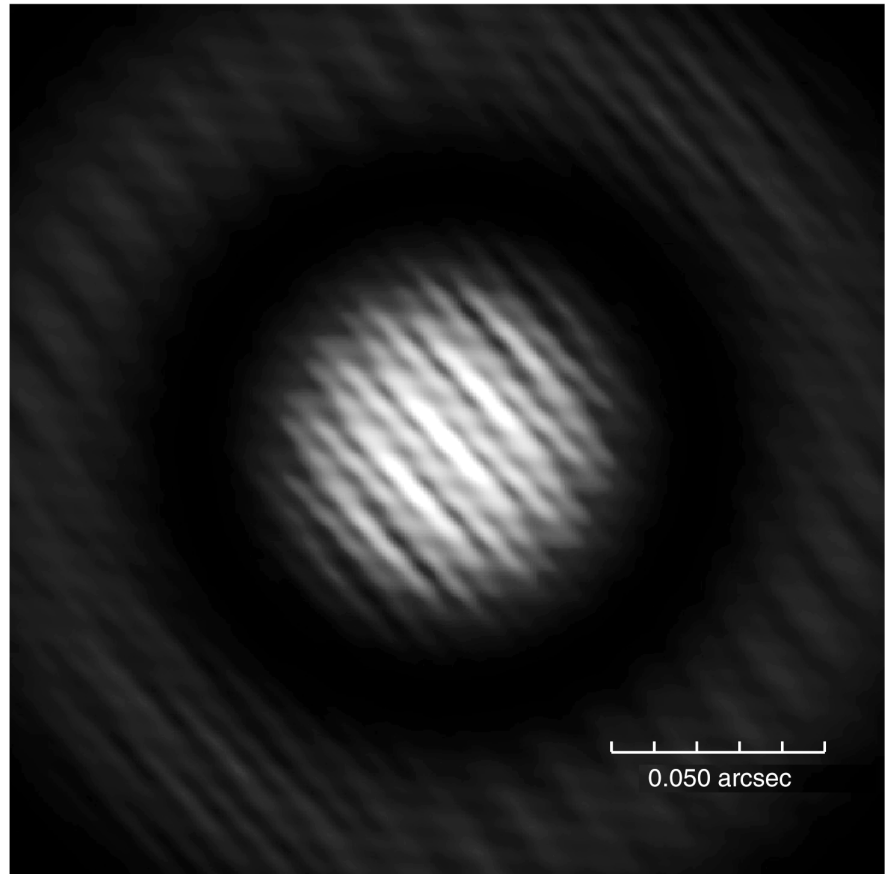


Figure 1: The reconstructed, two-dimensional interferometric point spread function (PSF) of the star Achernar observed in the K-band. The width of the central fringe is 3 by 15 milli-arcsec indicating the angular resolution limit of the VLTI for the baseline distribution shown in Figure 2. On the largest scale, the image is enveloped by the Airy disk of a single 8-m Unit Telescope. Its first minimum at 57 milli-arcsec off the centre can be clearly seen. The image provides a dramatic illustration of the 20-fold increase in resolution of the VLTI over a single 8.2-m telescope.

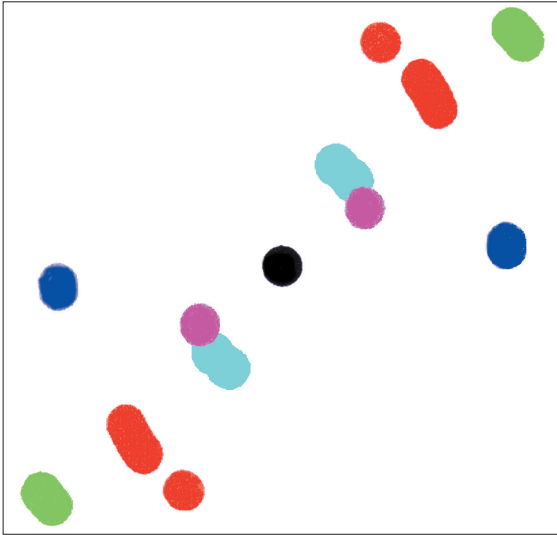
with the Unit Telescopes. The intensity distribution was reconstructed from the measurements with individual baselines by Fourier transforming the distribution of values displayed in Figure 2. Every balloon in that figure represents the result of a visibility measurement with one baseline vector. It is important to properly refer to baselines as baseline vectors in order to understand why the distribution of the balloons is considerably different from the distribution of Unit Telescopes at Paranal (see Fig. 3). The visibility function depends on the difference of telescope coordinates (projected perpendicular to the viewing direction of the star). For instance, two telescopes separated by 100 m along the north-south direction have exactly the same baseline vector as two other telescopes a few kilometres away that are also separated by 100 m along north-south.

The baseline vectors are displayed in the 'uv-plane', where the measured visibility forms the function value at the coordinate given by the length and the orientation of the baseline vector. Since the visibilities are derived from the intensity, a real and positive quantity, the visibility function is point symmetric; one visibility measurement de-

livers two function values, at (u, v) and at $(-u, -v)$.

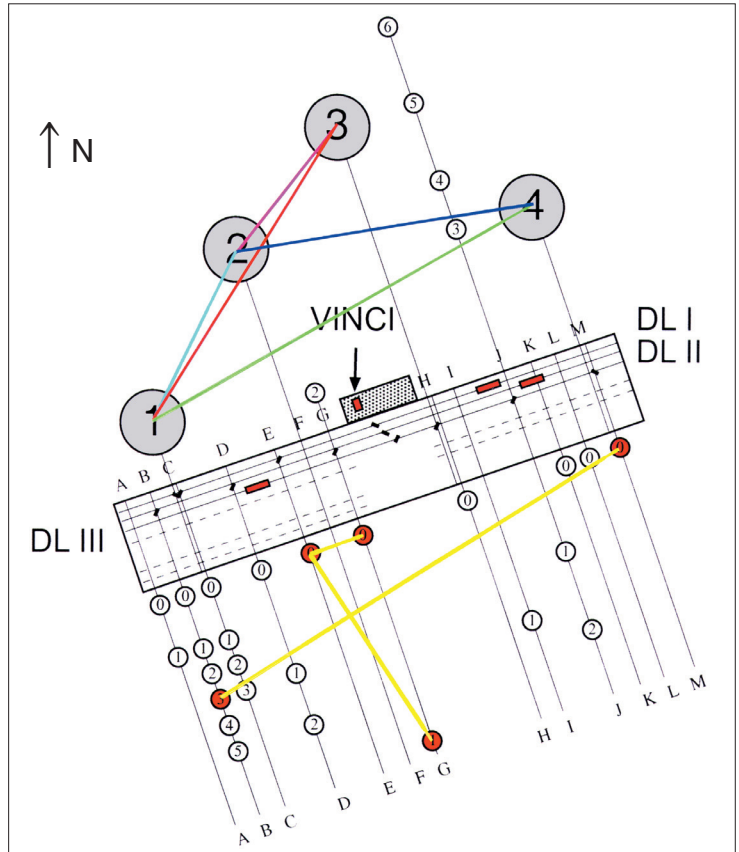
The balloons representing the measured visibilities in the uv-plane are small disks although a point would be expected when observing with an individual baseline. The reason is that the telescope is not a pinhole but an 8-m aperture allowing for a small variation of baselines around the 'centre-to-centre' baseline. Inside VINCI, optical fibres are used as spatial filters. The size of the optical fibres is exactly an Airy disk of the telescope, i.e. the field of view is one Airy disk. This spatial filtering is equivalent to performing an average over the visibilities inside the disk represented by the balloons.

For imaging it is important to note that one measures as many independent image points inside the Airy disk as one has baselines, i.e. as one has degrees of freedom. Fortunately, the number of baselines is not only determined by the number of telescopes but also by the duration of the observation. Due to the sidereal motion, the baseline projected onto the viewing direction changes all the time in length and orientation depending on the object coordinates. Some of the baselines that are displayed in Figure 2 have a slight peanut



▲ Figure 2: The set of baselines used for observing Achernar with the four Unit Telescopes. Each baseline is represented by two opposite, short arcs, symmetric around the origin (centre) of the diagram. The colour-coded pattern reflects the telescope pairs (ANTU-KUEYEN = magenta, ANTU-MELIPAL = red, ANTU-YEPUN = green, KUEYEN-MELIPAL = cyan, KUEYEN-YEPUN = blue).

Figure 3: The lines indicate the Unit Telescope and AT stations that have been combined at Paranal to date. The colour scheme for the UTs corresponds to the baselines shown in Figure 2.



shape due to the observing time of a few hours. Several individual measurements were taken during this time. Therefore, the number of individual points in the image will be considerably larger than six when observing with all four Unit Telescopes.

The present observations of Achernar give an impression of the point spread function of the VLTI because Achernar with an angular diameter of 2 milli-arcsec is smaller than the resolution limit of 3 milli-arcsec of the VLTI in the K-band. Due to the moderate number of baselines, the point spread function in Figure 1 shows a mix of a moderate number of individual fringe patterns. A larger number of visibility measurements would make the individual fringe patterns disappear, and only the central fringe would remain as the 'point' in the point spread function.

The particular distribution of baselines in Figure 2 is rather extended in the north-east/south-west direction (the baseline of ANTU-YEPUN) and rather narrow in the perpendicular direction because the baseline MELIPAL-YEPUN is missing. Consequently, the Fourier transform of this distribution is rather narrow in the north-east/south-west direction and rather wide in the perpendicular direction. The terms narrow and wide refer to the width of the central fringe. The central fringe in Figure 1 has a width of about 3 milli-arcsec in the direction of the longest baseline and of about 15 milli-arcsec in the perpendicular direction. Due to the processing technique, the Airy disk of an individual

8-m telescope shows up in the point spread function in Figure 1. The first dark ring of the Airy disk with a radius of 57 milli-arcsec in the K-band is readily apparent. This illustrates the gain in angular resolution with the VLTI compared to an individual Unit Telescope.

However, it is still a long way to go before the VLTI will do imaging of arbitrary objects since this requires measuring the phase of the visibility function in addition to its modulus i.e. its contrast. AMBER in 2003 will be a first step, being able to use three telescopes and performing a phase reconstruction via the closure phase technique. Eventually, from 2005 onwards, PRIMA will allow measuring the phase directly per baseline and, in addition, observe very faint objects. The scientific objectives of the PRIMA facility are described in [10].

3. Outlook

The coming year will be extremely busy, with integrations of new subsystems about every two months. FINITO, the fringe sensor unit, will be first, followed by two MACAO systems, by the first two Auxiliary Telescopes, by AMBER and by the carriages with cat's eyes of the three new Delay Lines. This is a big burden for the integration teams since the VLTI is not the only 'telescope' at Paranal.

In 2004, the remaining two MACAO systems and the third and fourth Auxiliary Telescopes will arrive at Paranal so that the VLTI will be able to combine the light from eight different telescopes, four Unit Telescopes and

four Auxiliary Telescopes. With six Delay Lines, a common focus of six telescopes can be used at any given moment. To fully exploit the VLTI infrastructure, the first second-generation instrument should clearly be a six-way beam combiner, measuring 15 baselines at once and 28 during a night, without reconfiguring the telescopes.

Amongst all these integration and commissioning activities one must not forget that the success of an observatory depends solely on the scientific output. MIDI will make a start next year, and 2004 will be largely devoted to science operations with the VLTI.

Acknowledgement

Over the last 20 months, the number of people both at ESO and in the community contributing to the VLTI has become too large to name here. I would like to thank not only those with the highest visibility but also the large number of contributors forming the base of the success by ensuring that every little piece of this complex machine works every night.

References

- [1] Kervella, P., et al. 2002, in *Exotic Stars as Challenges to Evolution*, IAU Symposium 187, in press.
- [2] Wittkowski, M. and Hummel, Ch. 2002, in *Interferometry for Optical Astronomy II*, ed. Traub, W., Proc. SPIE 4838, in press.
- [3] Richichi, A. and Wittkowski, M. 2002, in *The VLTI: Challenges for the Future*, eds. Garcia P.J.V., Glindemann A., Henning T., Malbet F., JENAM Workshop, in press.

- [4] Segransan, D., *et al.* 2003, *A&A Letters*, in press.
- [5] Paresce, F., *et al.* 2002a, in *Interferometry for Optical Astronomy II*, ed. Traub, W., Proc. SPIE 4838, in press.
- [6] Percheron, I., *et al.* 2002, in *The VLTI: Challenges for the Future*, eds. Garcia P. J. V., Glindemann A., Henning T., Malbet F., JENAM Workshop, in press.
- [7] Koehler, B., *et al.* 2002, *The Messenger*, this volume.
- [8] Kern, P., *et al.* 2002, in *Interferometry for Optical Astronomy II*, ed. Traub, W., Proc. SPIE 4838, in press.
- [9] Arsenault, R., *et al.* 2002, in *Adaptive Optical System Technologies II*, eds. Bonaccini, D., Wizinowich, P., Proc. SPIE 4839, in press.
- [10] Paresce, F., *et al.* 2002b, in *Interferometry for Optical Astronomy II*, ed. Traub, W., Proc. SPIE 4838, in press.

The Auxiliary Telescopes for the VLTI: a Status Report

B. KOEHLER¹, C. FLEBUS²

P. DIERICKX¹, M. DIMMLER¹, M. DUCHATEAU¹, P. DUHOUX¹, G. EHRENFELD³,
E. GABRIEL², P. GLOESENER², V. HEINZ³, R. KARBAN¹, M. KRAUS¹, J.M. MORESMAU¹,
N. NINANE², O. PIRNAY², E. QUERTEMONT², J. STRASSER, K. WIRENSTRAND¹

¹ESO, Garching, Germany; ²AMOS, Liège, Belgium; ³ESO, Paranal, Chile

1. Introduction

In June 1998, ESO signed a contract with the company AMOS (Belgium) for the supply of the Auxiliary Telescope System (ATS) for the VLTI. The original scope covered two movable Auxiliary Telescopes (ATs), as shown in Figure 1, as well as their associated site equipment including rails and interface devices for each observing station. An amendment was signed in September 1999 for the supply of a third AT and, last September, a fourth AT was ordered.

The contract with AMOS is based on top-level performance requirements and includes the design, manufacturing and testing of the complete system including all mirrors and cells, complete mechanical structure, drives, encoders, small mechanisms and low-level electronics. The main sub-contractors of AMOS are FISBA (Switzerland) for the coudé mirrors, PHASE (Italy) for the motors and CSEM (Switzerland) for the M2 hexapod mechanism.

ESO is in charge of the design and development of the telescope control hardware and software, as well as of the two star sensors located at the coudé focus.

After integration of the ESO control hardware and software, the telescope is fully tested in Europe at AMOS with the possibility of sky observation provided by an outside observing station included in the dedicated test facility. After this, ESO transports the ATs to Paranal, re-integrates them in the so-called Mirror Maintenance Building (MMB) and finally commissions them on the sky.

The project entered into manufacturing phase in mid-1999 and is now reaching the end of a very extensive testing and verification phase in Europe on AT#1 before its shipment to Paranal next year.

This article recalls the rationale at the origin of the ATS development, provides a description of the design and finally reports on the performance as measured in Europe so far.

2. Why Does the VLTI Need Auxiliary Telescopes?

The VLTI is primarily intended to combine coherently the four VLT 8-m Unit Telescopes (UTs). Obviously, the ultimate VLTI sensitivity will indeed be obtained when combining the UTs. However, the array of 1.8-m diameter ATs is a key element for the technical and scientific capability of the interferometer. The main reasons are listed below.

- It provides the best imaging capability of VLTI by complementing the array of UTs. It gives access to 30 telescope stations increasing therefore the number of accessible baseline vectors, a fundamental parameter for high-fidelity image reconstruction.
- It gives access to the longest VLTI baseline of $B = 200$

m versus a maximum of 130 m between UTs. This is needed to reach the ultimate angular resolution of the VLTI that scales as λ/B (i.e. 0.6 milli-arcsec in the visible and 2 milli-arcsec in the K band).

- It enables full-time use of the VLTI facilities, since the ATs are entirely dedicated to interferometric observations. This is an important factor for the VLTI scientific productivity (and for the amortization of its development cost!).

- It is required by the Narrow Angle Astrometry mode of PRIMA that



Figure 1: The first Auxiliary Telescope for the VLTI during final testing at AMOS in Liège (Belgium).

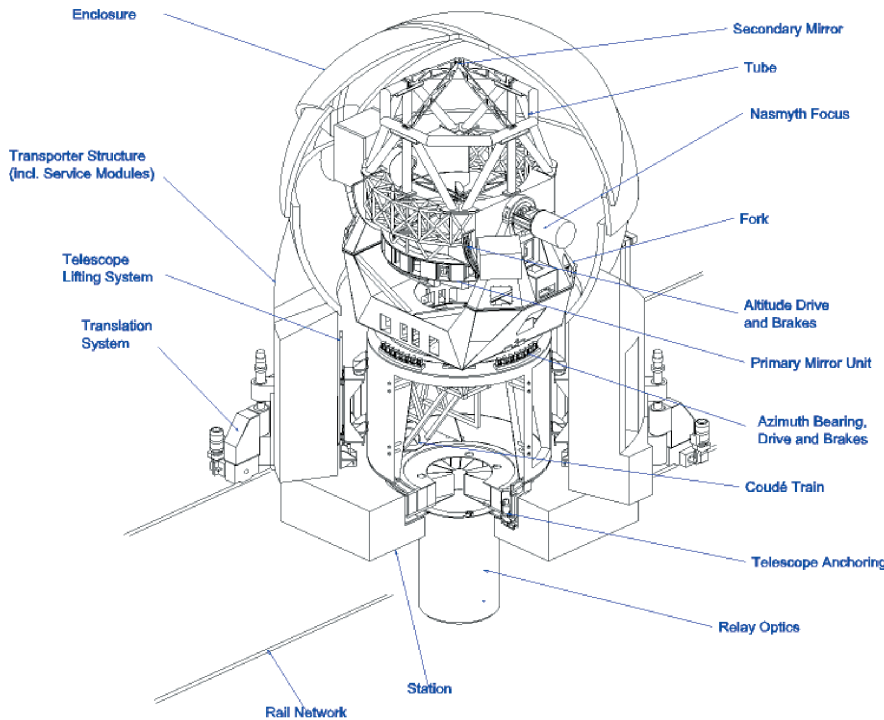


Figure 2: Overview of the Auxiliary Telescope System. The telescope is anchored on one of the 30 observing stations. It is surrounded by its built-in “Transporter” used to relocate the telescope, to support its enclosure and to house electronic cabinets and service equipment. Inside the station pit, the cylindrical structure contains the coudé sensors and the Relay Optics that sends a parallel beam to the Delay Line Tunnel trough underground light ducts.

needs regular and long-term monitoring out of reach with the highly subscribed UTs.

- It can be used for testing and commissioning of other VLTI facilities (e.g. for the 2nd generation of instruments) without using precious UT time.

For these reasons, the ATs are expected to become the ‘workhorses’ of the VLTI and to deliver a large amount of scientific results for those programmes that do not fundamentally need the sensitivity provided by the UTs.

The typical magnitude limits for the VLTI in the K band ($2.2 \mu\text{m}$) and in the N band ($10 \mu\text{m}$) are expected to be respectively $K = 11$ and $N = 4$ for the UTs equipped with Adaptive Optics. For the AT equipped fast tip-tilt correction only, these become $K = 9$ and $N = 1$.

The design of the VLTI infrastructure foresees up to eight Auxiliary Telescopes and eight Delay Lines. The reasons for increasing the number of tele-

scopes in the array are essentially linked to the imaging capability. Indeed, the fourth AT has recently opened the possibility for second-generation instruments to observe 6 baselines simultaneously. This will drastically improve the snapshot imaging capability, particularly useful for variable objects. Even with a 3-beam instrument like the VLTI instrument AMBER, the 6 baselines can then be observed quasi simultaneously by a fast switching of a mirror in the VLTI optical train instead of relocating the ATs, an operation that can be done during the day only. Similarly, the number of phase closures available per AT configuration will increase from 1 to 3. This represents a three-fold increase in observing efficiency in this powerful imaging mode where the phase errors introduced by the atmosphere can be cancelled out in order to retrieve the phase of the object, a critical parameter for image reconstruction. A fourth AT will also increase the limiting magnitude

by using the so-called ‘boot-straping’ technique where the fringes are tracked on the relatively short intermediate baselines while the low-visibility fringes are integrated on the extreme baseline. In addition, the fourth AT will permit to dedicate two ATs for the PRIMA astrometry mode while two others are being used by MIDI or AMBER. This may prove a fundamental advantage during the challenging commissioning phase of PRIMA by alleviating the possible conflicts with the regular VLTI science observation.

3. Specifications and Design Description

3.1 Basic conceptual choices and main specifications

The ATS specifications originate from its dedication to interferometric observations down to visible wavelengths. This calls for an extreme mechanical stability, at the level of a few nano-meters, together with the capability to easily relocate the telescope.

The following conceptual choices were made as a result of early feasibility studies.

- Primary mirror diameter 1.8 m, as a compromise between science capability and cost.

- Self-contained autonomous Telescope with built-in ‘Transporter’ enabling relocation of the telescope on observing stations connected by a rail network and built-in Enclosure ensuring survival in outdoor conditions (wind, earthquake).

- No active optics to limit control complexity already inherent in the interferometer, but 5-axis M2 support for remotely controlled alignment.

- Field acquisition and fast tip-tilt sensors at the coudé focus and provision for later implementation of Adaptive Optics.

- Stiff Alt-Az mount with Altitude axis 5 m high as a compromise between stiffness and ‘ground seing’ effects.

- Pseudo-kinematic interface between telescope and ground for high position and angular repeatability so that only fine remotely controlled alignment is required after a relocation.

- Mechanical bearing for both axes to limit maintenance and avoid hydraulic connections at station or on-board pumps.

- Direct drives for improved controllability associated with high accuracy optical encoders and analogue tachometers.

Table 1 summarizes the main performance requirements specified for the Auxiliary Telescope System. The most stringent ones imposed by interferometry are the excellent image quality, the high tracking accuracy and the Optical Path Length (OPL) stability. Other constraints imposed by the site

Table 1: Main AT performance requirements.

Optical quality of the complete telescope	< 110 nm r.m.s WFE
Wavelength range:	0.4 to 25 μm
Telescope position repeatability:	± 10 arcsec, ± 0.1 mm after any relocation
First telescope eigenfrequency:	> 10 Hz
Pointing accuracy:	< 1 arcsec r.m.s.
Tracking accuracy (blind):	< 0.1 arcsec r.m.s.
Tracking accuracy (Field Stab.):	< 0.025 arcsec r.m.s.
Optical Path Length Stability:	< 30 nm rms over 10 msec
Time to relocate to any station:	< 3 hours with 2 operators
Total Mass:	< 30 Tons
Design volume:	$H < 7.1\text{m}$, $W < 5.4$ m & $L < 5.8$ m



▲ Figure 3: The 1.8-m primary mirror in its cell during integration into the telescope at AMOS. The mirror is lightweighted to reduce its mass by a factor about 2. A 54-points waffle-tree axial support was selected to comply with the stringent image quality requirements.

Figure 4: The 140-mm diameter secondary mirror is mounted on an hexapod to enable remotely controlled focus, centring and angular alignment. The hexapod, built by CSEM (Switzerland) is a very compact, very high accuracy mechanical device featuring a resolution smaller than 0.2 microns and a very small cross-coupling between focus and tilt motions to avoid mispointing while re-focusing the telescope. ►



infrastructure such as the total mass and the design volume are also driving factors for the overall AT design.

3.2 Optical design

The AT optical design is similar to that of the UT and includes 11 mirrors. The first three (M1-M3) constitute a *Ritchey-Chrétien telescope* with a 1.8-m diameter primary mirror. A fast $f/1.4$ primary mirror was selected to provide a compact tube design and limit wind buffeting of particular concern for interferometric application where nanometer-level stability is required in the Optical Path Length (OPL). One consequence of that particular design is the high sensitivity of the telescope to the secondary mirror (M2) defocus & de-centre which places high demand on the stiffness of the tube structure. The Nasmyth focus of the Ritchey-Chrétien is unused for normal operation. It is re-imaged by the 5-mirror *coudé train* (M4-M8) to form a coudé focus located underground. In addition, the coudé train creates an image of the telescope pupil on M6 where a fast tip-tilt mirror (and possibly later an adaptive optics mirror) is located. Just above the coudé focus, a *dichroic mirror* (M9) transmits the visible to a CCD camera and an APD module (STRAP) for acquisition and fast guiding. The infrared light reflected by M9 is collimated by the *Relay Optics* (M10-M11) to form an 18mm parallel beam sent towards the VLT delay lines.

3.3 Telescope structure

An overview of the telescope design can be seen in Figure 2. The main drivers were the maximization of the first eigenfrequency, the minimization of the M1-M2 de-space and de-centre (typically $< 10 \mu\text{m}$) under gravity, wind load and thermal load as well as the minimization of the wind torque. This had to be achieved while complying with the constraints of mass, design volume, station interface and earthquake survival.

The *Tube* structure is a classical Serrurier strut made of hollow tubes connecting to a top-ring made out of full rods for weight balance. The M2 spiders were optimized in order to limit the design volume, to reduce the torque due to wind load on the top-ring and to increase axial stiffness in view of OPL stability. A particular feature of the tube design is the solution adopted, after several trade-offs, for the thermal compensation rendered necessary by the extreme sensitivity to M2 defocus. The compensation is provided by a proper selection of material for the Serrurier (steel), top-ring (steel) and M2 spider (invar). When the temperature increases, the tube expands and the top-ring diameter increases. This later creates a stress in the M2 spiders that results in a downward motion of M2 compensating the tube and M1 cell expansion. Several trade-offs were made on the centrepiece that is a main contributor to stiffness and wind torque. The latter constraint led to the final design based

on a complex strut structure with appropriate welded box/plates interfaces to the altitude shaft, Serrurier structure and M1 cell. On each side of the centrepiece, a semi-circular plate holds the magnets for the altitude motors and tachometers and a brake disk. For the support of M3, a spider was preferred over a more classical tower solution because it provides better static and dynamic results while easing the re-alignment after an M1 removal for the coating.

The tube is connected to the *Fork* on both sides by double row angular contact ball bearings providing high stiffness, low run-out and low friction. The Fork is a welded box structure with internal ribs highly optimized for stiffness and mass. At its lower part, the Fork connects to the Azimuth bearing, a key element to the overall telescope stiffness. The Azimuth bearing is a three-row roller bearing with very high radial, axial and tilt stiffness but, at the same time, very low friction torque necessary for the pointing/tracking accuracy.

Below the Azimuth bearing, the *Ground Interface Structure* (GIS) provides the connection to the ground through the pseudo-kinematic anchoring and clamping devices. This part of the telescope was also intensely optimized by FEM due to its importance in the first telescope eigenfrequency.

Inside the station pit the *Relay Optics Structure* (ROS), a double-skin welded box cylindrical structure, houses the Relay Optics and the coudé sensors. When relocating an AT on a new sta-



Figure 5: The first telescope on its test bench inside the dedicated hall at AMOS. In addition to tests at component level such as optical quality of each mirror, friction of the axis bearings, etc., the first telescope undergoes a thorough acceptance test programme including modal tests of the complete structure, dynamic response of the azimuth and altitude axis, OPL stability measurement, verification of structural deformation under gravity, pointing repeatability check and others.



Figure 6: The Transporter in its relocation configuration. The cylinder in the foreground houses the Relay Optics and the coude sensors (CCD and STRAP). The light beam exits the telescope by one of the two black openings. During relocation, the cylinder is lowered underground inside the station pit before the telescope is placed on top.

tion, this structure is lowered into the station hole on soft pads, the telescope is placed on top and a centring and clamping mechanism is activated between the structure and the Ground Interface Structure. The position repeatability is such that local alignment is not required after relocation. This holds also for the repeatability of the telescope anchoring system. The only telescope alignment necessary after relocation is performed remotely from the Control Room.

3.4 Drives, tachometer and encoders

The motors selected for both Altitude and Azimuth axes are direct drive, *brushless torque motor*, similar in concept to those installed in the UT. Two curved linear motor pads are used diametrically opposed for Azimuth and one pad is attached to each side of the fork for Altitude. Each motor is equipped with internal position sensors used in particular for motor commutation.

Each axis is equipped with an AC-DC *analogue tachogenerator* using the same magnet strip and similar pads as the motor. The power amplifier is based on fast DSP technology and provides motor current control, overspeed limitation and tachogeneration.

The axis position information is given by high accuracy Heidenhain *optical encoders*. The high interpolation factor leads to the very high angular resolution of 9 milli-arcsec on Altitude and 3 milli-arcsec on Azimuth.

3.5 Primary mirror unit

The M1 unit is shown on Figure 3. It consists of the primary mirror, its cell with axial and lateral supports and finally the interface with the telescope tube.

The *primary mirror* is made out of a 200-mm thick blank of Zerodur material from SCHOTT (Germany). Due to mass constraints, the mirror is light-weighted by drilling hexagonal pockets on its rear face as can be seen on Figure 3. It is polished to a hyperbolic shape.

The mirror *axial support* is the result of an intensive optimization by Finite Element Modelling in order to minimize the effect of gravity deflection. The selected solution compatible with the lightweight geometry and the low-level error budget is a 54-axial-point support mounted on a three-stage wiffle-tree system using flexible pivots.

For the *lateral support*, the retained optimal solution consists of 16 astatic levers using low-friction bearing and

counter-weights. In addition, three radial fixed points are located inside the M1 central hole.

The *M1 cell* consists mainly of a welded steel structure with a double skin for the bottom and lateral parts to improve the cell stiffness. The structure is made of two parts to facilitate the mirror integration and maintenance. The cell's lower part interfaces with the axial support while the upper part interfaces with the lateral support. The first eigenfrequency of the M1 unit is 20 Hz and the mirror degradation in its cell under gravity is less than 11 nm RMS surface.

3.6 Secondary mirror unit

Due to the selected fast f/1.4 primary mirror, the secondary *M2 mirror* is a rather small mirror 140-mm in diameter. However, its highly aspherical and fast (f/1.3) shape makes it a difficult mirror to manufacture. It is also made out of a blank of Zerodur, 25 mm thick.

The M2 is mounted on a *hexapod support* (see Fig. 4) providing defocus, de-centring and tip-tilt motions with sub-micron and arcsecond level resolution for remote alignment. Its design is primarily driven by the very limited space available (in the shadow of M2)

and the requirement to limit cross coupling between focus and tilt motion.

3.7 Enclosure

The basic enclosure concept is to provide good natural ventilation during the night to limit “dome and mirror seeing” and therefore to leave the part of the telescope above the altitude axis exposed to the outside wind (see Fig. 1). Following an analysis of the wind load, thermal requirements and mass and volume constraints, the selected design consists of composite spherical shells that open up with two hydraulic cylinders attached to each of the two upper shells. When closed, the two upper shells are clamped together by means of 6 electrical actuators and inflatable seals are inflated in-between each shell. The normal status of the enclosure is fully open or fully closed. However, it is possible to close totally or partially any of the two sides in order to act as a wind shield in case of high wind coming from S-E or N-W, the two dominant wind directions.

3.8 Transporter and Service Modules

The main function of the Transporter is to provide the handling means to relocate the telescope without the need for any additional external devices. A typical relocation sequence can be summarized as follows: (i) unclamp the Relay Optics Structure from the telescope, (ii) unclamp the Telescope, (iii) lift the Telescope, (iv) unclamp the Transporter, (v) lower down the Transporter wheel on the rails and lift the Transporter in driving position, (vi) drive the Transporter beside the station, (vii) attach the Relay Optics to its handling device integrated on the Transporter and lift it, and (viii) drive to the next station. When a change of direction is needed (at one of the rail crossing), the Transporter is stopped at the crossing, lowered and clamped on special interface plates. The wheels are lifted up and rotated by 90° before being lowered on the perpendicular rails. Unclamping and lifting the Transporter enables to drive to the next crossing. At the destination station, the reverse operations are performed.

The Transporter (see Fig. 2) consists of a *frame structure* made of hollow aluminium rectangular profiles. It has been optimized with respect to mass minimization (aluminium), space constraints and earthquake survival during observation and relocation (with telescope load). An inner cylindrical structure supports the enclosure and the Telescope lifting devices. An outer cylinder structure, covered with aluminium panels and equipped with access doors, provides protection of the electronics cabinets and the Service

Modules that are fitted in-between the two cylinders. The four *drive wheel* blocks, attached to the outer cylinder, include the electrically driven wheel and hydraulically driven lifting, rotation and blocking mechanisms. The *telescope lifting device* consists of 8 lifting actuators linked to cardan shafts which are driven by two electric motors. The Relay Optics handling device uses two electric linear actuators linked by a floating shaft.

The other functions of the Transporter are to provide air conditioning, cooling liquid, auxiliary power as well as hydraulic and pneumatic power for the various mechanisms. It also provides the space for the control electronics cabinets.

The *air conditioning system* provides temperature control during the day based on three temperature sensors located on the primary mirror, plus six other sensors distributed on the telescope structure. The mirror temperature is controlled to $\pm 0.5^\circ\text{C}$ of ambient air with the capacity to cool the mirror by 2°C in about 3 hours. The cooling power is injected with filtered, re-circulated air through a circular fabric duct with constant flow and high induction to ensure temperature homogeneity. The control is done through a PLC with an optimal set point computed by the ESO AT Control System based on outside temperature measurement and forecast for the next night.

The *liquid cooling module* is providing cooling power during observation for temperature control of electronic cabinets and heat-dissipating equipment such as motors, coude sensors and small mechanisms. The remaining heat dissipated in the vicinity of the optical beam is maintained below 25W and surface temperatures are kept at ambient $\pm 1.5^\circ\text{C}$. In order to avoid the vibration of the chiller during observation, the cooling energy is stored inside a tank of heat latent nodules. The cooling capacity is 1 kW during 12 h and is re-generated during the day by running the chiller.

Figure 7: The first Transporter sees the sun light for the first time at AMOS (Liège, Belgium) during its functional tests last October. A dummy station will permit testing of the telescope on the sky before shipment to Paranal.

The *auxiliary power module* consists of a set of batteries feeding a UPS to provide uninterrupted power to the control electronics as well as an electrogen group connected to the UPS to provide electric power during relocation when the telescope is unplugged from its station socket.

The *hydraulic group* provides the required oil pressure and flow for the various hydraulic mechanisms. Such mechanisms are used for the Transporter wheels 90° rotation, the Transporter lifting, the clamping of Transporter to ground, Telescope to ground and Relay Optics Structure to Telescope, as well as for the Enclosure opening/closing.

Finally, a *pneumatic system* is used to inflate/deflate the Enclosure seals and to activate the Telescope axes brakes.

3.9 Station equipment and rails

The station equipment consists of a set of *Telescope interfaces*, *Transporter interfaces* and a *station lid*. The telescope interface is made of a plate whose upper face is machined to provide a perfect supporting plane for the telescope anchoring counterparts. These counterparts are male elements consisting of a clamping finger placed inside a cone. They come into the corresponding conical part of the telescope clamping device to form a pseudo-kinematic interface. The station Lid is a composite hexagonal cover fitted with a seal. It ensures good thermal insulation, air tightness and resists to a 500-kg central load. It can be handled by two persons.

The *rails* are standard rolled steel profile with end cut at 45° to ensure smooth load transfer at the junctions. At a crossing, a specific design enables to transfer the load from the central rolling





Figure 8: Installation of the AT interface devices inside each of the 30 observing stations at Paranal. A high-precision alignment method using theodolite and specific tools is used to reach a positioning accuracy below a millimetre and an arcminute.

surface of the wheel to its two lateral flanges. At each track end, an end-stop is installed.

3.10 Control system

The design & implementation of the control system is shared between AMOS and ESO. AMOS is responsible for the Transporter control including the complete relocation sequence and the Service Modules while ESO is in charge of the complete Telescope Control including control of the axes, the M2 support, the field stabilization loop as well as the small telescope mechanisms such as M10.

On the AMOS side, two *Programmable Logical Controllers* (PLC's) perform the control tasks. The first one (Sauter) is dedicated to the Air Conditioning and Liquid Cooling Module while the second one (Siemens) controls the other Transporter functions including those needed during relocation. For the latter, the operation is done locally from a portable control panel (see Figure 7). Both communicate with the ESO Local Control Units (LCU's) for exchange of status information and commands when needed (e.g. switch on/off air conditioning, set reference temperature, open/close enclosure, etc.)

On the side of ESO, the control system adheres to the Hardware and Software standards adopted for the VLT. It is based on a distributed architecture of *workstations* (Unix) connected to the LCU's (VxWorks) via a LAN (Ethernet). For each AT, the control electronics located on-board the Transporter is connected through the station plug and the LAN optical fibres to the VLT or VLTI Control Room from where all control is done during regular operation (i.e. except for relocation).

The design of the *Software* makes extensive re-use of the Telescope Control Software (TCS) implemented on the UT with a few modifications required by the difference in hardware.

However, two significant new approaches have been applied on the AT. On the Hardware side, a fully digital control scheme was selected in place of the former analogue velocity controllers for the telescope axes. This was one of the first applications of what has become now a new VLT standard: the generic Tool for Advance Control (TAC). Its main advantage is the possibility to configure and optimize the control algorithm in a very flexible manner even at runtime. TAC is now used for several applications in the VLT/VLTI (OPD Controller, FINITO). On the Software side, the Unified Software Development Process with the Unified Modeling Language (UML) has been introduced at the beginning of the AT project.

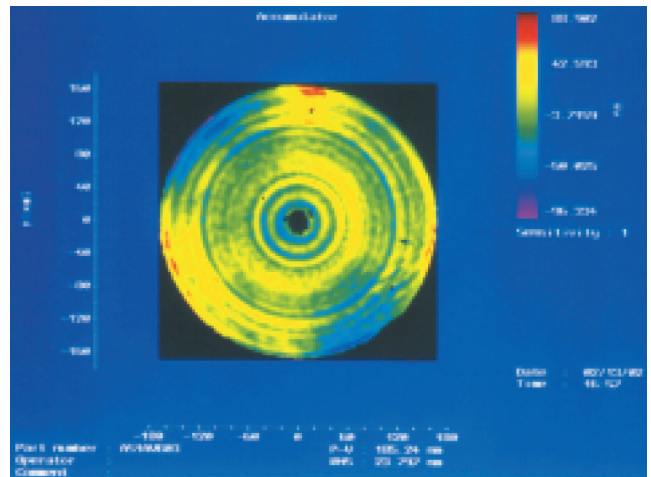
4. Current Status

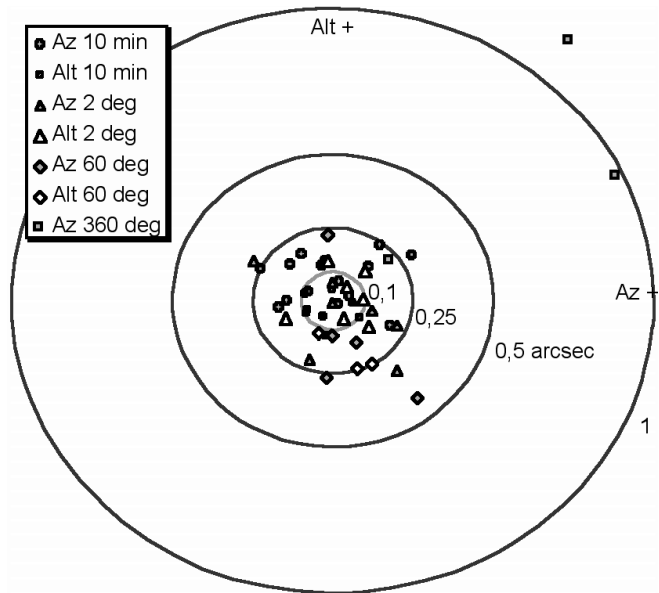
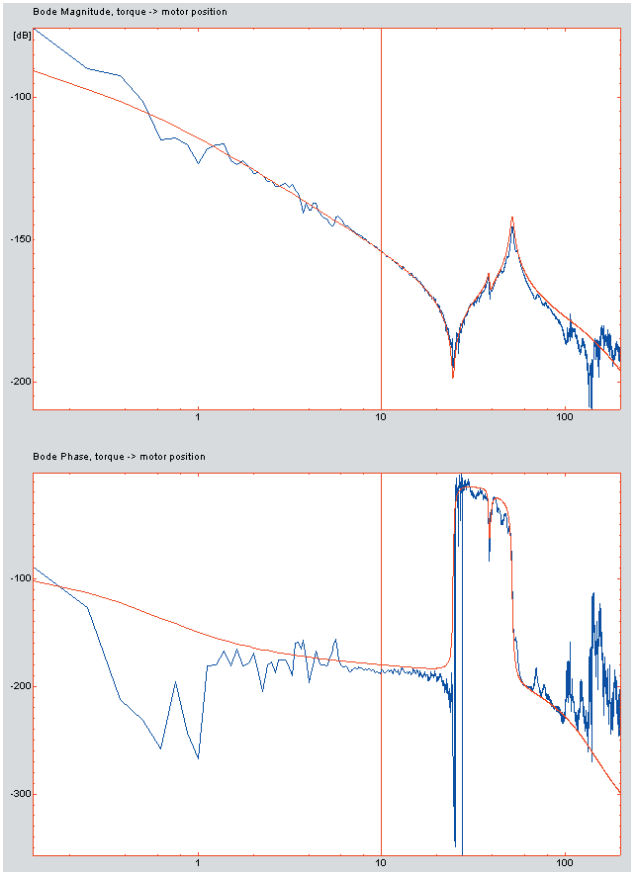
As far as optics are concerned, the full set of 11 mirrors is complete for each of the first three ATs except the primary mirrors for AT#2 and AT#3 that are respectively under final figuring and machining. The blank for AT#4 has been ordered and light-weighting will start before the end of the year. Each mirror has been successively polished within its very tight allocated specification derived from the global telescope image quality given in Table 1. As an example, the phase map of the first primary mirror for AT#1 is shown on Figure 9. The achieved wavefront error amounts to less than 24 nm RMS. This is an ex-

Figure 9: The 1.8-m primary mirror of AT#1 after polishing. The wavefront error is below 24 nanometers RMS

cellent achievement for the first mirror of this size and short focal ratio manufactured by AMOS.

Currently, the first AT is in its last testing phase at AMOS. The telescope, fully integrated with optics, is anchored on a dedicated station (see Fig. 5) where all the major performance tests have been completed, as described in the next section. Meanwhile, the Transporter has also been fully integrated and the second telescope – partially integrated – has been placed inside in order to proceed with an extensive functional test phase during which all motions required for the relocation have been exercised and tuned (see Fig. 7). One of the main remaining activities is the testing of the relocation performance, including the time to relocate (less than 3 hours) and the repeatability of the telescope positioning ($\pm 100 \mu\text{m}$ and $\pm 10 \text{ arcsec}$). The latter was already successfully tested on a breadboard during the design phase. The other important remaining test concerns the performance of the thermal control provided by the air conditioning module during the day and by the liquid cooling module during night observation. In January, the formal technical acceptance in Europe of the first AT will take





▲ Figure 11: Overview of measured non-repeatable pointing error in arcsec on the sky for various angular motions of the altitude and azimuth axes. The circles represent the requirement specifications for the various angular ranges.

◀ Figure 10: Azimuth axis dynamic response (measured and fitted model) used to verify the control bandwidths needed for accurate telescope tracking.

place. Subsequently, the system will be handed over to ESO for a 3-month test period in Europe where the ESO Control System will be tested and fine-tuned with a possibility for sky observations. The first AT will then be packed and sent to Paranal where re-integration will start mid-2003.

The second and third telescopes are currently in the assembly process. Most of the sub-contracted equipment for the telescopes such as the main drives, M2 hexapods, bearings are integrated. The Transporter for AT#2 is being assembled while the one for AT#3 is still under manufacturing.

At Paranal, the preparatory activities are taking up momentum in order to be ready to receive the first AT. The telescope interface devices have been installed and carefully aligned in each of the 30 stations (see Fig. 8) and the rail installation is about to start.

5. First Results from Telescope Performance Tests

In order to verify system-level performance requirements before the final commissioning on site, an extensive test program has been carried on AT#1 at AMOS. Some of the most important results are reported below.

5.1 Verification of the telescope axis dynamic response

The dynamic transfer function between the motor torque reference and

the signals from the tachometer or the position encoder is a critical characteristic for an accurate, high-bandwidth control of the telescope axes (under the responsibility of ESO). For this reason, the dynamic responses of both altitude and azimuth axes have been specified and measured. Figure 10 shows the result of the measurement to which a simplified dynamic model of the telescope could be fitted in order to verify that the control bandwidth and stability criteria will be met when ESO plugs in its telescope control system. The results are well within the specifications of 8 Hz bandwidth for the velocity loop and 2 Hz bandwidth for the position loop.

5.2 Verification of the Optical Path Length stability

One of the most unusual and difficult requirements for the AT is the stability of the Optical Path Length (OPL) inside the telescope that is required by interferometric observations. The OPL variation was a driving parameter of the telescope mechanical design where optimization processes were necessary to fulfil the specifications. The identified contributors to the OPL variation are the vibrations resulting from the dynamic wind load, the normal micro-seismic activity and the Transporter and telescope active sources during operation. In order to verify the contribution of the telescope internal vibrations to the total OPL stability budget, a dedicated OPL test set-up was designed using a com-

bination of laser interferometer and accelerometer measurements. The M1-M2 OPL variation was measured by means of two high-sensitivity accelerometers while the OPL variation from M2 to M11 was measured by means of an HP Doppler interferometer. The results of the OPL test were combined together with the other contributors to the OPL stability as computed by analysis such as the wind load and the micro-seismic disturbances. The consolidated budget appears to be compliant with the specifications.

5.3 Verification of non-repeatable pointing error

The pointing accuracy is particularly important for a telescope dedicated to interferometry. Indeed, the standard interferometric observing strategy consists in switching rapidly (every 1 to 3 minutes) between the scientific object and a calibrator of known diameter that is used to calibrate the time varying instrumental and atmospheric visibility losses. Poor pointing repeatability requiring full acquisition sequences can therefore seriously affect the efficiency of the observation. A test was dedicated to measure the non-repeatable part of the AT pointing accuracy for five pointing directions distributed over the operational range. A collimator and five folding mirrors were installed above the telescope. The collimated light, sent via one folding mirror, is focused at the coudé focus on a CCD. The image po-

sition is recorded before and after the telescope has been moved back and forth by a given angle (from 10 arcminutes, up to 60 or 360 degrees) in altitude and azimuth directions. Due to the very small pointing errors to be measured (0.1 to 1 arcseconds), particular attention had to be paid to the thermal environment and to the processing method in order to eliminate thermal drifts of the measurement set-up. Figure 11 gives an overview of the excellent results obtained, basically limited by the residual measurement noise of 0.13 arcsec.

6. Conclusion

This article provides an overview of the current development of the Auxiliary Telescopes for the VLTI. The main performance tests of the first telescope are completed. They have shown that the system is on track to meet the severe and specific requirements originating from its dedication to interferometry, in particular a high dynamic performance. The functional tests related to the relocation of the telescope have been successfully completed on the first Transporter and the

related performance tests are currently in progress. Early next year, the first AT will be ready for a short ESO test period in Liège to tune the telescope control system developed in parallel at ESO. The year 2003 will see the installation at Paranal of the first two ATs. This will considerably boost the scientific productivity of VLTI that will, at that time, be equipped with its two first-generation instruments: MIDI and AMBER. AT#3 is expected to be ready for scientific observation in mid-2004 and AT#4 in early 2005.

Paranal Observatory – 2002

ROBERTO GILMOZZI and JASON SPYROMILIO

We live in interesting times. Last year was our first with all four 8-m telescopes in operation. We had only one instrument per telescope but we were kept busy with UVES and ISAAC working round the clock and commissioning and installations during bright time when FORS1 and FORS2 were taking a breather. Now at the end of 2002 we look at Paranal and a very different picture appears in front of us.

We continued to operate with low technical time losses. In the period from April to October 2002 the down time was 3.6% on Antu, 4.4% on Kueyen,

2.9% on Melipal, and 3.1% on Yepun. Observing time losses due to adverse weather conditions represented 12% of the science time, somewhat more than in previous years. We archived 57,810 frames on ISAAC, 34,329 frames on UVES, 22,853 frames on FORS1 and 37,847 frames on FORS2.

NAOS/CONICA has been brought into operation in a major effort by the consortia that built it, ESO instrumentation division and Paranal. All parties pulled out all the stops to start science operations on the 1st of October 2002. NACO, as we now call the otherwise

unwieldy named instrument, is widely recognized as the most powerful adaptive optics facility instrument in the world. Already fabulous results have appeared in press releases and more are to come. The spectacular results on the Galactic centre have demonstrated the excellent capabilities of the instrument. UT4 now has two instruments and both dark and bright time are fully exploited for science.

VIMOS appeared, somewhat overweight and with all the challenges of what in effect is four imaging, multiobject spectrographs mounted on a single frame. Starting with two arms, it then had a leg added to it and another two arms making the whole thing quite a sight to be admired on the Nasmyth B platform of UT3. All of this under the careful supervision of Paranal engineering and extensive testing and discussions to ensure that nothing untoward occurred as we pushed the rotators beyond their specified and tested range. Again with a lot of work from the consortium and the support of the instrumentation division and the ever present Sandro D'Odorico, we have now reached the stage of Paranalization of the instrument and we have a fixed date with our customers on the 1st of April 2003. Already the PI (Olivier Le Fevre) has claimed success with the execution of the entire CFR Survey executed in a single exposure.

In the mean time FLAMES arrived in parts and has slowly grown to occupy the totality of the Nasmyth A platform of UT2. First OzPoz, the fibre positioner and then GIRAFFE the spectrograph to take the 130 spectra at medium resolution simultaneously. OzPoz did puzzle us for a while. Mostly it puzzled the consortium that built it. After a few interventions on the instrument to make sure it fit to the telescope properly and to make sure it could cope with the real



Figure 1: The VST enclosure taking shape at the edge of the Paranal platform.

operational temperatures, it worked well enough to give us confidence to offer the instrument to the community also on April 1st 2003. Paranalization is in full swing also for FLAMES and the visits from Australia to fix it are rare.

FORS1 moved back to UT1 to make dark time available to VIMOS. Now UT1, UT2 and UT4 have dark and bright time instruments attached and either offered or just about to be. UT3 with VIMOS is eagerly awaiting VISIR next year.

On UT4 we added a laser clean room, kindly provided by telescope division in Garching. This is a whole new platform under the Nasmyth B focus of UT4 with a fancy room to house the laser for the artificial guide star to be installed at the VLT in 2003. We mounted a small telescope on the back of the secondary of UT4 to check for flexures and entertained ourselves and Martin Cullum trying to work out where the thing was pointing. In any case the flexures are low and we await the laser and the fibre to carry the light plus the launch telescope during 2003.

This would be enough for most observatories to be going on. However, Paranal is more than a home for four 8-m telescopes. The interferometer continues to grow in capabilities and improves its operations. Last year we started the installation and first runs with the tip-tilt boxes at the coudé foci. Stabilized beams were fed from UT1 and UT3 into VINCI and excellent fringes were obtained. In 2002 the systems were stabilized operationally with very few nights of sky time. The other two coudé trains (UT2 and UT4) were installed aligned and tested. The reader should be aware that 11 mirrors appear in the normal coudé train before the beam is sent on the interferometer delay line tunnel. In September we obtained fringes with all four telescopes marking a major milestone in the development of the interferometric capabilities of Paranal.

In November, MIDI, our first fully fledged interferometric instrument arrived on site and is being integrated as this article is being written. First light should arrive soon. AMBER, FINITO and full coudé adaptive optics on the UTs for VLTI are all in the plan for 2003.

Three additional delay lines are being installed into the tunnels and variable curvature mirrors added to the system to better control the position of the pupil. The VLTI complex is reaching a maturity of operation at Paranal that is comparable to that of the UTs. We eagerly await the arrival of the first auxiliary telescope next year and the preparations on Paranal are ongoing with the alignment of the docking stations and the installation of the tracks.

In September of 2002, a set of boxes arrived on Paranal containing suspiciously Paranal blue metal pieces. At



Figure 2: The primary of UT3 coming out of the coating chamber with a reflectivity of 92% and a micro-roughness of 7 Ångströms. The best coating ever at Paranal.

the time of writing these pieces are starting to be placed on top of the VST concrete pier for the enclosure of our next telescope. The enclosure is expected to be finished in early 2003 and the telescope is to be installed soon after. A few weeks before the enclosure erection begun we received the boxes containing the VST 2.6-m primary and secondary mirrors. Unfortunately the primary mirror was destroyed during transport. Our colleagues at the Osservatorio di Capodimonte in Naples who are building the telescope very quickly ordered a replacement mirror and if all goes well we expect no significant delay to the project.

We welcomed the VISTA site supervisor to Paranal and we prepare for the start of the works to accommodate the 4-m infrared wide field telescope.

The smallest telescope on Paranal was also commissioned. Called Mascot (ask J.G. Cuby) it is an all-sky camera based on simple commercially available components and with some in house ingenuity it makes its images available in real time on the UT consoles. The operators still go out to have a look.

Coating mirrors on Paranal is a never ending story. However, in 2002 we have reached a peak of activity. At the time of

writing we are removing the primary and tertiary from UT1 and plan in the next few days to have the fourth 8-m coating this year. Moving these mirrors around and going through the cleaning and coating process, along with all the preventative maintenance that is performed on the domes and telescopes while the glass is out, is a major engineering effort organized to the minute and synchronized with great precision. The observatory is now undertaking the maintenance of the passive supports for the cell in an effort that is supported by La Silla who are providing the workshop space.

In January of 2002 we all moved into the new Paranal residence. The long stay in the containers is finally over and we now have a pleasant and comfortable environment in which to live. Work on Paranal is by necessity associated with long absences from family and friends and extreme weather conditions, in particular very low humidity. The new residence attempts, and we believe succeeds, to reduce the hardships associated with work on site.

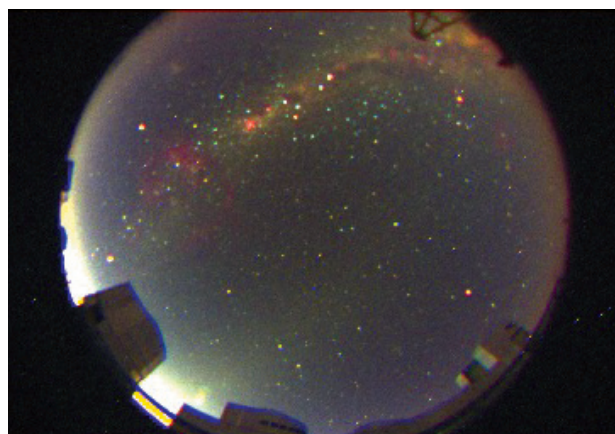


Figure 3: All-sky image from Mascot Camera which monitors the cloud cover on Paranal continuously during observations.

Some of the containers are being retained as we continue to build on Paranal (e.g. VST and VISTA) and often have more people working on site than are expected in a steady state of operation. The recent MIDI commissioning required for the reactivation of some containers for ESO and consortium staff. Not all were happy with the move back to the not-so-good-old days.

The new Visitor's Centre was concluded and is in use for the weekend visitor programme, and as a starting point for VIP visitors.

The scale of the Paranal operation is often difficult to appreciate. Ourselves on the mountain find it all fairly normal. To put it into context the ESO Paranal

casino serves approximately 100,000 meals every year and we have 40,000 overnight stays per year. Paranal is not connected to the Chilean electricity grid and has to generate its own power (up to three megawatts). Water is of course a necessary resource and we can store up to 1 million litres in our tanks. Keeping the observatory supplied requires a water tanker truck to arrive on site every 8 hours, every day of the year.

In 2002, Joerg Eschwey, who more than any other individual has personified the challenge and success of creating a whole observatory and its infrastructure in the middle of the Atacama desert, has moved on from the VLT to

the ALMA project. With this move a small shake up of the observatory organization was necessary and it has been a pleasure to welcome Frank Ruseler from the Santiago office of ESO to Paranal where he has taken over the logistics department.

The year ahead of us promises to be as exciting as this past one. VISIR, VST, OmegaCAM, MACAOs for the UTs, FINITO, AMBER, Auxiliary telescopes and the laser guide star all intend to arrive on Paranal. Times will continue to be interesting on Paranal for the foreseeable future. Exciting new facilities and capabilities continue to be added to this astronomy wonderland.

News from La Silla: Science Operations Department

O. HAINAUT

This year has seen a major restructuring of the internal workings of La Silla observatory. While this is not immediately obvious to the visiting astronomer, it prepares the observatory for the future and decreasing staffing levels. In particular, the engineering and telescope teams have been reorganized and now constitute two departments:

(1) La Silla Engineering Department (LED). This is a merger of the previous Mechanics, Electronics and Instrumentation teams. This department is responsible for the maintenance of the telescopes and projects taking place at La Silla.

(2) La Silla Science Operations (SciOp). This team actually operates the telescopes.

The Infrastructure Support Group (ISG), Software and Communications (SWC), Logistics, and Management departments all keep the same structure as before.

La Silla SciOp

This is a merger of the three former telescope teams (NTT, 3.6-CAT and Medium-Sized Telescopes) which were abandoned in order to optimize human resources. SciOp currently consists of 17 astronomers, 18 TIOs, and 2 operation engineers who are allocated to different "Instrument Forces". The astronomers and TIOs work within a specific instrument force to focus their expertise on instruments of a particular type. For example, the Infrared Instrument force consists of SOFI and TIMMI2. All people working within this force will support both of these instruments.

Each force is led by one of the Instrument Scientists, and primary responsibilities include implementing a coherent calibration plan, producing consistent documentation, observing templates, etc., and following-up developments and problems that may occur with the instruments within the instrument force.

The La Silla web pages will be restructured to reflect the organizational changes in the observatory, and in particular to make comparisons between instruments simpler. If you have a query about a particular instrument, you should contact the corresponding instrument force (see below). You can also contact La Silla SciOp by sending an email to lasilla@eso.org. This account is continuously monitored by the SciOp Shift Leader (one of the astronomers on duty) who will then forward your query to the correct person.

This email address is the best way to contact us in order to receive a fast reply.

The new web page of SciOp is available at <http://www.ls.eso.org/lasilla/sciops/>. Here you will find links to all the instrument pages, as well as more information on the new structure.

The RITZ!

For the visiting astronomer, most of the above will probably go largely unnoticed. The one big change for visitors is the opening of the new control building (nicknamed "RITZ", for Remote Integrated Telescope Zentrum). This new, central observing hub of La Silla is located at the bottom of the NTT access ramps in front of the "Sarcophagus" (Figure 1). It is 300 metres square and will ultimately host the con-

Instrument Force	Instruments	Contact email
Imaging	WFI 2.2-m SUSI2 NTT	ls-imaging@eso.org
Visible Spectro-Imagers	EFOSC2 3.6-m EMMI NTT	ls-spectro@eso.org
Infrared	TIMMI2 3.6-m SOFI NTT ADONIS 3.6-m	ls-infrared@eso.org
High-Res. Spectroscopy	FEROS 1.5-m/2.2-m CES 3.6-m HARPS 3.6-m EMMI-Echelle NTT	ls-hires@eso.org
Telescopes	NTT, 3.6-m, 2.2-m	ls-telescopes@eso.org

trol rooms of the NTT, 3.6-m and 2.2-m telescopes in a common area, allowing us to operate the telescopes more efficiently.

The RITZ was built with the comfort of its inhabitants in mind. Toward the west, it has many large windows overlooking the valley and ocean, with a fantastic view of the sunset (and potential green-flashes). On the other hand, its walls are almost completely blind toward the north-east since this is the direction from which the wind blows most of the time. All of the control computers are located in separate rooms behind the consoles, allowing us to keep the computers cold and the control room temperate. These computer rooms also provide additional thermal insulation for the main working area, and keep it free from the noise of the many workstations. The floor plan of the main control room, as well as the materials chosen for the walls and ceiling are ergonomically optimized, ensuring that sounds are damped and glare from the windows is avoided.

Since October 18, the NTT has been operated fully remotely from the RITZ. We hope to move the 2.2-m control room this year, and the 3.6-m early next year.

News from the Instruments and Telescopes

From the start of Period 70 (start of October), and as reported in previous *Messenger* articles, the two 1.5-m telescopes on La Silla are no longer offered to the ESO community. The ESO 1.52-m will be operated until the end of 2002, with 100% of the time allocated to Brazilian observers, and the Danish 1.54-m will continue to be used by the Danish community only.

A few months ago, the red CCD of EMMI was upgraded to a mosaic of 2×1 MIT/LL $2k \times 4k$ chips. The quantum



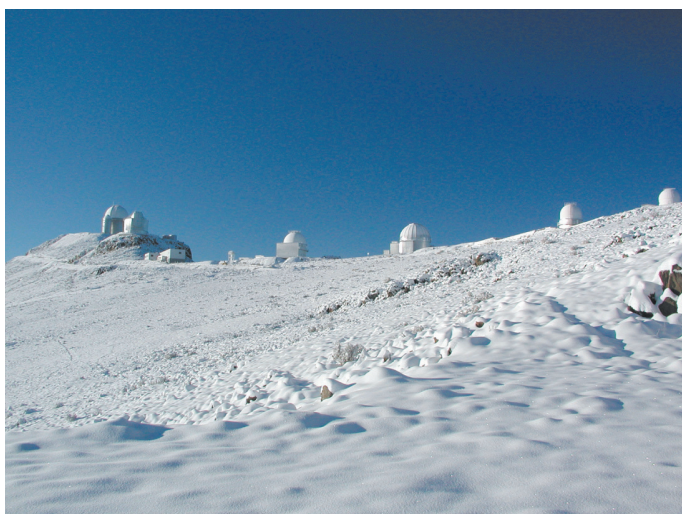
efficiency of the mosaic is significantly higher than that of the former Tektronix CCD and the larger size of the CCDs leads to a wider field of view. In addition, the pixel size (0.166") gives a better sampling in good seeing images and permits narrower slits to be used. However, the most striking feature of the new detector is its read-out time: thanks to the FIERA controller, the 4k chips are read in only 18 seconds, with very low read-out noise. More information can be found on the updated EMMI web pages.

FEROS, the high-resolution, fibre-fed spectrograph that used to be mounted on the ESO 1.52-m telescope, has been transferred to the 2.2-m, where it is now installed in parallel with the Wide Field Imager. The move took place in early October and the instrument is currently being commissioned in its new home. We expect that this will

result in an improvement of the spectrograph's performance by a factor of 2. Keep an eye on the FEROS pages for up-to-date information.

TIMMI2, the mid-IR spectro-imager mounted at the 3.6-m, is currently undergoing a major upgrade: the control electronics and software are being entirely replaced by an IRACE controller and VLT-software. This will improve the performance of the instrument, but more notably, it will make its operation and maintenance much more straightforward. Also, for the observer, the main difference will be that TIMMI2 will be operated from the standard P2PP-BOB interfaces.

Finally, ADONIS, the adaptive optics system at the 3.6-m, was retired at the end of August after almost 10 years in service. The field of high resolution imaging is now carried by NAOS-CONICA on the VLT.



Two unusual views of La Silla. The left-hand picture shows La Silla immediately after the snow storm of 28 August 2002. Some weeks later the desert around La Silla was for a short time transformed into a sea of flowers. Photos by Peter Sinclair.

Extra-Solar Planets

N.C. SANTOS, M. MAYOR, D. QUELOZ, S. UDRY

Observatoire de Genève, Sauverny, Switzerland

Introduction

The widely accepted picture of stellar formation tells us that a planetary system is a simple by-product of the stellar formation process. When a cloud of gas and dust contracts to form a star, conservation of angular momentum induces the formation of a flat disk around the central newborn “sun”. By a process still not fully understood, this disk is believed to be the stage for the planetary formation. According to the traditional paradigm, dust particles and ice grains in the disk are gathered to form the first planetary seeds (e.g. Pollack et al. 1996). In the “outer” regions of the disk, where ices can con-

densate, these “planetesimals” are thought to grow in a few million years. When such a “planetesimal” achieves enough mass (about 10 times the mass of the Earth), its gravitational pull is sufficiently strong for it to start accreting gas in a runaway process that gives origin to a giant gaseous planet similar to the outer planets in our own Solar System. Later on, in the inner part of the disk, where temperatures are too high and volatiles cannot condensate, silicate particles are gathered to form the telluric planets like our Earth.

In the past decade, images taken by the NASA/ESA Hubble Space Telescope (HST) have revealed a multitude of such proto-planetary disks in the

Orion stellar nursery, showing that disks are indeed very common around young solar-type stars. This supports the idea that extra-solar planets should be common. However, such systems have escaped detection until very recently.

In fact, it was not until 1995, following the discovery of the planet orbiting the solar-type star 51Peg May95, that the search for extra-solar planets had its first success¹. This long wait was mainly due to the difficulty of detecting such bodies. Planets are cold objects, and their visible spectrum results basically from reflected light of the parent star. As a result, the planet/stellar luminosity ratio is of the order of 10^{-9} . Seen from a distance of a few parsec, a planet is no more than a small “undetectable” speckle embedded in the diffraction and/or aberration of the stellar image.

The detection of exoplanets has thus been based, up to now, upon “indirect” methods. In particular, all the planetary discoveries were only possible due to the development of high-precision radial-velocity techniques. These methods, that measure the motion of a star along the line of sight (by measuring the Doppler shift of spectral lines), have now achieved precisions of the order of a few m s^{-1} ($\Delta\lambda/\lambda \sim 10^{-8}$). Such a high precision is indeed needed to find a planet: for example, Jupiter induces a periodic perturbation with an amplitude of only 13 m s^{-1} on the Sun!

In this article we will review the current status of planetary searches, presenting the major challenges that we are facing at this moment. We will then discuss how new and future generation instruments and missions will help to answer the most important questions. We will concentrate mostly on the results we can expect from future radial-velocity campaigns with state-of-the-art instruments like HARPS on the ESO 3.6-m telescope (see article by Pepe et al. in this issue).

A Diversity of Planets

Today, about 100 extra-solar planetary systems have been unveiled

¹Before this discovery, only planets around a pulsar had been detected (Wolszczan & Frail 1992); however, these are probably second-generation planets. In this article we will concentrate on planets around solar-type stars.

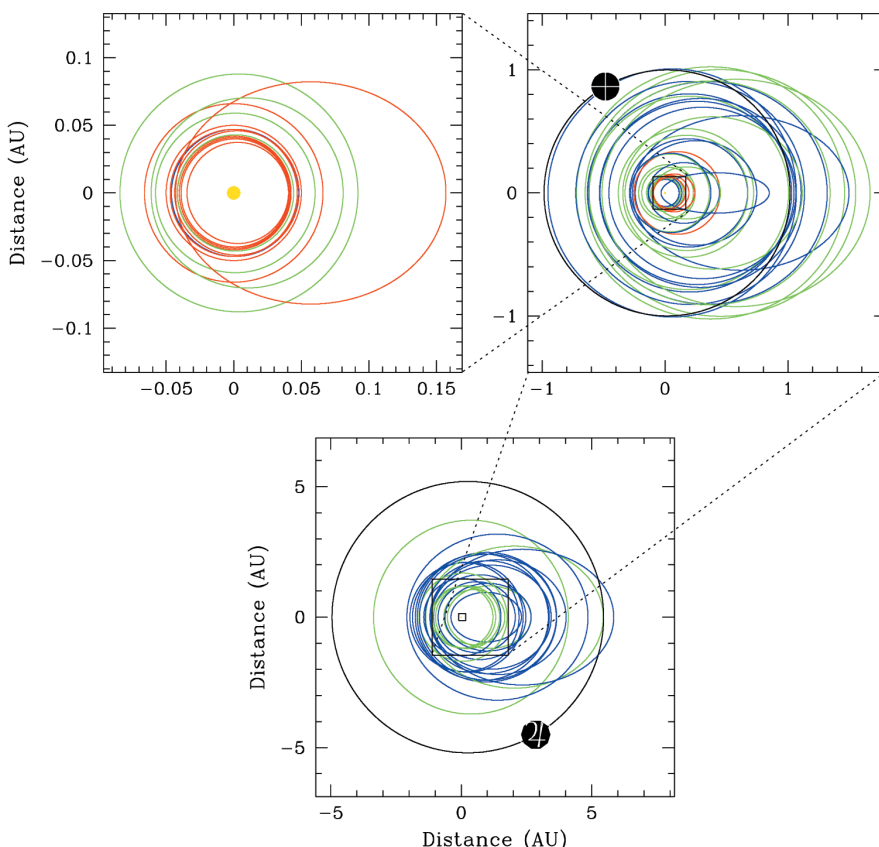


Figure 1: Schematic orbital configurations for some of the newly found extra-solar planets in three different scales. In the upper-left panel we represent the orbits of the shorter-period companions. The Sun (yellow circle) is drawn to scale. This plot illustrates well both the proximity of these planets to their host stars, and the complete lack of planetary companions orbiting closer than a certain distance (see text for more details). The upper-right and lower panels illustrate the situation concerning longer orbital period planets. In these two plots, the orbits of the Earth and Jupiter are also drawn for comparison (with the usual symbols). These three panels clearly illustrate the huge variety of orbital parameters presented by the extra-solar planets.

around stars other than our Sun². These discoveries, which include ~ 10 multi-planetary systems, have brought to light the existence of planets with a huge variety of characteristics, opening unexpected questions about the processes of giant planetary formation.

The diversity of the discovered extrasolar planets is well illustrated in Figure 1. Unexpectedly, they don't have much in common with the giant planets in our own Solar System. Contrarily to these latter, the "new" worlds present an enormous and unexpected variety of masses and orbital parameters (astronomers were basically expecting to find "Jupiters" orbiting at ~ 5 A.U. or more from their host stars in quasi-circular trajectories). The majority of the discovered planets were not even supposed to exist according to the traditional paradigm of giant planetary formation (e.g. Pollack et al. 1996). Their masses vary from sub-Saturn to several times the mass of Jupiter. Some have orbits with semi-major axes smaller than the distance from Mercury to the Sun, and except for the closest companions, they generally follow eccentric trajectories, contrarily to the case of the giant-planets in the Solar System.

These findings have put into question the former planetary formation paradigm. However, the relatively large number of discovered planets is already permitting us to undertake the first statistical studies of the properties of the exoplanets, as well as of their host stars. This is bringing new constraints to the models of planet formation and evolution. Let us then see in more detail what kind of problems and information these new discoveries have brought.

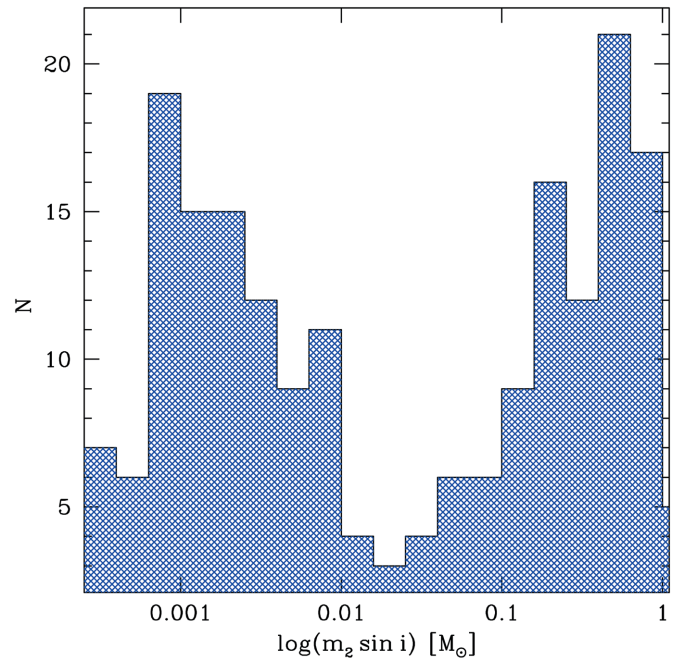
The Period Distribution

One of the most interesting problems that appeared after the first planets were discovered has to do with the proximity to their host stars. The first planet discovered (around 51Peg – Mayor & Queloz 1995) is exactly the first such example: it orbits its star once every 4.2 days, corresponding to an orbital radius of only 0.05 A.U. This is much less than the distance from Mercury to the Sun.

The problem that was raised with the finding of these 51Peg-like planets (usually called "hot-Jupiters") resides in the fact that at such close distances the temperatures are too high for ices to condensate, and there does not seem to exist enough available material to form a Jupiter-mass planet. It is thus very difficult to imagine that such worlds could be formed so close to the central stellar furnace.

²For a complete and updated list of the known exoplanets, see e.g. table at <http://obswww.unige.ch/exoplanets>.

Figure 2: Distribution of minimum masses for the currently discovered low-mass companions to solar-type stars. Although the radial-velocity method has a higher sensitivity to higher-mass companions, the observed distribution rises very steeply towards the low-mass domain. From this mass up to the stellar regime, only a few objects were detected; this region is usually denominated the "Brown-Dwarf desert". This gap in the mass distribution of low-mass companions to solar-type stars supports the view that the physical mechanisms involved in the formation of these two populations (planets vs. stars) are very different.



In order to explain the newly found systems, several mechanisms have thus been proposed. Current results show that *in situ* formation is very unlikely, and we need to invoke inward migration, either due to gravitational interaction with the disk (Goldreich & Tremaine 1980) or with other companions to explain the observed orbital periods. In other words, the observed close-in planets could simply have been formed far from their host star, and then migrated inwards.

But the migration mechanisms, that have broken long-lasting ideas of "stability" of the planetary systems, have some problems to solve. According to the models, the timescales of planetary migration in a disk are particularly short. This means that more than worrying about how planets migrate after or during their formation, we need to understand how migration can be stopped (and/or slowed down)!

One particularly interesting clue comes from the observation that there is a clear pile-up of planetary companions with periods around 3 days, accompanied by a complete absence of any system with a period shorter than this value. This result, which is in complete contrast with the period distribution for stellar companions (we can find double stars with periods much shorter than 3 days), means that somehow the process involved in the planetary migration makes the planet "stop" at a distance corresponding to this orbital period. To explain this fact, several ideas have been presented. These invoke different mechanisms like e.g. a magnetospheric central cavity of the accretion disk (once the planet gets into this cavity it will no longer strongly interact with

the disk and consequently stops the migration), photo-evaporation, tidal interaction with the host star, or Roche-lobe overflow of the young inflated giant planet (processes resulting in an increase of the orbital radius of the planet, thus opposing the migration tendency)³.

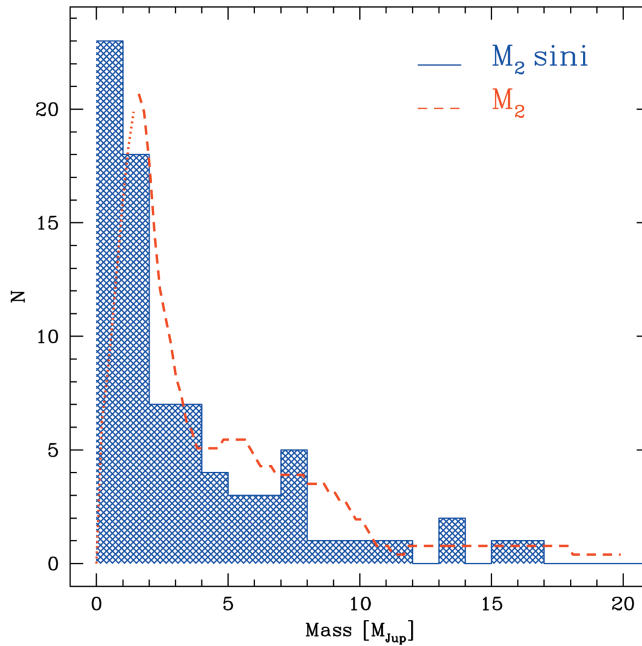
In any case, even if these mechanisms are able to explain how the shorter period planets have stopped migration, they do not explain how the longer period ones (like Jupiter itself) did not migrate to distances closer to their host stars. The key to this might have to do with a combination of parameters, like the disk masses, lifetimes, viscosities, and initial planetary masses and/or number of bodies formed, that will affect the final orbital configuration of a planet. Some of these parameters are not well known (maybe the planetary formation itself is controlling them), something that complicates the discussion.

The Mass Distribution

Very important information is brought to us by the analysis of the mass spectrum of the planetary companions. In particular, a plot showing the mass distribution of companions to solar-type stars (as shown in Figure 2), shows a clear discontinuity for the mass regime between about 30 and 50 times the mass of Jupiter: there are basically no companions found to date having those masses. This result is even more striking if we note that the radial-velocity

³Planets migrating more than this approximate limit might "simply" also evaporate/transfer material to the host star, and thus disappear or become too low-mass to be detected.

Figure 3: Distribution of exoplanet masses. The histogram represents the observed minimum mass distribution, while the red line represents the statistical true planetary mass distribution resulting from a deconvolution of the unknown orbital inclinations. The distribution reaches “zero” at a mass of about 10 times the mass of Jupiter, which probably corresponds to the upper limit for the mass of a giant planet. The nature of the objects with masses between 10 and ~17 times the mass of Jupiter is still an open question. As in Jorissen et al. (2001).



technique is more sensitive to massive companions than to their lower mass counterparts.

This gap, usually called the “brown dwarf desert”, separates the low mass “planetary” companions from their high mass “stellar” counterparts, and is probably telling us something very important about the physical processes involved in the formation of these two populations: stars, even the low mass ones, are thought to be formed as the result of the gravitational collapse and fragmentation of a cloud of gas and dust. On the other hand, a planet forms in a circumstellar accretion disk.

More information is provided if we analyse the shape of the distribution for the planetary mass regime (Fig. 3). This distribution is observed to decrease smoothly with increasing mass, reaching “zero” at about 10 Jupiter masses (Jorissen et al. 2001). This limit is clearly not related to the Deuterium-burning mass limit of $\sim 13 M_{\text{Jup}}$, sometimes considered as the limiting mass for a planet (this latter value is in fact an arbitrary limit used as a possible “definition”, but it is not related to the planetary formation physics). As it was recently shown by several authors (e.g. Jorissen et al. 2001), this result is not an artefact of projection effects (the unknown orbital inclination implies that we can only derive a minimum mass for the companion from the radial-velocity measurements), but a real upper limit for the mass of the planetary companions discovered so far.

The Period-Mass Relation

Recent results have also unveiled some interesting correlations between the planetary mass and its orbital period. In fact, there seems to exist a paucity of high-mass planetary com-

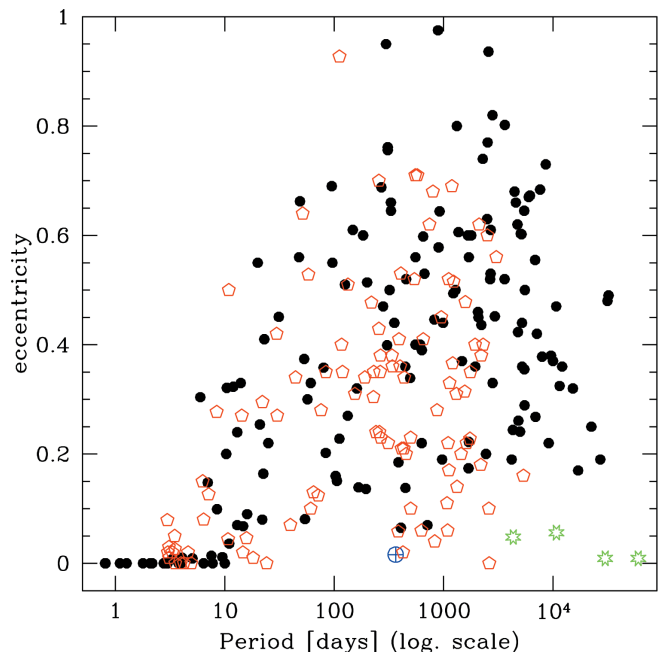
panions ($M > 2 M_{\text{Jup}}$) orbiting in short period (lower than ~ 40 -days) trajectories. Similarly, there seems to be a lack of long-period and very low-mass planets.

These results are further helping us to understand the mechanisms of planet migration, since they are compatible with the current ideas about planetary orbital evolution (either due to an interaction with the disk or with other companions), that suggest that the higher the mass of a planet, the more slowly (and less) it will migrate.

The Eccentricity

One of the most enigmatic results found to date has to do with the analy-

Figure 4: Eccentricity vs. orbital period (in logarithmic scale) for the discovered extrasolar planets (red pentagons), stellar binaries (filled dots), and for the giant planets in our Solar System (green stars). The earth is represented by the usual symbol. Although some long-period exoplanets exist having low values for the eccentricity, most of the systems present much higher eccentricities than those observed for the Solar System giant planets. Possible explanations invoke mechanisms capable of pumping the eccentricity, like gravitational interactions between planets in a multi-planetary system, or with a distant stellar companion.



sis of the orbital eccentricities of the planetary-mass companions. According to the traditional paradigm of planetary formation, a planet (formed in a disk) should keep a relatively circular (low eccentricity) trajectory. Current models shown indeed that the interaction (and migration) of a low mass companion within a gas disk has the effect of damping its eccentricity (Goldreich & Tremaine 1980). However, opposite to expectations, if we look at the eccentricities of the planetary companions we can see that they are spread through values that go from nearly zero to more than 0.9 for the planet orbiting the star HD80606!

In Figure 4 we plot the eccentricity as a function of orbital period for the planetary companions to solar-type stars, as well as for the stellar companions. First of all, it is important to describe the general tendencies observed in the plot. The low eccentricity observed for short-period binaries is the result of a well known effect: the proximity to their primary stars induces tidal interactions that have the effect of damping the eccentricity. Since the tidal effect decreases very fast with distance, above a given orbital period (about 10 days for dwarf star binaries), tidal circularization is no longer effective, and all companions having periods longer than a given value simply keep their “initial” orbital eccentricity.

While both distributions show the signature of tidal effects on the eccentricity, a first glimpse also tells us that there is no clear difference between the two groups of points: stars and planets have a similar distribution in this diagram. This poses the problem of understanding how planetary companions formed in a disk can have the same ec-

centricity distribution as their stellar mass counterparts. And how can this be fit into the picture of a planet forming (and migrating) in a disk?

The explanation for these facts may be other processes capable of exciting the eccentricity of the planetary orbits. These include the interaction between planets in a multiple system or between the planet and a disk of planetesimals, the simultaneous migration of various planets in a disk, or the influence of a distant stellar companion. All or at least some of these physical processes might play an important role in defining the “final” orbital configuration.

Although still not clear, a close inspection of Figure 4 permits us to find a few differences between the eccentricities of the stellar and planetary companions. In particular, for periods in the range of 10 to 30 days (clearly outside the circularization period by tidal interaction with the star), there are a few planet hosts having very low eccentricity, while no stellar binaries are present in this region. The same and even stronger trend is seen for longer periods, suggesting the presence of a group of planetary companions with orbital characteristics more similar to those of the planets in the Solar System (with low eccentricity and long period). On the other hand, for the very short period systems, we can see some planetary companions with eccentricities higher than those found for “stars”. This features may be telling us that different formation and evolution processes took place: for example, the former group may be seen as a sign for formation in a disk, and the latter one as an evidence of the influence of a longer period companion on the eccentricity.

Clues from the Planet Hosts: the Stellar Metallicity

Up to now we have been reviewing the results and conclusions obtained directly from the study of the orbital properties and masses of the discovered planets. But another fact that is helping astronomers understand the mechanisms of planetary formation has to do with the planet host stars themselves. Indeed, they were found to be particularly metal-rich, i.e. they have, on average, a higher metal content than the stars without detected planetary companions (see Santos et al. 2001 for the most recent results) – see Figure 5.

A possible and likely interpretation of this may be that the higher the metallicity of the cloud that gives origin to the star/planetary system (and thus the dust content of the disk), the faster a planetesimal can grow, and the higher the probability that a giant planet is formed before the proto-planetary disk dissipates. In other words, the metallicity seems to be playing a key role in the

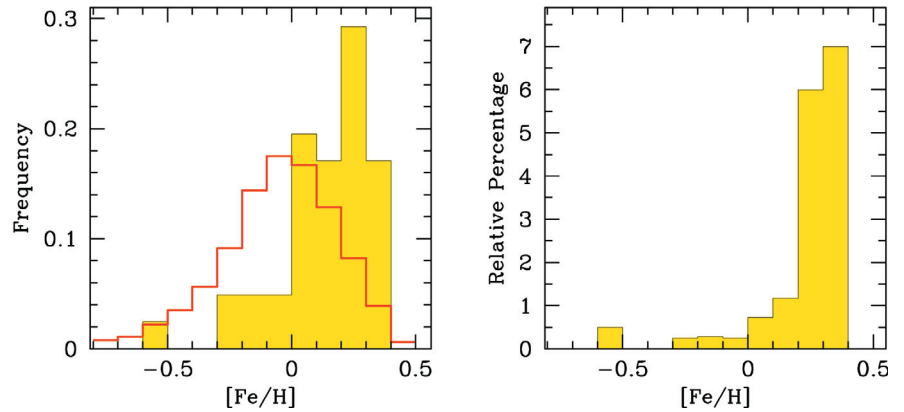


Figure 5: Left: Metallicity ($[Fe/H]$) distributions for stars with planets (yellow histogram) compared with the same distribution for field dwarfs in the solar neighbourhood (open red histogram). In this panel, both distributions are normalized by the total number of points. The $[Fe/H]$ scale is logarithmic, and the Sun has by definition $[Fe/H] = 0$. Most planet hosts are more metal-rich than our Sun; Right: the percentage of stars that have been found to harbour a planet for each metallicity bin, plotted as a function of the metallicity. This plot clearly shows that the probability of finding a giant planet increases with the metallicity of the star. As in Santos et al. (2001).

formation of the currently discovered extra-solar planetary systems.

Boss (1997) has suggested that besides the core accretion scenario (see introduction), giant planets might also be formed as a result of disk instability processes: by the formation and condensation of clumps of gas and dust in the protoplanetary disk. This process is, however, not very dependent on the metallicity. In other words, if the disk-instability models were the most important mechanism involved in the formation of giant planets, we should not expect to see a strong dependence on the rate of planet detection as a function of the metallicity. The huge dependence observed is thus probably a sign that the core accretion scenario is the important mechanism involved in the formation of giant planets.

It is, however, important to stress that it is not precisely known how the metallicity is influencing the planetary formation and/or evolution; for example, the masses of the disks themselves, which can be crucial to determine the efficiency of planetary formation, are not known observationally with enough precision.

A Case of Stellar “Cannibalism”

Recent observations also suggest that planets might be engulfed by their parent stars, whether as the result of orbital migration, or e.g. of gravitational interactions with other planets or stellar companions. Probably the clearest evidence of such an event comes from the detection of the lithium isotope ${}^6\text{Li}$ in the atmosphere of the planet-host star HD 82943 (Israeli et al. 2001). This fragile isotope is easily destroyed (at only 1.6 million degrees, through (p,α) reactions) during the early evolutionary stages of star formation. At this stage, the proto-star is completely convective, and the relatively cool material at the

surface is still deeply mixed with the hot stellar interior (this is not the case when the star reaches its “adulthood”). ${}^6\text{Li}$ is thus not supposed to exist in stars like HD 82943, and the simplest and most convincing way to explain its presence is to consider that planet(s), or at least planetary material, have fallen into HD 82943 sometime during its lifetime.

The most recent and detailed analysis seems to clearly confirm the presence of this isotope. The question is then turned to know whether this case is isolated or if it represents a frequent outcome of the planetary formation process. How much can this process increase the observed metallicity of the planet hosts? Current results suggest that at least the degree of stellar “pollution” is not incredibly high (Santos et al. 2001).

Black Sheep

When measuring the spectrum of a star we are obtaining the integrated light of the whole stellar disk, and gathering photons coming from different points in the stellar surface. Each individual point has its own spectrum, with a different Doppler shift that is a function of the velocity field in that specific region of the stellar photosphere. As a consequence, any phenomenon capable of changing the velocity field of a given region in the stellar surface will change the global spectrum Doppler shift, and consequently the measured radial-velocity.

This result has an important impact when dealing with radial-velocity measurements: the radial-velocity technique is not sensitive only to the motion of a star around the centre of mass of a star/planet system, but also to eventual variations in the structure of the stellar surface.

In fact, phenomena such as stellar pulsation, inhomogeneous convection or the presence of dark spots (e.g. Saer

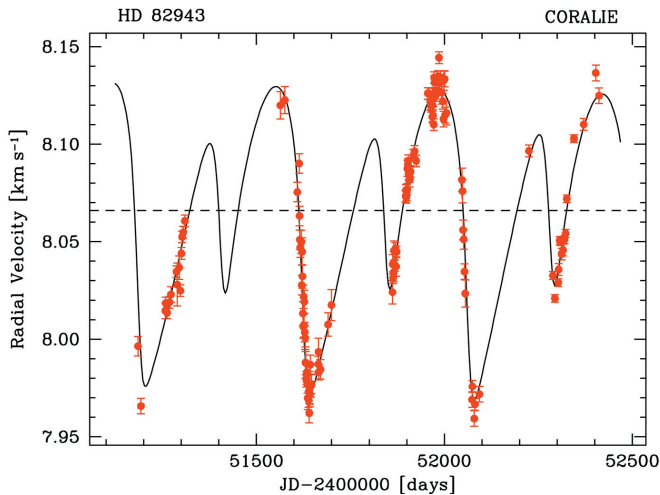


Figure 6: Radial-velocity measurements and best 2-planet Keplerian solution for HD 82943. The radial-velocity measurements show that this star has a system of two resonant planets, orbiting it with periods of ~ 220 and 440 days, respectively. This same star was found to have ${}^6\text{Li}$ in its atmosphere, a signature of possible planet engulfment (Israelian et al. 2001).

& Donahue 1997) are expected to induce radial velocity variations. Furthermore, contamination from the spectrum of other stellar companions can also induce spurious radial-velocity signals. These cases can prevent us from finding planets (if the perturbation is larger than the orbital radial-velocity variation), but perhaps more importantly, they might give us false candidates if they produce a periodic signal (e.g. a rotating stellar spot). The radial-velocity technique is thus most efficient for low chromospheric activity single “old” dwarfs.

A few good examples of spurious periodic radial-velocity variations can be found in the literature. The first to be described was the periodic signal observed for the dwarf HD 166435, that was shown to be due to the presence of a dark spot rather than to the gravitational influence of a planetary companion.

At the current (and increasing) level of precision obtained using the radial-velocity techniques, such kinds of examples might become more and more common. It is thus very important to develop ways to disentangle e.g. activity-related phenomena from real planetary candidates. Such methods might be based on the study of the shape of the spectral lines (usually called the “bisectors”), the photometric variability of the star, and/or of chromospheric activity indexes. This is very important for projects like HARPS, for which the barrier of the 1 ms^{-1} will be achieved.

Guidelines for the Future

The study of extra-solar planetary systems is just beginning. After only 7 years, we can say that at least 5% of solar-type dwarfs have giant planetary companions in relatively short period orbits (≤ 3 years). However, and as we have seen in the previous sections, many interesting but troubling problems still await a solution. In fact, the newly-found planets have clearly disturbed the long-standing theories of giant planetary formation and evolution. The def-

inition of a planet itself is currently under debate.

To solve this problem, there are high expectations from new or soon-to-be available instruments (see the paper on the HARPS spectrometer in this issue). The incredible precision gain achieved by these radial-velocity “machines” will be crucial in this aspect. But what are exactly the important lines of study to follow? And what kind of answers can we expect in the next few years?

Increasing the Statistics

As we have seen above, the observed correlations between the orbital parameters of the newly found planets are giving astronomers a completely different view on the formation and evolution of planetary systems. We no longer have the Sun as the only example, and today we have to deal with the peculiar characteristics of the “new” extra-solar planets: a huge variety of periods, eccentricities, masses.

To clear up current uncertainties we need more data. Only a large and statistically uniform set of data may enable us to clarify the current situation. In this sense, the hundreds of new planets expected to be discovered in the next few years will have a very important outcome.

Lower and Lower Masses

One clear result of the increase in precision of the current and future radial-velocity surveys is the ability to find lower-mass planets.

As we have seen above, the mass function for planetary companions around solar-type stars is rising toward the low-mass regime. But given that the radial-velocity technique is more sensitive to the more massive companions, the lower mass bins in the plot of Figure 2 are definitely not well represented. How then does this function behave for the lower-mass regime? What is the minimum mass of a giant planet? How does this depend on the orbital pe-

riod? The increase in long-term precision, and the continuation of the current high-precision radial-velocity programmes, will also give us the opportunity of finding more and more long-period planets. Current models predict that the planetary formation and evolution processes should produce more long-period planets than their short period counterparts. In fact, the current surveys are just starting to discover exo-planets with periods comparable to the ones found for the Solar System giants. This is an essential goal in order to improve the statistics of these objects, and to check if the Solar System is anomalous or common.

Of course, other problems will arise and become more important as a consequence of the dramatic increase in precision. In particular, the intrinsic stellar radial-velocity “jitter” produced by e.g. chromospheric activity related phenomena (e.g. Saar & Donahue 1997) might impose serious (and still unknown) limits on the final precision, and on the consequent ability to find very low-mass (and long-period) systems. This is particularly true for the youngest stars. Some effort should thus be put into the development of diagnostics capable of confirming the planetary nature of the radial-velocity signal. Furthermore, we might even imagine that the spurious radial-velocity variations caused by activity might be modelled and corrected, leaving only the real gravitational effects on the signal.

Planets Around M Dwarfs

Although more than 100 exoplanet candidates are now in the lists, only two planetary companions around M dwarfs have been detected (both in the solely system Gl 876). The very low number of M-dwarf planetary companions can in fact be largely explained by observational biases: the very low mass dwarfs are faint and it is difficult to obtain accurate radial velocities for them.

However, to constrain the various scenarios of planetary-system formation and evolution, it is now crucial to obtain better statistics for planets around the most numerous stars in our galaxy. M dwarfs compose 80% of the main sequence stars. How many of them have planets? How these planets differ from those orbiting the more massive G dwarfs is totally unknown. These questions await the future capabilities of instruments like HARPS.

The Chemical Link

Planet host stars seem to be, on average, particularly metal-rich. This interesting result probably reflects the importance the quantity of available rocky material in the disk has on the formation of giant planets.

As discussed above, this link might hold the key to understanding how giant planets are formed. The two competing theories (core accretion and disk instability) should have different sensitivities to the metallicity. If most planets were formed by the latter of these two processes we should not expect any special metallicity sensitivity.

Although the metallicity trend is clearly seen (Santos et al. 2001), there are nevertheless a few planet hosts that are particularly metal poor (see e.g. case of HD 6434). How can this be explained? One elegant way of solving this puzzle is to look for the frequency of planets around metal-poor halo dwarfs. If, as expected, no planetary mass objects are found around such a sample of stars, then the disk instability model is clearly put into question. However, if some are found, giant planets might be formed by different processes.

There are also some traces of stellar "pollution" among the planet host stars (Israelian et al. 2001). This opens the question of understanding how much planetary material might fall into the convective envelope as a consequence of the planetary formation process itself. How much can this change the metallicity of the star? If important, this could have consequences even for studies of the chemical evolution of the galaxy.

Although current results seem to refute any strong generalized stellar pollution among planet hosts, it is important to cross-check. One interesting way of addressing this problem might then be the study and comparison of the chemical contents of stars in visual binary systems composed of similar spectral type solar-type stars, one (or both) of which having planetary-mass companions. Strong differences found would be interpreted as a sign that stellar pollution is quite common. However, only one clear case has been studied to date: the double visual system 16 Cyg A and B, where the B component is known to harbour a planet. This case does not show any clear difference in the iron abundance, while a curious lithium abundance difference is found.

Transit Candidates

Another important result of instruments like HARPS will be their ability to follow up planetary-like transit signatures detected by photometry.

There are currently more than 20 groups around the world trying to look for signatures of the presence of planets around field dwarfs by looking for the brightness dimming as a putative planet crosses its disk. In spite of the efforts, only very few results have been announced, and none of these was confirmed to have a planetary origin. The only clear case of a real planetary transit detected so far was found for the

star HD 209458, a dwarf that was previously discovered to host a very-short period planetary companion (Charbonneau et al. 2000).

This detection, and the subsequent related studies, have had an enormous impact for the understanding of these systems. For example, it was possible to estimate the mean density of the planet, and to prove that it is orbiting in the same direction and plane as the star's equator.

In the near future we can expect that other such events might be brought to light. In particular, many hundreds of photometric transit candidates are expected from space missions like COROT, Kepler or Eddington. However, based only on photometry we cannot determine whether the observed transiting body is a planet or simply a low-mass star (since the effect is of similar magnitude because of the large degeneracy of the radius of these objects). The follow-up of the photometric observations by radial-velocity surveys is thus essential and will permit us to obtain the real mass of the planet.

With such data we can hope to derive empirical relations between variables such as the planet's mean density and its distance from the star, its mass, and the stellar metal abundance. In this sense it is important to say that the very high precision of HARPS, together with the relatively large aperture of the ESO 3.6-m telescope, will play an important role, since it will give the opportunity to obtain masses (or at least meaningful upper limits) for the least massive planets detected by the photometric missions.

Multiple Systems: Dynamical Interactions

Among the many planets that are expected to be found, some will surely belong to multi-planetary systems. Today, only about 10 such cases are known, but many stars that are already known to harbour a planet also show systematic trends in radial velocity, indicating that at least a second companion is present in the system. While for the majority of cases this tendency might be simply due to the presence of low-mass stellar companions, in some others they might be the telltale signatures of a multi-planetary system. The gain in precision with instruments like HARPS will definitely permit us to search the already known planet hosts for other planet-mass companions, and to increase the number of known multiple systems.

There is in fact much interesting information that can come from these cases. Current results have shown that planets in multiple systems come frequently in resonant orbits (see e.g. HD82943 – Figure 6). This is telling us a lot about the formation and migration of the exoplanets.

On the other hand, the strong interaction between planets in such systems will be reflected as an observable evolution of their orbital parameters. A dynamical analysis of this will give us the opportunity to obtain information on the masses and relative orbital inclinations for the companions.

Planets in Binaries

To date, several planets have been discovered in known multiple stellar systems. Moreover, a fraction of stars known to host planets exhibit a drift in the γ -velocity indicating the presence of an additional distant companion.

These observations show that despite the gravitational perturbation of the stellar companion, planets may form and survive around stars in multiple systems. The properties of such planets hold important clues on the mechanisms of planetary formation. For example, according to the standard core accretion model of planetary formation, a giant planet is formed by the accretion of gas around a ~ 10 earth mass core of rocky material. This is supposed to take place at distances comparable to the Jupiter–Sun separation (~ 5 A.U.). Opposing this model, Boss (1997) has proposed that giant gaseous planets might also be formed from the condensation of clumps resulting from gravitational instabilities in the disk. How can we distinguish these two scenarios?

One of the keys may come from the study of planets in binaries. The presence of a stellar companion possibly plays an important role in the formation of planets. It has been shown, for example, that a stellar companion can truncate the proto-planetary disk at a radius that depends mainly on the distance between the two stars. If so, and considering the core accretion scenario, we should not be able to see planets around stars members of binary systems that are closer than a given limit. How close can a star have a companion and still have planets? The answer to this question is very important to understand how giant planets are formed.

Concluding Remarks

As the planet search programmes are on their way, many more planetary companions are expected to be discovered in the next few years. Many hopes are now placed on instruments like HARPS, that will provide radial velocities of stars with a precision of 1 ms^{-1} or better. This will give us the opportunity to dramatically improve the samples.

Other major contributions will come from future space missions like COROT, Eddington, or Kepler, which will unveil thousands of short-period planets around stars in the solar neigh-

bourhood. And, of course, the use of high-precision astrometric measurements with instruments like the VLTI or the Keck interferometer will survey "nearby" stars for long-period systems. Altogether, these coming observational facilities will definitely help us to construct a new and more complete view of how planetary systems are born and how they evolve.

References

Boss A.P., 1997, *Science* **276**, 1836.
 Charbonneau D., Brown T.M., Latham D.W., Mayor M., 2000, *ApJ* **529**, L45.
 Goldreich P., Tremaine S., 1980, *ApJ* **241**, 425.
 Israelian G., Santos N.C., Mayor M., Rebolo R., 2001, *Nature* **411**, 163.
 Jorissen A., Mayor M., Udry S., 2001, *A&A* **379**, 992.

Mayor M., Queloz D., 1995, *Nature* **378**, 355.
 Pollack J.B., Hubickyj O., Bodenheimer P., Lissauer J.J., Podolak M., Greenzweig Y., 1996, *Icarus* **124**, 62.
 Saar S.H., Donahue R.A., 1997, *ApJ* **485**, 319.
 Santos N.C., Israelian G., Mayor M., 2001, *A&A* **373**, 1019.
 Wolszczan A., Frail D. A., 1992, *Nature* **355**, 145.

FIRES: Ultradeep Near-Infrared Imaging with ISAAC of the Hubble Deep Field South

I. LABBÉ¹, M. FRANX¹, E. DADDI³, G. RUDNICK², P.G. VAN DOKKUM⁴,
 A. MOORWOOD³, N.M. FÖRSTER SCHREIBER¹, H.-W. RIX⁵, P. VAN DER WERF¹,
 H. RÖTTGERING¹, L. VAN STARKENBURG¹, A. VAN DE WEL¹, I. TRUJILLO⁵, and
 K. KUIJKEN¹

¹Leiden Observatory, Leiden, The Netherlands; ²MPA, Garching, Germany;

³ESO, Garching, Germany; ⁴Caltech, Pasadena (CA), USA; ⁵MPIA, Heidelberg, Germany

1. Introduction

Between October 1999 and October 2000 an undistinguished high-galactic latitude patch of sky, the Hubble Deep Field South (HDF-S), was observed with the VLT for more than 100 hours under the best seeing conditions. Using the near-infrared (NIR) imaging mode

of the Infrared Spectrometer and Array Camera (ISAAC, Moorwood 1997), we obtained ultradeep images in the J_s (1.24 μm), H (1.65 μm) and K_s (2.16 μm) bands. The combined power of an 8-metre-class telescope and the high-quality wide-field imaging capabilities of ISAAC resulted in the deepest ground-based NIR observations to date, and

the deepest K_s -band in any field. The first results are spectacular, demonstrating the necessity of this deep NIR imaging, and having direct consequences for our understanding of galaxy formation.

The rest-frame optical light emitted by galaxies beyond $z \sim 1$ shifts into the near-infrared. Thus, if we want to compare $1 < z < 4$ galaxies to their present-day counterparts at similar intrinsic wavelengths – in order to understand their ancestral relation – it is essential to use NIR data to access the rest-frame optical. Here, long-lived stars may dominate the total light of the galaxy and the complicating effects of active star formation and dust obscuration are less important than in the rest-frame ultraviolet. This therefore provides a better indicator of the amount of stellar mass that has formed. Compared to the selection of high-redshift galaxies by their rest-frame UV light, such as in surveys of Lyman Break Galaxies (LBGs, Steidel et al. 1996a,b),

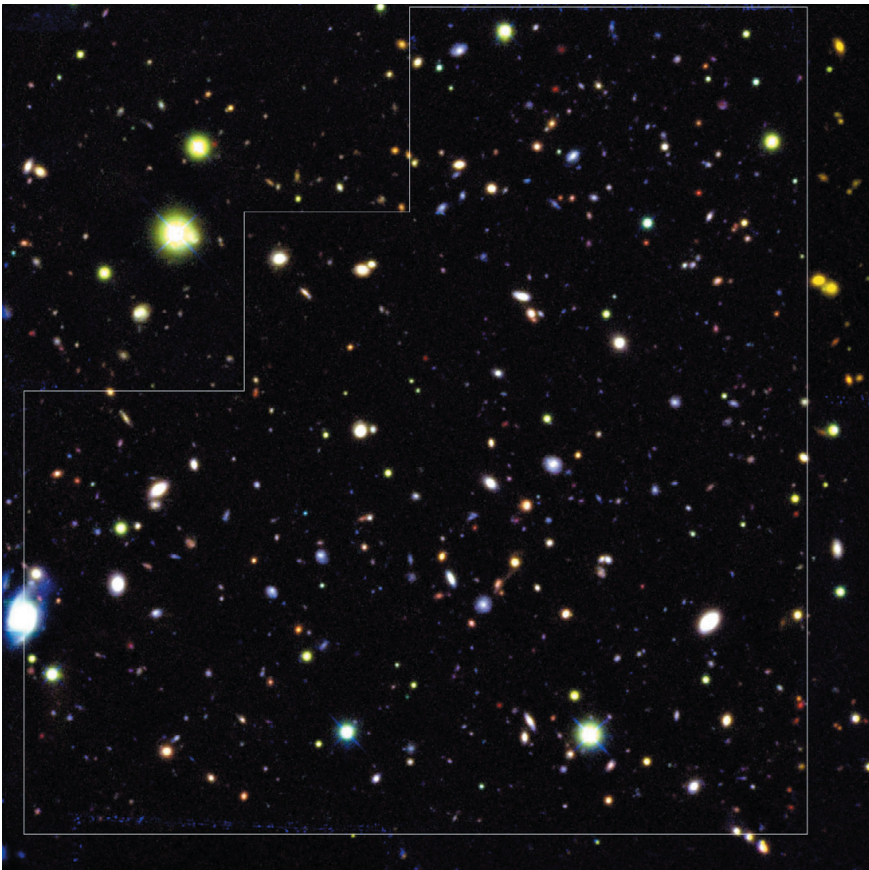


Figure 1: Three-colour composite image of the ISAAC field on top of the WFPC2 main-field, outlined in white, and parts of three WFPC2 flanking fields. The field of view is approximately 2.5×2.5 arcminutes and North is up. The images are registered and smoothed to a common seeing of $\text{FWHM} \approx 0.46''$, coding WFPC2 I_{814} in blue, ISAAC J_s in green and ISAAC K_s in red. There is a striking variety in optical-to-infrared colours, especially for fainter objects. A number of red sources have photometric redshifts $z > 2$ and are candidates for relatively massive, evolved galaxies. These galaxies would not be selected by the U-dropout technique because they are too faint in the observer's optical.

selection in the NIR K_s -band gives a more complete census of the galaxies that contribute to the stellar mass content of the early universe. And, by studying these systems over a substantial redshift range, we can directly see how they were assembled as we look further back in time. Very deep optical-to-infrared data in many filters are required not only to access the rest-frame optical light of galaxies and constrain their stellar composition, but also to determine the redshifts of faint distant galaxies from their broadband photometry alone. The majority of the galaxies detected are too faint to be observed spectroscopically, even with powerful telescopes like the VLT.

Here, we discuss the full NIR data set of the HDF-S. The observations, reduction techniques, the catalogue of sources, and the photometric redshifts are described in detail in Labbé et al. (2002). Throughout, we will assume a flat Λ -dominated cosmology ($\Omega_M = 0.3$, $\Lambda = 0.7$, $H_0 = 100h \text{ km s}^{-1} \text{ Mpc}^{-1}$) and all magnitudes are expressed in the Johnson photometric system unless explicitly indicated by the subscript *AB* for the AB magnitude system.

2. Observations

The observations of the HDF-S are part of the Faint InfraRed Extragalactic Survey (FIRES, Franx et al. 2000), a large public programme carried out at the VLT consisting of very deep NIR ISAAC observations of two selected fields with existing deep optical WFPC2 imaging. The second and somewhat shallower field around the $z \approx 0.83$ cluster MS1054-03 (Förster Schreiber et al. in preparation) was observed for 80 hours over an area four times larger than the HDF-S. The full NIR data set of the HDF-S consists of 33.6 hours of imaging in J_s , 32.3 hours in H , and 35.6 hours in K_s with ISAAC, which has a $2.5' \times 2.5'$ field of view. The effective seeing in the reduced images is approximately $0.46''$ in all bands, close to the best seeing that can be reasonably obtained from Paranal. We reach a depth of 25.9 in J_s , 24.8 in H , and 24.4 in K_s (total magnitude for point sources, 3σ). Complemented by ultradeep HST/WFPC2 imaging (version 2, Casertano et al. 2000) in the optical filters U_{300} , B_{450} , V_{606} , and I_{814} bands (the subscript indicating the effective wavelength), we assembled a K_s -selected catalogue containing 833 sources, of which 624 have seven-band photometry, covering $0.3\text{--}2.2 \mu\text{m}$. We determined the photometric redshifts of all extragalactic sources using a method detailed in Rudnick et al. (2001, 2002a in preparation). Comparison with spectroscopic redshifts available for 49 sources in the field shows excellent agreement: $|z_{\text{spec}} - z_{\text{phot}}| / (1 + z_{\text{spec}}) \approx 0.08$.

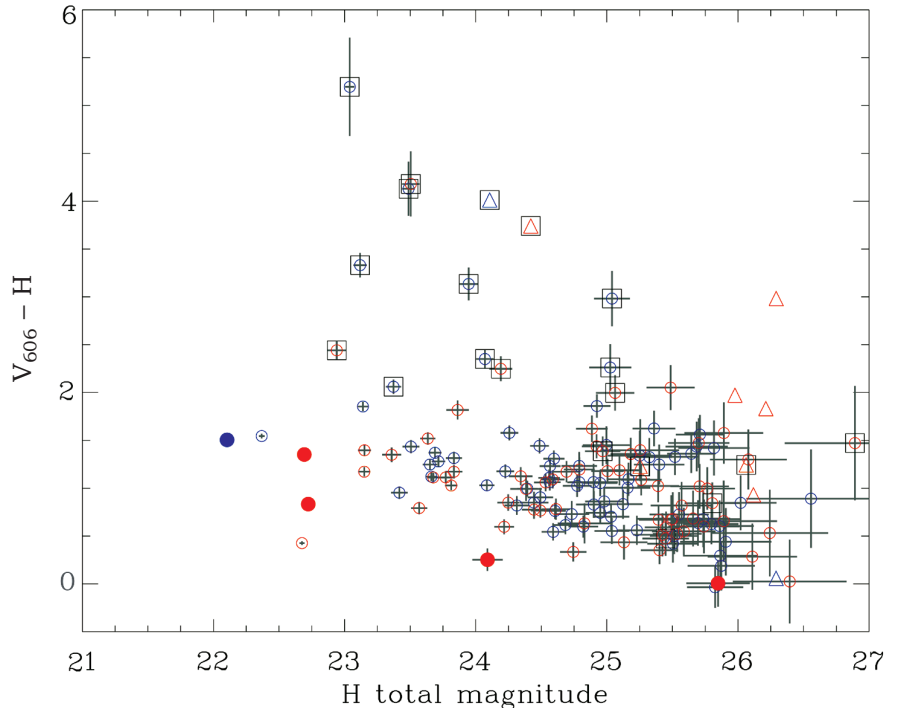


Figure 2: $V_{606} - H$ versus H colour-magnitude diagram (on the AB system) for galaxies in the HDF-S K_s -selected catalogue with $1.95 < z_{\text{phot}} < 3.5$. Filled symbols indicate galaxies with spectroscopy and the data points are grouped into two redshift ranges: $1.95 \leq z < 2.7$ (red) and $2.7 \leq z < 3.5$ (blue). We find 7 galaxies redder than $V_{606, AB} - H_{AB} > 3$ and brighter than $H_{AB} < 25$, compared to only one in the HDF-N. Galaxies with $S/N < 2$ for the V_{606} measurement (triangles) are plotted at the 2σ confidence limit in V_{606} , indicating a lower limit on the $V_{606} - H$ colour. Galaxies having red $(J_s - K_s)_J > 2.3$ colours (open squares) are also shown. The number of candidates for red, evolved galaxies is much higher than in the HDF-N for a similar survey area, as shown in an identical plot in Figure 1 of Papovich, Dickinson & Ferguson (2001). The transformation of the $V_{606} - H_s$ colour from the AB system to the Johnson magnitude system is $(V_{606} - H)_J = (V_{606} - H)_{AB} + 1.26$.

The colour image shown in Figure 1 combines HST I -band data with ISAAC data in the J_s and K_s bands. Most sources visible are very faint distant galaxies and a rich variety in their optical-to-infrared colours is readily apparent. Some high-redshift galaxies, visible as red sources, are hardly detected or even absent in the optical I -band but are quite bright in the NIR K_s .

3. Evolved Galaxies at High Redshift

Remarkably, the HDF-S contains many high-redshift sources that are relatively bright in the infrared and extremely faint in the optical, whereas the HDF-N contains far fewer such galaxies. This is clearly visible in Figure 2, which shows $V_{606} - H$ colours versus the infrared H band magnitudes of NIR selected galaxies between redshifts $2 < z < 3.5$. The filters are chosen to match those used in Figure 1 in Papovich, Dickinson & Ferguson (2001), allowing a direct comparison with the HDF-N. For a similar survey area and similar limiting depth, we find 7 galaxies redder than $V_{606, AB} - H_{AB} > 3$ and brighter than $H_{AB} < 25$ (on the AB magnitude system), compared to one in the NIR sample of HDF-N. These systems are probable candidates for relatively massive

and evolved galaxies with comparatively low star-formation rates, and models of galaxy formation must allow for their formation in sufficient numbers at $z \sim 3$. It appears that in recent hydrodynamical simulations (Weinberg, Hernquist & Katz 2002) high-redshift galaxies are converting gas into stars continuously and at a fairly high rate, keeping them blue or “unevolved”. While this is qualitatively consistent with the lack of red galaxies in the HDF-N, the situation in the HDF-S is significantly different.

All high-redshift galaxies with very red $V_{606} - H$ colours also have very red infrared $J_s - K_s$ colours. Redshifting model spectra of galaxies shows that such red colours are produced by evolved systems at redshifts $z > 2$. In our K_s -band selected catalogue we find 13 relatively bright galaxies ($K_{\text{tot}} < 22$) that have red $J_s - K_s > 2.3$ colours (Franx et al. in preparation), compared to 37 U-dropouts to the same flux limit. The photometric redshifts of these galaxies, determined from the optical-to-infrared spectral energy distributions (SEDs), are between $2 < z_{\text{phot}} < 4$. Yet, most of the red galaxies are so faint in the observers optical that they would be missed by standard optical selection criteria, such as the U-dropout method. In principle, the red colours can be

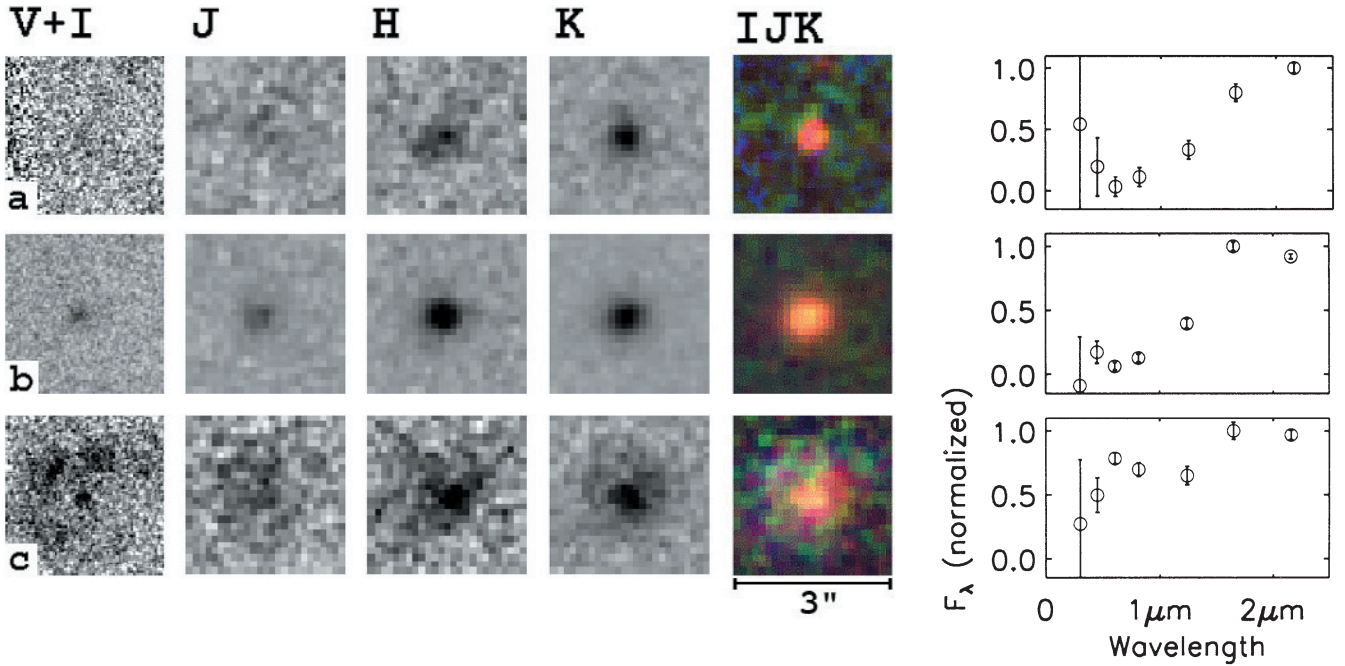


Figure 3: Morphology of bright red $J_s - K_s > 2.3$ galaxies in the HDF-S. The left grayscale panels show the averaged WFPC2 V+ I data, and right-hand panels show our VLT/ISAAC J_s , H, K_s data. The intensity is proportional to F_λ , with arbitrary normalization for each galaxy. The colour images show a combination of I, J_s , K_s data, after matching the image quality to that of the K_s -band. The right-hand column shows the spectral energy distributions. Many of these galaxies are small and show prominent breaks in the infrared (rest-frame optical). Note that the galaxy in the top row is barely visible even in J_s . The SED of the object in the middle is consistent with a strong Balmer/4000Å break at $z \sim 2.5$. The galaxy in the bottom row is very extended in the rest-frame optical. It shows faint emission in the H-band out to $1''$, consistent with an exponential profile.

caused by dust, by contribution of prominent emission lines falling in the K_s -band, or by the redshifted Balmer or 4000 Å break, which indicates the presence of evolved stars. Although emission lines have been detected in spectroscopically confirmed $J_s - K_s > 2.3$ galaxies in the FIRES MS1054-03 field by van Dokkum et al. (in preparation), their contribution to the broadband NIR photometry is estimated to be small. In many cases the spectral energy distributions show a clear break between J_s and K_s , which is more easily explained as an aging effect than as a result of dust reddening. These galaxies contribute significantly to the rest-frame optical luminosity density (Rudnick et al. 2002a in preparation) and from their red rest-frame optical colours – implying high mass-to-light ratios – we estimate that they contain a substantial fraction of the total stellar mass present in all galaxies at $z \sim 3$.

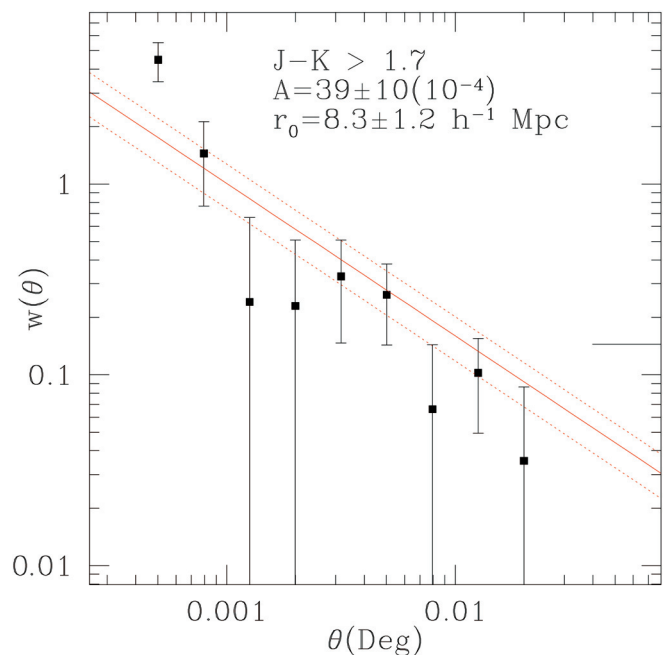
The morphologies of the red galaxies are generally very compact at all wavelengths, as can be seen in Figure 3. A notable exception is the galaxy in Figure 3c which is clearly extended and has an exponentially decreasing surface brightness profile out to $1''$ radius in the H-band. This galaxy seems to host blue knots which could form a spiral arm in the optical WFPC2 images, while it has an extended disk-like appearance with a prominent bulge in the centre in the ISAAC H and K_s images; possibly these are actively star-forming sites embedded in a larger mature host galaxy.

4. Strong Clustering of Faint Red Galaxies at $2 < z_{phot} < 4$

Presumably, high-redshift galaxies with red $J_s - K_s$ colours are among the oldest and most massive galaxies at their cosmic epoch and they have formed at the highest density peaks in the matter distribution at significantly earlier times. If so, this population should be more clustered than less massive and less evolved (bluer) objects at similar redshifts. Using the FIRES data of the HDF-S, Daddi et al. (2002) have studied the clustering be-

haviour of K_s -selected galaxies at $2 < z_{phot} < 4$, finding that the amount of clustering depends strongly on the $J_s - K_s$ colour of galaxies, with red galaxies more clustered than blue galaxies, very similar to what is observed in the optical in the local universe. Dividing the sample at $J_s - K_s = 1.7$ in two subsamples reveals that the galaxies with $J_s - K_s > 1.7$ colours have the largest-ever level of clustering measured for $z > 2$ galaxies (see Fig. 4). The derived correlation length for the faint red galaxies is $r_0 = 8.3 \pm 1.2$ Mpc (comoving): a factor of 3–4 higher than that of Lyman

Figure 4: The angular two-point correlation function for galaxies with red $J_s - K_s > 1.7$ colours between redshifts of 2 and 4, with the best fitting power-law (solid line) and 1-sigma errors (dotted lines). A positive and large clustering signal is detected, suggesting that these red FIRES galaxies are strongly clustered in real space, with a correlation length $r_0 = 8.3 \pm 1.2 h^{-1}$ Mpc comoving. This is the largest level of clustering ever found for distant, $z > 2$ galaxy populations.



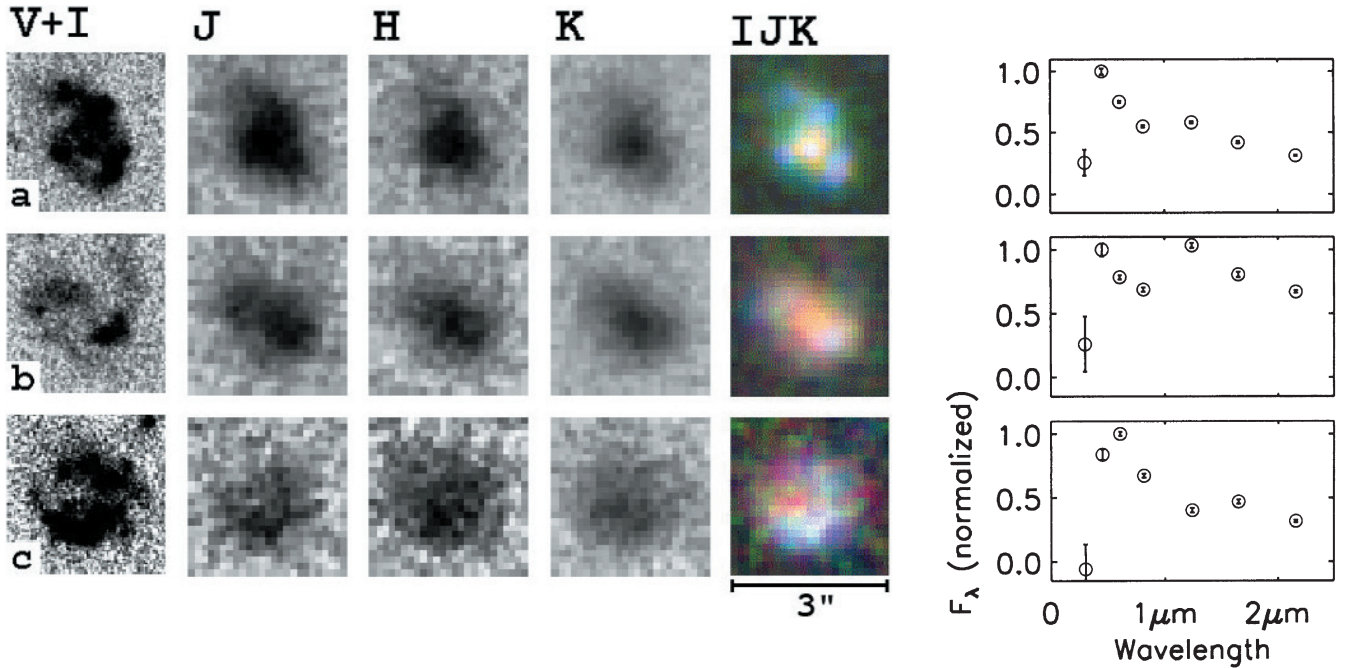


Figure 5: Same as Figure 3 for the three largest Lyman-break galaxies in the HDF-S. The K -band images (rest-frame optical) are more centrally concentrated than the WFC2 images; this is a real change in light distribution and not caused by the decreased image quality in the NIR. The redshifts of galaxies (a) and (c) have been confirmed spectroscopically; they have $z = 2.027$ and $z = 2.793$ respectively, implying a scale length of $10h^{-1}\text{kpc}$ for the latter.

Break galaxies over similar redshift ranges and with similar number densities. The overall properties of this red $J - K > 1.7$ strongly clustered population suggests that they are the progenitors of present-day massive ellipticals and extremely red objects (EROs) at $z \sim 1.5$.

5. Large Disk-Like Galaxies at High Redshift

The high-redshift galaxies in HDF-S show a large variation in both morphologies and spectral energy distributions. Spectacularly, we find some $z > 2$ galaxies that are very large in the rest-frame optical and show profound differences between the intrinsic ultraviolet and optical morphologies (Labbé et al. in preparation). Three of the galaxies, shown in Figure 5, are LBGs (selected by applying the U-dropout criteria of Madau et al. 1996), while one is the previously described red galaxy in Figure 3c. Their spectral energy distributions show a pronounced break in the rest-frame optical, identified as the age-sensitive Balmer/4000 Å break. They are amongst the brightest and reddest in the rest-frame optical and they are probably the most massive galaxies at $z \sim 2-3$.

The I -band morphologies (probing rest-frame 2000–2700 Å) are complex with a patchy distribution that is not concentrated towards the centre. Conversely, the NIR light is compact and peaks right in the centre of the I -band structure, surrounded by a diffuse and extended disk-like distribution. The most straightforward explanation is that

these systems are very luminous giant spiral galaxies, with patchy star formation residing in a diffuse disk with a red bulge in the centre. It is well possible that we have discovered the predecessors of the large disk galaxies we see in the lower-redshift universe. Morphological studies in the rest-frame UV light of LBGs have always emphasized the compact and small sizes of the galaxies (Giavalisco et al. 1996, Lowenthal et al. 1997), as indeed is true for the bulk of our sample. However, galaxies that are large in the rest-frame optical with classical spiral morphologies have never been seen before, in particular not in the HDF-N (Dickinson et al. 2000) even though such structures would have been well recognizable in their deep WFC2 and NICMOS imaging.

Follow-up VLT/FORS spectroscopy (Rudnick et al. 2002b in preparation) confirmed the redshift of the galaxy in Figure 5c, a disk-like U-dropout at $z_{\text{spec}} = 2.793 \pm 0.003$, implying a scale length of $10 h^{-1}\text{kpc}$. Vanzella et al. (2002) found an identical redshift for this galaxy and for another, shown in Figure 5a, they found $z_{\text{spec}} = 2.027$. Theories of disk formation generally predict that large disk galaxies have been assembled recently ($z < 1$), and that high-redshift $z > 2$ disks are small and dense, with typical sizes of \sim few kpc. Producing large disk-like galaxies with reasonable likelihood may therefore pose a challenge to the current hierarchical models.

6. Summary

These first results on the HDF-S demonstrate the necessity of extending

deep optical observations to near-IR wavelengths for a more complete census of galaxies in the early universe. In particular, the deepest-ever K_s -band data have proven to be invaluable, probing well into the rest-frame optical at $2 < z < 4$, where long-lived stars may dominate the light of galaxies.

Provided with a new window on the early universe we find previously undiscovered populations of galaxies, with possible far-reaching consequences for our understanding of galaxy formation. We find that the HDF-S has many more galaxies at $z \sim 3$ with very red $V_{606} - H$ colours than the HDF-N; these are candidates for relatively massive evolved systems. Closely connected, we find a substantial population of red $J_s - K_s > 2.3$ galaxies at $z > 2$, many of which are barely detectable even in the deepest optical images, and would be missed by optical colour selection techniques such as the U-dropout method. Yet, these galaxies probably contribute substantially to the total stellar mass present in the early universe at $z \sim 3$. We detect strong clustering ($r_0 = 8.3 \pm 1.2$ Mpc, comoving) of galaxies with $J_s - K_s > 1.7$ colours at $2 < z_{\text{phot}} < 4$. The strong clustering and their red $J_s - K_s$ colours, suggest that there is a direct evolutionary link between these systems, EROs at $z \sim 1.5$, and massive elliptical galaxies in the local universe. We also find high-redshift systems that are very large in the rest-frame optical with morphologies similar to those of nearby giant spiral galaxies, containing a red bulge surrounded by a diffuse disk and with scattered patches of star formation. While these are only a few

examples, it is currently not clear whether galaxy formation models can produce objects of comparable colours and sizes in sufficient numbers to be consistent with our observations.

Lastly, the substantial differences between HDF-N and HDF-S demonstrate that results based on such small fields can be seriously affected by cosmic variance. The results of the second field in the FIRES survey, the much larger MS1054-03 field, should decide which one of the fields is atypical. We are pursuing extended follow-up programmes to obtain more spectroscopic confirmation of the above results, allowing us to fully investigate the nature of these galaxies and the clues they provide for models of galaxy formation. Updates on the FIRES programme and access to the reduced images and catalogues can be found at our website <http://www.strw.leidenuniv.nl/~fires>.

Acknowledgements

We wish to thank the ESO staff for operation of the VLT and ISAAC and their kind assistance. We are grateful for their enormous efforts in obtaining these data in service mode and making them available to us.

References

- Moorwood, A.F.M., "ISAAC: a 1-5 μ m imager/spectrometer for the VLT", in *Optical telescopes of today and tomorrow*. A.L. Ardeberg ed., *proc. SPIE* **2871**, pp. 1146–1151, 1997.
- Steidel, C.C., Giavalisco, M., Dickinson, M., & Adelberger, K.L., *AJ* **112**, pp. 352–358, 1996.
- Steidel, C.C., Giavalisco, M., Pettini, M., Dickinson, M., & Adelberger, K.L., *ApJ* **462**, L17, 1996.
- Rudnick, G. et al., *AJ* **122**, pp. 2205–2221, 2001.
- Labbé, I.F.L. et al., *AJ* accepted, 2002.
- Förster Schreiber, N.M. et al., in preparation, 2002.

- Oke, J.B. 1971, *ApJ*, **170**, 193.
- Franx, M. et al., "FIRES at the VLT: the Faint InfraRed Extragalactic Survey", *The Messenger* **99**, pp. 20–22, 2000.
- Casertano, S. et al., *AJ* **120**, pp. 2747–2824, 2000.
- Papovich, C., Dickinson, M., & Ferguson, H.C., *ApJ* **559**, pp. 620–653, 2001.
- Weinberg, D.H., Hernquist, L., & Katz, N., 2002, *ApJ*, **571**, 15.
- Daddi, E. et al., *ApJ*, submitted, 2002.
- Madau, P., Ferguson, H.C., Dickinson, M.E., Giavalisco, M., Steidel, C.C., & Fruchter, A., *MNRAS* **283**, pp. 1388–1404, 1996.
- Giavalisco, M., Steidel, C. C., & Macchetto, F.D., *ApJ* **470**, 189, 1996.
- Lowenthal, J.D. et al., *ApJ* **481**, pp. 673–688, 1997.
- Rudnick, G. et al., in preparation, 2002a.
- Rudnick, G. et al., in preparation, 2002b.
- Dickinson, M., "The first galaxies: structure and stellar populations" *Philos. Trans. R. Soc. London A* **358**, p. 2001, 2000.
- Dickinson, M. et al., *ApJ* **531**, pp. 624–634, 2000.
- Vanzella, E. et al., *A&A* accepted, 2002.

OTHER ASTRONOMICAL NEWS

Summary of the Workshop on

EXTRAGALACTIC GLOBULAR CLUSTER SYSTEMS

hosted by the European Southern Observatory in Garching on August 27–30, 2002

By M. KISSLER-PATIG

Extragalactic Globular Clusters, a Booming Field of Research

Globular cluster systems were established in the last decade as powerful

tools for the study of galaxy formation and evolution. For this purpose they are used in nearby galaxies with as much success as the diffuse stellar populations and complement the latter studies

by being superior in several practical aspects. For instance, globular clusters are better chronometers than the diffuse stellar population since each globular cluster can be identified as a single-age population. The age determination of the major globular cluster subpopulations allows one to precisely date the star formation events in the host galaxy.

Further, the study of globular cluster systems is the easiest way to detect multiple old or intermediate-age subpopulations within a galaxy. These in turn can trace multiple major star-formation episodes at early times, invisible in the studies of the diffuse galaxy light in which all populations are mixed.

Another advantage is that globular clusters can be traced far out in the halo, probing stellar populations and kinematics at several effective radii of the host galaxy – a range inaccessible to diffuse stellar light studies. The globular clusters can be used for dynamical studies at outer radii, shedding light on the assembly histories of the systems and the host galaxies.

Finally, globular clusters are very good calibrators at all wavelength for single stellar population models, an es-



Figure 1: NGC 6946 – a nearby spiral with a large number of very luminous young stellar clusters. Taken from Larsen's contribution. The observations were made with the ALFOSC instrument on the Nordic Optical Telescope on La Palma. ALFOSC is a twin instrument of DFOSC on the Danish 1.54-m and mounted on the NOT; it has a field size of about 6×6 arcmin. The colour image was generated from a mosaic of 3 pointings with red channel = $V + I + H\alpha$; green channel = V ; blue channel = B .

sential tool for all galaxy formation and evolution studies.

In summary, globular clusters are a very strong complement to diffuse galaxy-light studies. They are very good tracers of the major star-formation episodes of galaxies, including extreme conditions such as star-burst during violent merger events. The study of these systems allows us to learn not only about the formation of the globular clusters and their systems, but also about the formation and evolution of galaxies.

The ESO Workshop, a Follow-up on the Pucon IAU Symposium

Last year's IAU Symposium 207 on "Extragalactic Star Clusters" in Pucon (the first IAU symposium to be held in Chile) highlighted preliminary results from some of the currently ongoing, extensive programmes to study globular cluster systems. The size of the meeting did not lend itself to interactive discussions. However, the talks presented at this Symposium underlined the dramatic progress currently underway in this field.

This motivated us to follow it up a year and a half later with a workshop on a more focused aspect, namely "Extragalactic Globular Cluster Systems". The meeting was held at the headquarters of ESO in Garching, profiting from the freshly renovated Auditorium. About 60 participants enjoyed 4 days of lively discussion and excellent presentations. The low mean age of the researchers in this dynamic field spoke for the timeliness of the research. Participants who pioneered the research a couple of decades ago (such as W.E. Harris, and D. Hanes) expressed several times the joy of seeing the field blossom, even if it implied that they are now regarded as "dinosaurs" by the young graduates and post-graduates.

The workshop programme was planned such that no less than 2 hours for lunch break and another one hour

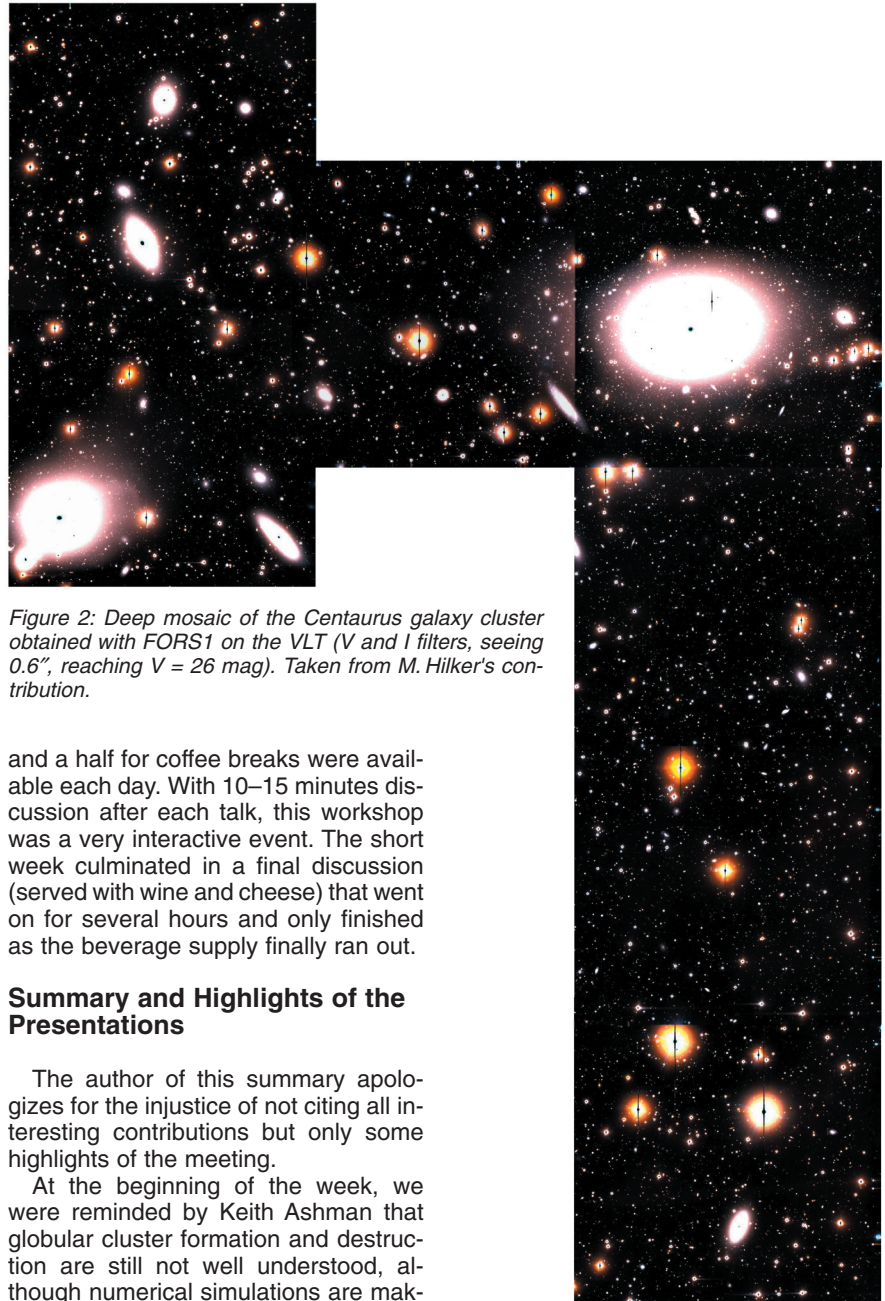


Figure 2: Deep mosaic of the Centaurus galaxy cluster obtained with FORS1 on the VLT (V and I filters, seeing 0.6", reaching $V = 26$ mag). Taken from M. Hilker's contribution.

and a half for coffee breaks were available each day. With 10–15 minutes discussion after each talk, this workshop was a very interactive event. The short week culminated in a final discussion (served with wine and cheese) that went on for several hours and only finished as the beverage supply finally ran out.

Summary and Highlights of the Presentations

The author of this summary apologizes for the injustice of not citing all interesting contributions but only some highlights of the meeting.

At the beginning of the week, we were reminded by Keith Ashman that globular cluster formation and destruction are still not well understood, although numerical simulations are making steady progress in explaining the evolution of globular cluster systems

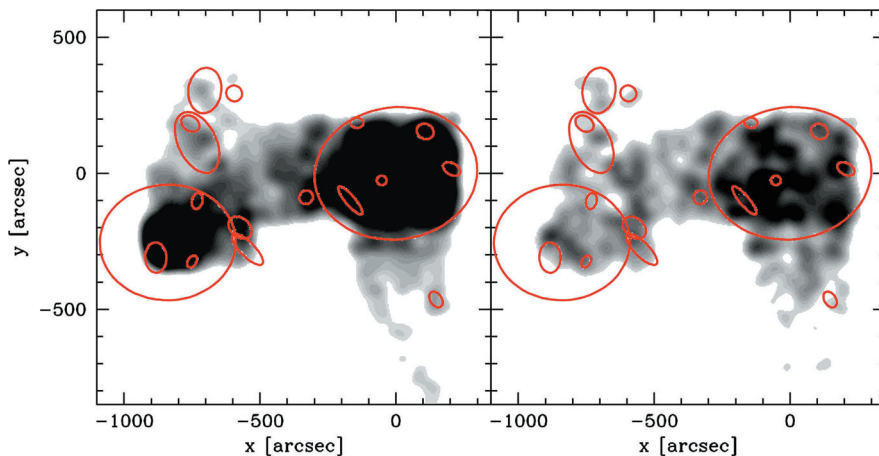


Figure 3: The smoothed density map of globular cluster candidates shows clear over-densities outside the isophotes of the major galaxies. Centaurus must host a significant population of free floating, intra-galaxy globular clusters.

(e.g. the presentation of Enrico Vesperini).

Young star clusters are, however, extensively observed and studied as a whole session demonstrated. The main current result is that these young clusters get better and better connected with their old counter-parts and that little doubt remains that a vast number of the observed massive young clusters will evolve into objects similar to the old globular clusters observed today, although their initial properties might contain surprises (e.g. S. Mengel's review).

Early- and late-type giant galaxies remain the favourites for studying cluster systems as a whole. Spectroscopic studies with 8- to 10-m telescopes produce impressive results both on the kinematics of the outer regions of galaxies (e.g. the many hundred velocities collected in the outskirts of NGC

1399 by Tom Richtler and his group), as well as on the chemistry of the old clusters (e.g. Puzia et al.). A number of studies also reported on large intermediate age populations of globular clusters in early-type galaxies, detected both by a combination of optical and near-infrared photometry as well as by spectroscopy (e.g. Hempel et al., Goudfrooij et al.). Interestingly, the globular clusters in dwarf galaxies look “almost but not quite unlike” their counterparts in giant galaxies as Jennifer Lotz showed us. Despite the similarity, populations in dwarfs can extend to very low metallicity.

Interestingly (even if not unexpectedly), globular clusters are found in large numbers in the intergalactic medium of galaxy clusters. Michael Hilker and collaborators show clear evidence for globular clusters floating through the Hydra I and Centaurus galaxy clusters.

Finally, globular clusters, as the oldest objects known in the sky, are now being put in a cosmological context. Mike Beasley investigated the constraints that they put on semi-analytic models in the hierarchical clustering scenario of galaxy formation. Michael Santos presented a model in which the

old metal-poor globular clusters formed prior to re-ionization.

Clearly, extragalactic globular clusters currently dominate the study of stellar populations in nearby galaxies. Their properties set hard constraints on galaxy formation and evolution models, but also shed new light on the star formation history of the universe. This research area will clearly produce a number of astonishing results in the next 5 years.

The organizers would like to warmly thank Christina Stoffer who perfectly controlled the logistics of the conference, as well as Pam Bristow for helping in the proceedings editing.

The VLTI: Challenges for the Future

WORKSHOP AT JENAM 2002 IN PORTO

A. GLINDEMANN, ESO

On the verge of becoming a major science facility, the VLTI was the subject of one of the workshops at this year's Joint European and National Astronomical Meeting in Porto (Portugal) in September. The two and a half day workshop had the aim of introducing interferometry and the VLTI to the non-expert. About 65 participants, many of them young and from outside the interferometric community (the two essentials for success) showed the large interest in interferometry.

After an introduction to interferometry, to the VLTI and its instruments, and to the two other large interferometers –

the Keck Interferometer and the Large Binocular Telescope – on the first day, the second day was devoted to science. In 16 presentations, stellar astrophysics was addressed including accretion disks and outflows of young stellar objects, surface structure and circumstellar envelopes of Mira stars, diameter of Cepheids, and mass loss of Wolf-Rayet stars. The possibilities of observing nuclear regions of AGNs with the VLTI were also explored. The emphasis of the presentations was on the possibilities with the VLTI. Some of the presentations contained results of interferometric observations with smaller interferometers. The report on

Mira was based on new observations done with the VLTI and made public through the regular VLTI releases.

On the last day, the discussion on the future of the VLTI and on projects for second-generation instrumentation concluded the workshop.

This workshop was a success in attracting the non-interferometrists in the astronomical community and in summing up the scientific topics to be tackled in the near future. It became evident that it is now important to finally make the observations and produce the results that have been discussed over the last years.

Summary of a Meeting on Science Operations with ALMA, held on Friday, 8 November 2002

P. SHAVER (ESO) and E. VAN DISHOECK (Leiden)

With the recent approvals by the ESO Council and the US National Science Board for the construction of the Atacama Large Millimeter Array (ALMA), it was thought timely to update the European astronomical community on the project and to solicit input on the plans for science operations and user support. To this end, a one-day meeting was held at ESO Headquarters in Garching on Friday, 8 November. It was very well attended; the auditorium was filled to capacity with some 100 participants from all over Europe.

The meeting began with an overview of the project and its current status by S. Guilloteau. Three very stimulating talks reviewed some of the major science drivers for ALMA: the high-redshift

Universe (S. Lilly), star and planet formation (A. Natta), and late-type stars (H. Olofsson).

The meeting then moved on to consider operations: concepts and plans for the operations phase were outlined by E. van Dishoeck, D. Silva talked about the relevant operational lessons from the VLT, and R. Lucas discussed the ALMA data reduction software and observing tools. After lunch P. Cox discussed the coordination of the European astronomical community and preparation for ALMA, including the opportunities within the EU Framework 6 programme. The discussion session then started with seven short contributions on a variety of topics, which led on to a very stimulating and useful open dis-

ussion chaired by J. Richer and E. van Dishoeck. Topics of discussion included the role and nature of a possible European Regional Support Centre (RSC) which could assist users in the observation preparation and data analysis processes, and ideas and priorities concerning software, receiver bands, surveys, future enhancements, and preparation for ALMA science. In view of the success of this meeting, there will probably be more such meetings for the community as the project evolves.

The viewgraphs from the invited talks given at the meeting are posted on the ALMA website, <http://www.eso.org/projects/alma/doclib/talks/>, where more details on the ALMA project can also be found.

Celebrating ESO's 40th Anniversary

C. MADSEN, ESO

ESO has always been a forward-looking organization, focussed on present and future programmes and projects. In its 40th year, this is as true as ever, as ESO keeps its eyes on implementing the VLTI, initiating the development of the second-generation instrumentation for the VLT and, of course, embarking on Phase II of the ALMA project, for which the ESO Council gave the green light at its mid-year meeting in London. Still, a 40th anniversary warrants a look at the decades passed and a reflection on the role and achievements of the organization during a period of time in which our science has progressed tremendously. That ESO has achieved its goals is undisputed, providing evidence of the wisdom of those astronomers who gathered in Leiden in early 1954 to formulate the need for this organization and justifying the trust displayed by the five countries, which were the original signatories to the 1962 convention that formed the legal base for ESO.

There were many milestones on ESO's road to success. Not surprisingly, many of them were recalled – and retold – during the various celebrations in September and October this year, described in the Anniversary issue of *The Messenger*, as well as, undoubtedly, in numerous conversations among members of the ESO 'family', be it former or present staff, members of committees or Council – or users in the scientific community.

Rather than organizing a single, high-profile central celebration event, ESO opted for a series of events, beginning with the official visit on 9



Dr. Uwe Thomas addressing an invited audience during his visit to the ESO Headquarters on 9 September.

September by Dr. Uwe Thomas, Secretary of State for education and research of the German Federal Government. Speeches by Dr. Thomas, Prof. Ralf Bender (LMU), Prof. Wolfgang Hillebrandt (MPA), ESO's Director General and Dr. Arno Freytag, President of the ESO Council, were followed by a screening of a (pre-premiere) version of the anniversary film 'Europe Reaches for the Stars – Forty Years ESO'. Also, the anniversary book 'Geheimnisvolles Universum – Europas Astronomen entschleiern das Weltall' by German science journalist Dirk Lorenzen was shown for the first time with hand-

bound copies presented to Dr. Thomas, Dr. Freytag, Mr. Manfred Solbrig, the Mayor of Garching, and to ESO's Director General.

On 14 October, a joint celebration by the Garching staff and the ESO Council took place, with speeches by ESO's Council President, the Director General and Claudio Cumani, Chairman of the ESO International Staff Association. The event was 'broadcast' via ESO's video-conference system. The anniversary film was shown to the entire staff, both in Garching and at simultaneous anniversary parties in Santiago, at La Silla and Paranal.

As mentioned in the last issue of *The Messenger*, ESO's anniversary is also a public event. Perhaps most visible is the new planetarium show, produced by the Association des planétariums de langue française (APLF) in collaboration with ESO. It is entitled 'Mysteries of the Southern Sky' and will become available in French, German, English, Dutch, Spanish and possibly other languages. Until now, about 40 planetaria in France and seven other countries have signed up and will stage the show in the coming weeks and months.

The formal premiere took place on 11 October at the Cité de l'Espace in Toulouse. The premiere event for an invited audience encompassed scientific talks by Drs. Françoise Combes and Marc Lachieze-Rey and an evening reception accompanied by live Latin American tunes.

Meanwhile, the ESO anniversary film is available on a three-language DVD (English, French, German), as well as



The newly refurbished auditorium in Garching was packed during the anniversary celebration on 14 October.



ESO's Director General addressing the invited audience at the premiere of the planetarium show in Toulouse.



In spite of the decidedly unpleasant weather in Garching on 14 October, good catering contributed to the convivial atmosphere in the party tent, as about 250 people gathered for the dinner for staff and Council.

in single-language versions on VHS tapes. Among other places, the DVD will be widely available through those planetaria staging the ESO show.

Finally, the CD-ROM (in English) entitled '3D Atlas of the Universe', is now

scheduled for early December. The CD-ROM, which is produced in a collaboration between ESO, USM (Munich) and Planetary Visions (University College, London), includes video clips, photos and texts about ESO as well as

some of the most spectacular astronomical images based on observations at La Silla and Paranal combined with advanced 3D simulation software. It will be commercially available all over Europe.

Breaking the Ground for the European Research Area – The Conference 'European Research 2002'

C. MADSEN, ESO

In the days November 11–13, about 9000 scientists, science administrators and policy makers gathered in Brussels to attend the Launch Conference for the '6th Framework Programme of the European Community for research, technological development and demon-

stration activities' – or for short, 'FP-6'. While most participants came from the member states of the European Union, candidate countries and associated states, the meeting was in fact attended by people from 65 countries, demonstrating the wide scope and the

importance of the process set in motion to create the European Research Area. Some 50 TV teams and 230 journalists from the print media covered the event, which *El País*, the leading Spanish newspaper, described as 'The Science Summit in Brussels'. The strong media interest bears witness to the fact that science and technology (and with them, also education) are playing an increasingly important and visible role in the public sphere and that the organization and execution of research, as well as the exploitation of scientific results, are assuming importance in the mainstream political debate.

Winds of Change

The background for the strong participation to the meeting is certainly to be found in the notion of a change of the political climate in Europe with respect to science and technology. The Lisbon declaration by the European Council in March 2000, stated that the EU should 'become the most competitive and dynamic knowledge-based economy in the world, capable of sustainable economic growth with more and better jobs and greater social cohesion'. It was re-



The ESO stand formed a part of the EIROforum area.



The EIROforum stand was packed with attendants as the EIROforum charter was signed.

inforced by the decision at the Barcelona summit in March 2002 to aim for a 50% increase in research spending in Europe, to reach the 3 % level of the GDP by the year 2010. One of the most important elements in the effort to revive European competitiveness in R&D is the concept of the European Research Area (ERA) and the 6th Framework Programme is explicitly described as a tool to help facilitate the formation of the ERA.

Clearly, creating the ERA is a complex process with a diversity of actors and stakeholders. The conference provided a forum for discussions among all groups involved, from science ministers to the scientists themselves, who turned up in huge numbers.

The subjects under discussion included 'Research and Innovation', 'Human resources and mobility', 'European research in a global context', 'Infrastructures for the European Research Area' as well as 'Science and Society'. In parallel, 'how-to' seminars gave practical advice for scientists planning to seek project funding under the new Framework Programme.

Furthermore, the 'Participants' forum' comprised more than 80 workshops and events covering a wide spectrum of topics – from fusion research, genomics, 'e-science' and grid technologies to intellectual property rights and science communication.

EIROforum and the ERA

One of the first tangible results of the ERA process was the collaboration between the European Intergovernmental Research Organizations (CERN, EFDA-JET, EMBL, ESA, ESO, ESRF, ILL), leading to the formation of the EIROforum. EIROforum has been active for a while and already achieved significant, practical results and the collaboration was formally sealed at the conference in Brussels. On Tuesday, November 12, the Directors General of the organizations signed the EIROforum Charter in the presence of Philippe Busquin, European Commissioner for Research, and numerous journalists. 'The establishment of EIROforum is a concrete example of

the dynamic created by the European Research Area. Europe has unquestioned excellence in science. By working together, Europe's leading research organizations can make that more visible on the European and world stage,' said Busquin in a press statement.

The signing of the charter was also marked by the launch of the EIROforum web site (www.eiroforum.org) and a brochure describing the aims and the specific elements of the collaboration.

EIROforum at the Conference

Indeed, EIROforum maintained a high visibility at the conference. Representatives of the member organizations took part in several round-table discussions and workshops, and the EIROforum exhibition attracted many visitors and provided inspiring surroundings for many discussions. The EIROforum stand covered 400 square metres with an open-plan architecture, providing individual space for each of the seven member organizations and a centrally located common area for the EIROforum itself. The press event in connection with the signing of the EIROforum Charter took place directly on the stand.

The ESO Stand

Featuring prominently on the 36 square metres ESO stand was a scale

model of the 100-m OWL telescope. It caught the attention of many visitors and was also shown in 'The Sixth Sense', the daily conference newspaper. Apart from the OWL project, subjects covered on the ESO stand were the VLT/VLTI and the ALMA project as well as those programmes for which the European Commission has provided major financial support, e.g. for Adaptive Optics, the Astrophysical Virtual Observatory (AVO) and the educational outreach programmes, notably 'Life in the Universe' and 'Physics on Stage'. Clearly, exposing ESO and its activities and future projects to such a huge, but select audience, was important, and the seven ESO staff that took turns on the stand had many interesting exchanges with the visitors.

'European Research 2002' sent a clear signal that the European research landscape is undergoing a major transformation, leading Le Figaro, the French daily, to talk about 'a new spirit for European scientists'. In two years time, when FP-6 reaches its half-term, the follow-up meeting, announced by Commissioner Busquin, will surely be able to determine to what extent this new spirit has produced tangible progress for European science.

A Nobel Prize for Riccardo Giacconi



Riccardo Giacconi has been awarded the Nobel Prize „for pioneering contributions to astrophysics, which have led to the discovery of cosmic X-ray sources". In the words of The Royal Swedish Academy of Sciences, „he detected for the first time a source of X-rays outside our solar system and he was the first to prove that the universe contains background radiation of X-ray light. He also detected sources of X-rays that most astronomers now consider to contain black holes. Giacconi constructed the first X-ray telescopes, which have provided us with completely new – and sharp – images of the universe. His contributions laid the foundations of X-ray astronomy." (<http://www.nobel.se/>). Over the last two decades he has also been a leader in other fields of astronomy, and served as ESO's Director General over the years 1993–1999. ESO and its community send Riccardo their congratulations on this great honour.

Agreement Between the Government of the Republic of Chile and ESO for Establishing a New Centre for Observation in Chile – ALMA

Reproduced from ESO Press Release 18/02 (23 October 2002)

On October 21, 2002, the Minister of Foreign Affairs of the Republic of Chile, Mrs. María Soledad Alvear, and the ESO Director General, Dr. Catherine Cesarsky, signed an Agreement that authorizes ESO to establish a new centre for astronomical observation in Chile.

This new centre for astronomical observation will be for the Atacama Large Millimeter Array (ALMA), the largest ground-based astronomical project for the next decades.

On this occasion, Minister Alvear stated that “we want to have ALMA working as soon as possible, which will constitute a pride not only to Chilean scientists but for the whole country and in particular, for the community of the Antofagasta Region”.

ESO Director General Cesarsky said that “signing this agreement between the Government of Chile and ESO is a historical step in the astronomical



Signing of the new Agreement that authorizes ESO to establish a new centre for astronomical observation in Chile. General view.

collaboration between Chile and ESO and it will allow Chile to host, once again, a project of worldwide interest and impact”.

ALMA is a joint project on equal basis between ESO and AUI (Associated Universities, Inc.). These organizations represent the scientific interests of Europe on one side and the United States with Canada on the other side. Chilean astronomers are closely involved with the

project, and 10 % of the observing time will be reserved for Chilean science.

ALMA will be built in the Andes, on the Plateau of Chajnantor, 5000 metres above sea level and 60 km east of the town of San Pedro de Atacama. The array will be comprised of 64 antennas with unprecedented sensitivity and angular resolution that will allow studying the origin of galaxies, stars and planets, opening new horizons for astronomy, and being able to observe galaxies across the universe where stars are being formed.

The agreement now signed between ESO and the Government of the Republic of Chile recognizes the interest that the ALMA Project has for Chile, as it will deepen and strengthen cooperation in scientific and technological matters between the parties.



Chilean Minister of Foreign Affairs of the Republic of Chile, Mrs. María Soledad Alvear (seated, right) and the ESO Director General, Dr. Catherine Cesarsky (seated, left).

Eighty Nights Up a Mountain

By SARA ELLISON



For the last two years, I have worked as a fellow at the Santiago offices of the European Southern Observatory (ESO) with support responsibilities at the Very

Large Telescope (VLT) on Cerro Paranal in the north of Chile. This is es-

A version of this article first appeared in August 2002 in the online publication Next Wave (www.nextwave.org), published by Science Magazine on the occasion of the UK joining ESO.

As Sara Ellison describes, she has been a Paranal Fellow for the past two years and is currently in her third year at the Pontificia Universidad Católica de Chile in Santiago.

entially a postdoctoral position; I started here directly after I completed my

PhD at the University of Cambridge in the summer of 2000.

There are many possibilities open to a completing graduate student and it can be quite daunting filtering through the various options, academic and otherwise. For me, the decision was based on a few fundamental academic and personal priorities. I wanted a destination that was going to provide an interesting and fulfilling lifestyle, preferably with the chance to learn a new language. I was also looking for a working environment that would offer diverse opportunities for professional development. Working in an observatory was therefore very appealing, and at that time (as is still the case a few years later) there were plenty of positions as observatories expanded their horizons to the new generation of large telescopes. In addition, as an undergraduate, I had spent five consecutive summer vacations working at various observatories in locations including Australia, Hawaii, and the Canary Islands, and undertaking support work and dabbling in instrumentation seemed a good complement to my scientific research.

Therefore, many of my postdoc applications were aimed at observatories, and I was particularly excited by the possibility of moving to Chile. The fellowship application consists of a straightforward form (no long research proposal like most places!) followed by an interview at the ESO headquarters near Munich in Germany with a video link to Chile. Applicants are selected on the combined criteria of a strong scientific record and suitability for support work (particularly important for Chile-bound fellows). Priority for posts goes to nationals of ESO member countries, and at that time the UK was not a member (it joined this July). However, because Chilean fellows have to fulfill very specialist duties at the telescopes, there are fewer suitable applicants (and usually fewer people who want to move to Chile) and this criterion is therefore relaxed. Because the ESO fellowship was my first choice amongst the various positions I applied for, it was an easy decision when, just before the start of the Christmas holidays, I was offered a position to start the following autumn.

Many people expect that moving to Chile may involve a large culture shock. Although it is certainly not the same as Europe, the facilities and infrastructure in Santiago are very well developed and settling in was not a problem at all. ESO has been dealing with Europeans moving to Chile for many years and has a well-oiled system that handles everything from moving your household and getting your local ID and visa processed to helping you find somewhere to live and opening a bank account. Chile fellows are allocated duty stations at either Paranal (like me) or La Silla, ESO's

first Chilean telescope site. Contractually, we spend 80 nights a year (usually in bite-size shifts of 1 week) on the mountain doing support work, plus up to a month doing duty-related work in Santiago. The rest of the time is your own to pursue whatever scientific research takes your fancy. The advantage in this set-up is that your duty responsibilities can be quite easily compartmentalized: When you're on the mountain you do support and when you're in Santiago you do science.

For every week you spend on the mountain, you officially get the following week off as 'compensation time'. However, most people tend to only take a few days off in order to maximize the time they can spend on their science, as research output is always an important factor in securing the next job. For Chile fellows, the contracts are nominally four years (a recent – and welcome – change from the old style 3-year contracts); the first three years are spent divided between research and support whilst there are various options available for the final year. You might continue working at ESO Chile, but with only 40 nights of support work, or you might go back to the headquarters in Germany and do a similar duty load in one of the divisions there. Alternatively, you can elect to go to one of the Chilean universities where you will do 100% research and have the benefits of applying for telescope time as a Chilean. Due to the relatively small number of Chilean astronomers compared to the large number of telescope hours they are entitled to, this offers a great opportunity to collect lots of data. A final option that has just been approved is that fellows may return to a university department that is willing to 'adopt' them in any ESO member country with their salary still paid by ESO. This is a particularly attractive option for many as it gives fellows who have been away from their home countries for three years the opportunity to advertise themselves to universities that they see as potential employers when their fellowship ends. This latter option also offers the potential to gain some teaching or supervisory experience, opportunities that are limited at ESO itself.

The flexibility, diversity, and four guaranteed years are just a few of the advantages of the ESO fellowship scheme. Other professional pluses include the opportunity to meet the large number of European astronomers that pass through to conduct their observations, providing ample possibilities for forming new collaborations and making yourself known within the community. In addition, it is generally attractive for future employers to see that you have had experience with

instrumentation and observatory work, which is a good complement to independent research. ESO fellowships are also very well regarded and prestigious, so it is certainly a good position to have held.

On the practical side, ESO fellows are well paid, with allowances for being overseas and having to spend time on the mountain, and the salary is essentially tax-free. There are also salary benefits if you are married and have children (who additionally receive an education allowance). Taking into account the lower cost of living in Chile, you can certainly live very well on the salary you take home, and there are lots of opportunities to live well in Chile! The lifestyle here is definitely an attraction – Santiago has the beach, mountains, and vineyards on its doorstep and all of the trappings of a big city such as cinemas, restaurants, and theatres.

Of course, every job has its associated drawbacks, and fellowships are no exception. The support work is very demanding, requires a lot of commitment, and involves a lot of travelling (it's 6 hours door-to-door to Paranal) and night work. You also have to spend a significant fraction of your time away from your family, and spouses do not have work status. Also, the support work obviously means you can spend less time on science, although this is something you have presumably accepted if you are considering an observatory job. For me, I have actually found that my productivity has not seriously suffered and that time away at the telescope is a refreshing change from the office. The key to success is definitely effective short-term time management; it is important to be able to plan your work on time scales of a few weeks between each telescope shift. This means breaking down large tasks into smaller jobs and setting goals and deadlines on a weekly basis. Focusing in this way has allowed me to be much more efficient with my time when I'm not on the mountain, a technique that will be useful even when I'm no longer working at ESO.

My contract with ESO will come to an end in September 2003. However, I already have a tenure-track job lined up at the University of Victoria in Canada, allowing me to satisfy my 'wanderlust' still further and get to know another new country. Apart from my research profile, the experience and skills I have developed at ESO are definitely part of what secured this position, as Canada increases its access to large telescopes and its involvement in future projects such as NGST and ALMA. I'll certainly be sad to leave Chile though, although I'm sure it will only be *hasta luego* and not *adios*.

ANNOUNCEMENTS

FIRST ANNOUNCEMENT

ESO WORKSHOP ON High Resolution Infrared Spectroscopy in Astronomy

ESO-Headquarters, Garching near Munich, November 18–21, 2003

Infrared spectroscopy at a resolution of a few km/s offers a unique tool to study rotational-vibrational transitions of many abundant molecules as well as important atomic lines in a multitude of interesting astrophysical environments. Applications include the possible direct detection of extrasolar planets, measurements of the abundances and magnetic fields of stars, studies of ISM chemistry and the kinematics of stars and gas in galactic centres.

The ESO VLT will shortly be equipped with two unique spectrometers which not only offer this high spectral resolution but also spatial resolutions of $\sim 0.2''$:

- CRIRES, an adaptive optics fed 1–5 μm spectrograph yielding a resolution of 3 km/s
- VISIR, which includes a high-resolution mode yielding a resolution of < 8 km/s between 8 and 13 μm

The aims of this workshop are to:

- present the latest status of the high-resolution infrared spectroscopic capabilities of the VLT and other observatories
- bring together the community interested in the application of high resolution infrared spectroscopy and to foster new collaborations
- provide ESO with feedback in the phase when operating and data reduction software is being defined and coded

For space reasons the number of participants is limited to 110.

Scientific Organizing Committee:

Bengt Gustafsson (Uppsala, chair), Catherine de Bergh (Meudon), Ewine van Dishoeck (Leiden), Artie Hatzes (Tautenburg), Ken Hinkle (Tucson), Ulli Käufel (ESO), Alan Moorwood (ESO, co-chair)

More details, preliminary programme and registration form can be retrieved from <http://www.eso.org/gen-fac/meetings/ekstasy2003> or contact

ekstasy2003@eso.org for further information

Symposium Secretary: Christina Stoffer

European Southern Observatory, Karl-Schwarzschild-Str. 2,
D-85748 Garching bei Muenchen, Germany
Fax: +49 89 3200 6480; E-mail ekstasy2003@eso.org

ESO Workshop on Large Programmes and Public Surveys

Dates: 19–21 May 2003
Location: Garching, Germany

An evaluation of the scientific success of the first completed Large Programmes at the VLT and public surveys should take place before the survey telescopes VST and VISTA start operating. To assess the scientific return of the Large Programmes, ESO is organizing a three-day workshop in Garching from 19 to 21 May 2003.

To ESO it will offer an opportunity to hear directly from major users of the facilities of their experiences, problems and wishes. The relation of surveys to other forms of observational programmes should be discussed.

GEORGIEVA, Radostina (BG), Associate
HAUPT, Christoph (D), System Engineer
KOLB, Johann (F), Student
LARSEN, Soeren (DK), Fellow
LOMBARDI, Marco (I), Fellow
PANGOLE, Eric (F), System Engineer
PIGNATA, Giuliano (I), Student
REJKUBA, Marina (HR), Fellow
RUDOLF, Hans (D), System Engineer
SOENKE, Christian (D), Associate
SOMMER, Heiko (D), ALMA Software Developer
VERDOES KLEIJN, Gijsbert (NL), Fellow
VERINAUD, Christophe (F), Associate
VICENTE, Silvia (PL), Student

CHILE

ANDERSSON, Andreas (S), Associate SEST
CLARKE, Fraser (UK), Fellow
GANDHI, Poshak (IND), Fellow
HUELAMO, Nuria (E), Fellow
MEDVES, Giuseppe (I), Paid Associate ALMA
NAKOS, Theodoros (GR), Student
O'BRIEN, Kieran (UK), Operations Staff Astronomer
VREESWIJK, Paul (NL), Fellow

PERSONNEL MOVEMENTS

International Staff

(1 October – 31 December 2002)

ARRIVALS

EUROPE

BASTIAN, Nathan (USA), Student
DOLENSKY, Markus (D), System Engineer

DEPARTURES

EUROPE

ARNOUITS, Stéphane (F), Fellow
BACHER, Arntraud (A), Associate
BERGOND, Gilles (F), Associate
CAVADORE, Cyril (F), CCD Detector Specialist
CORREIA, Serge (F), Associate
EULER, Christa (D), Administrative Assistant
HOSE, Jürgen (D), Associate
TOPLAK, Nenad (HR), Associate
ZIEBELL, Manfred (D), Head of Technical Division

CHILE

DAHLEM, Michael (D), Operations Staff Astronomer
DELSANTI, Audrey (F), Student
FAURE, Cécile (F), Student
ZALTRON, Paolo (I), Associate

Local Staff (1 September – 30 November 2002)

ARRIVALS

CANIGUANTE BARCO, Luis Alejandro, Electronic Engineer
HENRIQUE LEON, Juan Pablo, Mechanical Technician

Manfred Ziebell Retires



It's hard to believe, but by the end of November, Manfred's sounding footsteps will no longer be heard at ESO Garching.

Manfred initiated his engineering career at ESO when the 3.6-m telescope was in the design phase and had to be brought into a reality. New servo controls, positioning systems, communication protocols were his lot; a time when ESO struggled to reach its autonomous design maturity. Manfred proved to be a key figure for the future technological challenges.

Faced with a jungle of technical initiatives, he managed to develop electronic standards that merged successfully into the VLT design.

Manfred assembled design and support teams for the telescope and the instrumentation controls. Convincing rather than imposing was his style, a style that was very much appreciated and highly respected by his colleagues.

Service-minded, he became a paradigm of support endeavours, by solving technical problems, contractual issues and human relations. He was ready to tackle any issue, including Hausmeister and safety functions.

Problems? Ask Manfred!

Manfred was on the phone with Chile or... in Chile!

The VLT encoding units failed? Manfred was already negotiating alternatives!

As Head of the Technical Division, he established a support culture that placed ESO on the trail to success.

Manfred's hurried and sounding steps will be missed at ESO.

"Un hombre de primeras aguas, ahora otras aguas lo esperan"

Daniel Hofstadt

Thirty-Seven Years of Service with ESO!



On December 1st, 2002, after thirty-seven years of service, first in Chile and then in Garching, Ms. Christa Euler will leave ESO to enjoy a well-deserved retirement. Among the current staff, she is probably the only person who started her career at ESO just four years after the Organization was founded.

Christa joined ESO Chile on April 1st, 1966, at the time when Prof. Heckmann was Director General. In these early days she was responsible for all secretarial work in the Santiago

office, which was first located in the Guesthouse before moving to the Vitacura building. Three years later, upon the arrival of Prof. B.E. Westerlund, she took over the post of secretary to the ESO Director in Chile. With the exception of a ten-month period spent in the Personnel Department in Hamburg, she held this position until mid-1976. Her definitive move to ESO Europe took place in September 1976. At the newly installed Headquarters in Garching, she took up

LEIVA BECERRA, Alfredo, Instrumentation Engineer
ROA FIGUEROA, Luis, Mechanical Technician
ROJAS CHANAMPA, Chester, Instrument Technician
TORRES ZAMORANO, Manuel, Maintenance Electronic Technician

DEPARTURES

ALVAREZ CASTELLON, Pedro,
Precision Mechanic
CASTRO CASTRO, Wilson, Mechanic
MIRANDA MANRIQUEZ, Marcela,
Administrative Secretary

duty in the Visiting Astronomers' Section then headed by Dr. A.B. Muller.

During the twenty-six years that Christa worked in this Section, apart from being the key person whose diligence was much appreciated by all the astronomers having to travel to Chile, she has – among many other things – very efficiently handled over 20,000 observing proposals, and organized about fifty OPC meetings, including the corresponding "exclusive" OPC dinners. Today, her name is familiar to most European astronomers as well as to many others overseas, as demonstrated by the numerous expressions of heartfelt gratitude received for the farewell booklet that was presented to her on November 28, on the occasion of the OPC dinner, which was held in her honour.

Friends, colleagues and astronomers will certainly miss Christa Euler. We wish her all the best for the years to come.

Jacques Breysacher

New ESO Proceedings

The Proceedings of the Topical Meeting, held in Venice from 7 to 10 May 2001

Beyond Conventional Adaptive Optics

(ESO Conference and Workshop Proceedings No. 58)

have now been published. The price for the 490-page volume, edited by E. Vernet, R. Ragazzoni, S. Esposito and N. Hubin, is € 50.– (prepayment required).

Payments should be made to the ESO bank account 2102 002 with Commerzbank München (BLZ 700 400 41, S.W.I.F.T. Code: COBADEFF 700) or by cheque, addressed to the attention of

ESO, Financial Services, Karl-Schwarzschild-Str. 2
D-85748 Garching bei München, Germany

ESO Workshop Proceedings Still Available

Many ESO Conference and Workshop Proceedings are still available and may be ordered at the European Southern Observatory. Some of the more recent ones are listed below.

No.	Title	Price
45	ESO/EIPC Workshop "Structure, Dynamics and Chemical Evolution of Elliptical Galaxies", 1993	€ 45.–
46	Second ESO/CTIO Workshop on "Mass Loss on the AGB and Beyond", 1993	€ 35.–
47	5th ESO/ST-ECF Data Analysis Workshop, 1993	€ 15.–
48	ICO-16 Satellite Conference on "Active and Adaptive Optics", 1994	€ 45.–
49	ESO/OHP Workshop on "Dwarf Galaxies", 1994	€ 45.–
50	ESO/OAT Workshop "Handling and Archiving Data from Ground-based Telescopes", 1994	€ 20.–
51	Third CTIO/ESO Workshop on "The Local Group: Comparative and Global Properties", 1995	€ 25.–
52	European SL-9/Jupiter Workshop, 1995	€ 40.–

ESO, the European Southern Observatory, was created in 1962 to "... establish and operate an astronomical observatory in the southern hemisphere, equipped with powerful instruments, with the aim of furthering and organising collaboration in astronomy..." It is supported by ten countries: Belgium, Denmark, France, Germany, Italy, the Netherlands, Portugal, Sweden, Switzerland and the United Kingdom. ESO operates at two sites in the Atacama desert region of Chile. The new Very Large Telescope (VLT), the largest in the world, is located on Paranal, a 2,600 m high mountain approximately 130 km south of Antofagasta, in the driest part of the Atacama desert where the conditions are excellent for astronomical observations. The VLT consists of four 8.2-metre diameter telescopes. These telescopes can be used separately, or in combination as a giant interferometer (VLTI). At La Silla, 600 km north of Santiago de Chile at 2,400 m altitude, ESO operates several optical telescopes with diameters up to 3.6 m and a submillimetre radio telescope (SEST). Over 1300 proposals are made each year for the use of the ESO telescopes. The ESO headquarters are located in Garching, near Munich, Germany. This is the scientific, technical and administrative centre of ESO where technical development programmes are carried out to provide the Paranal and La Silla observatories with the most advanced instruments. There are also extensive astronomical data facilities. ESO employs about 320 international staff members, Fellows and Associates in Europe and Chile, and about 160 local staff members in Chile.

The ESO MESSENGER is published four times a year: normally in March, June, September and December. ESO also publishes Conference Proceedings, Preprints, Technical Notes and other material connected to its activities. Press Releases inform the media about particular events. For further information, contact the ESO Education and Public Relations Department at the following address:

EUROPEAN
SOUTHERN OBSERVATORY
Karl-Schwarzschild-Str. 2
D-85748 Garching bei München
Germany
Tel. (089) 320 06-0
Telefax (089) 3202362
ips@eso.org (internet)
URL: <http://www.eso.org>
<http://www.eso.org/gen-fac/pubs/messenger/>

The ESO Messenger:
Editor: Peter Shaver
Technical editor: Kurt Kjær

Printed by
Universitätsdruckerei
WOLF & SOHN
Heidemannstr. 166
D-80939 München
Germany

ISSN 0722-6691

No.	Title	Price
53	ESO/ST-ECF Workshop on "Calibrating and understanding HST and ESO instruments", Garching, Germany. P. Benvenuti (ed.)	€ 30.-
54	Topical Meeting on "Adaptive Optics", October 2-6, 1995, Garching, Germany. M. Cullum (ed.)	€ 40.-
55	NICMOS and the VLT. A New Era of High Resolution Near Infrared Imaging and Spectroscopy. Pula, Sardinia, Italy, May 26-27, 1998	€ 40.-
56	ESO/OSA Topical Meeting on "Astronomy with Adaptive Optics - Present Results and Future Programs". Sonthofen, Germany, September 7-11, 1999. D. Bonaccini (ed.)	€100.-
57	Bäckaskog Workshop on "Extremely Large Telescopes". Bäckaskog, Sweden, June 1-2, 1999. T. Andersen, A. Ardeberg, R. Gilmozzi (eds.)	€ 30.-

Contents

TELESCOPES AND INSTRUMENTATION

L. Pasquini et al.: Installation and Commissioning of FLAMES, the VLT Multifibre Facility	1
F. Pepe, M. Mayor, G. Rupprecht: HARPS: ESO's Coming Planet Searcher. Chasing Exoplanets with the La Silla 3.6-m Telescope	9
K. Kuijken et al.: OmegaCAM: the 16k×16k CCD Camera for the VLT Survey Telescope	15
A. Glindemann: The VLTI - 20 Months after First Fringes	18
B. Koehler, C. Flebus, P. Dierickx, M. Dimmler, M. Duchateau, P. Duhoux, G. Ehrenfeld, E. Gabriel, P. Gloesener, V. Heinz, R. Karban, M. Kraus, J.M. Moresmau, N. Ninane, O. Pirnay, E. Quertemont, J. Strasser, K. Wirenstrand: The Auxiliary Telescopes for the VLTI: a Status Report	21
Roberto Gilmozzi and Jason Spyromilio: Paranal Observatory - 2002	28
O. Hainaut: News from La Silla: Science Operations Department	30
Two unusual views of La Silla	31

REPORTS FROM OBSERVERS

N.C. Santos, M. Mayor, D. Queloz, S. Udry: Extra-Solar Planets	32
I. Labbé, M. Franx, E. Daddi, G. Rudnick, P.G. van Dokkum, A. Moorwood, N.M. Förster Schreiber, H.-W. Rix, P. van der Werf, H. Röttgering, L. van Starckenburg, A. van de Wel, I. Trujillo, and K. Kuijken: FIREs: Ultradeep Near-Infrared Imaging with ISAAC of the Hubble Deep Field South	38

OTHER ASTRONOMICAL NEWS

M. Kissler-Patig: Summary of the Workshop on Extragalactic Globular Cluster Systems hosted by the European Southern Observatory in Garching on August 27-30, 2002	42
A. Glindemann: The VLTI: Challenges for the Future. Workshop at Jenam 2002 in Porto	44
P. Shaver and E. Van Dishoek: Summary of a Meeting on Science Operations with ALMA, held on Friday, 8 November 2002	44
C. Madsen: Celebrating ESO's 40th Anniversary	45
C. Madsen: Breaking the Ground for the European Research Area - The Conference 'European Research 2002'	46
A Nobel Prize for Riccardo Giacconi	47
Agreement Between the Government of the Republic of Chile and ESO for Establishing a New Centre for Observation in Chile - ALMA	48
Sara Ellison: Eighty Nights Up a Mountain	48

ANNOUNCEMENTS

First Announcement of an ESO Workshop on High-Resolution Spectroscopy in Astronomy	50
ESO Workshop on Large Programmes and Public Surveys	50
Personnel Movements	50
Daniel Hofstadt: Manfred Ziebell Retires	51
Jacques Breysacher: Christa Euler - Thirty-Seven Years of Service with ESO!	51
New ESO Proceedings	51
ESO Workshop Proceedings Still Available	51